mathematics

MDPI

Article

Conscious Neighborhood-Based Jellyfish Search Optimizer for Solving Optimal Power Flow Problems

Mohammad H. Nadimi-Shahraki [1], Mahdis Banaie-Dezfouli [2,3,*] and Hoda Zamani [2,3]

[1] International Graduate School of Artificial Intelligence, National Yunlin University of Science and Technology, Yunlin 640301, Taiwan; nadimi@yuntech.edu.tw
[2] Faculty of Computer Engineering, Najafabad Branch, Islamic Azad University, Najafabad 8514143131, Iran; hoda_zamani@sco.iaun.ac.ir
[3] Big Data Research Center, Najafabad Branch, Islamic Azad University, Najafabad 8514143131, Iran
* Correspondence: m.dezfouli@sco.iaun.ac.ir

Abstract

Optimal Power Flow (OPF) problems are essential in power system planning, but their nonlinear and large-scale nature makes them difficult to solve with traditional optimization methods. Metaheuristic algorithms have become increasingly popular for solving OPF problems due to their ability to handle complex search spaces and multiple objectives. The Jellyfish Search Optimizer (JSO) is a metaheuristic algorithm that performs well for solving various optimization problems. However, it suffers from low exploration and an imbalance between exploration and exploitation. Therefore, this study introduces an improved JSO called Conscious Neighborhood-based JSO (CNJSO) to address these shortcomings. The proposed CNJSO suggests a new movement strategy named Best archive and Non-neighborhood-based Global Search (BNGS) to enhance the exploration ability. In addition, CNJSO adapts the concept of conscious neighborhood and the Wandering Around Search (WAS) strategy. The proposed CNJSO facilitates exploration of the search space and strikes a suitable balance between exploration and exploitation. The performance of CNJSO was evaluated on CEC 2018 benchmark functions, and the results were compared with those of ten state-of-the-art metaheuristic algorithms. In addition, the results were statistically validated using the Wilcoxon rank-sum and Friedman tests. Additionally, the effectiveness of CNJSO was assessed through the resolution of OPF problems. The experimental and statistical results confirm that the proposed CNJSO algorithm is competitive and superior to the compared algorithms.

Keywords: optimization; metaheuristic algorithms; swarm intelligence; jellyfish search optimizer; optimal power flow problem

MSC: 68T20

check for updates

Academic Editor: Anna Sciomachen

Received: 1 August 2025
Revised: 1 September 2025
Accepted: 4 September 2025
Published: 24 September 2025

Citation: Nadimi-Shahraki, M.H.; Banaie-Dezfouli, M.; Zamani, H. Conscious Neighborhood-Based Jellyfish Search Optimizer for Solving Optimal Power Flow Problems. *Mathematics* **2025**, *13*, 3068. https://doi.org/10.3390/math13193068

Copyright: © 2025 by the authors. Licensee MDPI, Basel, Switzerland. This article is an open access article distributed under the terms and conditions of the Creative Commons Attribution (CC BY) license (https://creativecommons.org/licenses/by/4.0/).

1. Introduction

Metaheuristic algorithms offer an efficient approach to solving complex optimization problems, often outperforming exact algorithms in terms of computational efficiency and execution time [1–3]. They can effectively handle problems with diverse characteristics, including high dimensionality, multimodality, and non-differentiability [4]. Many of these algorithms are inspired by phenomena observed in nature. They are classified as Nature-Inspired (NI) algorithms [5], which use randomness and probabilistic rules to explore the search space, enabling them to identify near-optimal solutions. Typically, NI algorithms

operate in two main phases: exploration, which broadly searches the solution space, and exploitation, which refines promising solutions. Effectively balancing these phases helps prevent stagnation in local minima and increases the likelihood of achieving optimal solutions [5,6].

NI algorithms have limitations that can hinder their ability to achieve the global optimum in different problem-solving scenarios. In addition, the No-Free Lunch (NFL) theorem emphasizes that an algorithm's effectiveness on one optimization problem does not guarantee its success on all other optimization problems [7–9]. There is no universally superior algorithm; each is tailored to specific problem types [8]. Therefore, different algorithms were introduced by the inspiration of nature, such as Evolution Strategy (ES) [10], Genetic Algorithm (GA) [11], Particle Swarm Optimization (PSO) [12], Ant Colony Optimization (ACO) [13], Gravitational Search Algorithm (GSA) [3], Grey Wolf Optimizer (GWO) [14], Jellyfish Search Optimizer (JSO) [15], Tunicate Swarm Algorithm (TSA) [16], Fossa Optimization Algorithm (FOA) [17], and Teaching–Learning-based Optimization (TLBO) [18]. These algorithms can be employed to solve complex optimization problems in a variety of domains, such as optimal power flow problems [19,20], engineering [21–23], feature selection [24–28], planning [29–31], community detection [32,33], financial issues [34], virtual machine placement [35], medical diagnosis [36,37], and clustering [38–40].

Among NI algorithms, the JSO is a recently developed NI algorithm inspired by the behavior of jellyfish [15]. It captures four movement types—ocean current following, bloom following, and both active and passive motions—coordinated by a time-control mechanism. Despite its straightforward design, JSO may suffer from premature convergence, which limits its ability to explore and the quality of its solutions [41,42]. Recently, many research studies have been introduced to enhance the JSO algorithm, such as Enhanced JSO (EJSO) [41], Fractional-Order modified and Gaussian mutation mechanism JSO (FOGJS) [42], Orthogonal Learning JSO (OLJSO) [43], and Multi-Objective Quasi-Reflected Jellyfish Search Optimizer (MOQRJFS) [44]. To address the constraints of the JSO, this study introduces an improved version of the algorithm, termed the Conscious Neighborhood-based JSO (CNJSO). This enhancement draws inspiration from the concept of conscious neighborhoods introduced in the Conscious Neighbor-hood-Based Crow Search Algorithm (CCSA) [45]. It aims to enhance the exploratory capability and balance between exploration and exploitation.

The novelty of this study lies in introducing a new movement strategy named Best Archive and Non-neighborhood-based Global Search (BNGS), which utilizes an archive and multiple trials to enhance the algorithm's exploration capabilities. CNJSO utilizes the conscious neighborhood to perceive the search space and choose movement strategies consciously. Moreover, CNJSO employs the wandering around search (WAS) strategy to improve individuals who are not performing well and cannot achieve better fitness. The CNJSO's performance is assessed and compared with some state-of-the-art swarm intelligence algorithms: PSO [12], Krill Herd (KH) [4], GWO [14], Whale Optimization Algorithm (WOA) [46], Exploration-Enhanced GWO (EEGWO) [47], Henry Gas Solubility Optimization (HGSO) [48], Jellyfish Search Optimizer (JSO) [15], Tunicate Swarm Algorithm (TSA) [16], Mountaineering Team-based Optimization (MTBO) [49], and Fossa Optimization Algorithm (FOA) [17] on the benchmark test functions of CEC 2018 [50]. Furthermore, CNJSO and the comparative algorithms are statistically evaluated using the Wilcoxon rank sum test and the Friedman test. Finally, the applicability of CNJSO is evaluated for solving the optimal power flow problem for the IEEE 30-bus and the IEEE 118-bus systems. These evaluations and statistical tests prove that the proposed CNJSO outperforms other comparative algorithms.

The remainder of this study is organized as follows: Section 2 briefly reviews the background and related works. Section 3 presents the problem definition. Section 4 describes the proposed algorithm. Section 5 conducts extensive experiments. Section 6 examines the applicability of CNJSO for solving optimal power flow problems. Finally, we conclude this study in Section 7.

2. Related Work

Nature-Inspired algorithms represent a collection of innovative search strategies and methods for solving problems based on the principles observed in the natural world. These algorithms are comprised of four groups: evolutionary algorithms, physics-based algorithms, human-related algorithms, and swarm intelligence algorithms [51,52]. An in-itial random population is used in an evolutionary algorithm, and it evolves over generations to generate new solutions through crossover and mutation. The worst solutions are then eliminated to increase the fitness value [53]. Some popular evolutionary algorithms are Evolution Strategy (ES) [10], Genetic Programming (GP) [54], Genetic Algorithm (GA) [11], and Differential Evolution (DE) [55]. These algorithms have been effectively applied to various real-world problems [56,57]. Among them, DE algorithms stand out for their robustness in tackling complex issues [58]. Several enhancements to the DE algorithm have been developed, including JADE [59], SHADE [60], LSHADE [61], iL-SHADE [62], QUATRE-EAR [63], and MTDE [64], as they suffer from low diversity and premature convergence.

Algorithms grounded in physics propose solutions for numerical optimization challenges by employing concepts from physics and mathematics observed in nature. They create new potential solutions by utilizing natural laws, including gravitational and magnetic forces, chemical reactions, the bending of light, the principle of inertia, and molecular dynamics. There are some well-known algorithms in this group, such as Big Bang-Big Crunch (BB-BC) [65], Gravitational Search Algorithm (GSA) [3], Charged System Search (CSS) [66], Black Hole (BH) [67], Atom Search Optimization (ASO) [68], Ray Optimization (RO) [69], and Henry Gas Solubility Optimization (HGSO) [48] was proposed based on Henry's law be-havior, which specifies the solubility of low-solubility gases in liquids. These algorithms have been used for solving various problem domains, such as the optimal design of truss structures [70], clustering [71], classification [72], global optimization [73,74], maximum power point tracking [75], power system network problems [76–78], photovoltaic energy generation systems [79], and genome biology [80].

Human-based metaheuristic algorithms that mimic human behavior are developed through the mathematical modeling of various human-centric evolutionary processes. The most renowned among these is the Teaching-Learning-Based Optimization (TLBO) [18], which draws inspiration from the dynamics of teacher-student interactions within a classroom setting. Similarly, the Poor and Rich Optimization (PRO) algorithm [81] is conceptualized from the economic behaviors of different socioeconomic classes. The Human Mental Search (HMS) algorithm [82] is crafted by simulating human strategies in online auction environments to attain success. Lastly, the Doctor-Patient Optimization (DPO) algorithm [83] is designed around the medical interactions involving disease prevention, diagnostics, and treatment processes. The Teaching-Based Learning Algorithm (TBLA) [84] was inspired by the influence of a teacher on learners' output in the class. The Corona-virus Herd Immunity Optimizer (CHIO) [85] is inspired by the concept of herd immunity as a strategy to fight the COVID-19 pandemic. This algorithm simulates the distribution of the coronavirus through interaction between contaminated persons and other people.

Swarm intelligence algorithms are computational methods that draw inspiration from the social behaviors of animals, such as the flocking of birds, herding of animals, and

foraging patterns of ants. Each member guides the group towards optimal solutions within a search space through cooperative interactions. Notable examples of these algo-rithms include PSO [12], artificial bee colony (ABC) [86], KH [4], grey wolf optimizer (GWO) [14], whale optimization algorithm (WOA) [46], crow search algorithm (CSA) [87], Harris hawks optimization (HHO) [88], butterfly optimization algorithm (BOA) [89], salp swarm algorithm (SSA) [90], cuckoo search (CS) [91], and ant lion optimizer (ALO) [92]. These algorithms have been effectively applied to address a variety of optimization problems, both continuous and discrete [84,93,94].

While Swarm Intelligence (SI) algorithms have demonstrated their efficacy in addressing optimization problems, they are not without limitations. These algorithms can become trapped in local optima, experience early convergence, and exhibit a decline in solution diversity [95]. Enhanced SI algorithms have been developed to counteract these issues, fortifying their problem-solving capabilities. The representative-based grey wolf optimizer (R-GWO) [96] proposes an improved version of the GWO, addressing some common limitations of the original algorithm, such as becoming stuck in local optima and premature convergence. R-GWO utilizes a representative-based approach to enhance exploration and maintain population diversity. An improved version of the Salp Swarm Algorithm, named Cosine Decline and Chaos Crossover (CDCSSA) [97], was proposed, which updates the leader's position using the cosine decline strategy. The CDCSSA improves the SSA's exploration and exploitation.

Another enhanced version of GWO is the Intelligent Grey Wolf Optimizer (IGWO) [98], which incorporates two mathematical frameworks: an efficient sinusoidal truncated function to enhance exploration and exploitation, and an opposition-based learning concept to improve exploration. Additional crossover and mutation operators were incorporated into the Hybridized GWO algorithm in HGWO [99] to address the economic dispatch problem. This algorithm enhances the rate of convergence. The Multi-trial vector-based Monkey King Evolution (MMKE) algorithm [100] integrates innovative components such as the Best-history Trial Vector Producer (BTVP) and the Random Trial Vector Producer (RTVP), which collaborate with the standard MKE through a multi-trial vector framework. This algorithm enhances global search proficiency, maintains a robust balance between exploration and exploitation, and prevents premature convergence. JSO, like many SI algorithms, has several weaknesses, including premature convergence, imbalanced exploration and exploitation, and slow convergence speed. Therefore, these shortcomings encouraged researchers to produce improved versions of JSO.

Several improvements have been made to the JSO algorithm, and this study has conducted further research on these enhancements. Enhanced JSO (EJSO) [41] is proposed with three improvements: a sine and cosine learning factors strategy, a local escape operator, and an opposition-based learning and quasi-opposition learning strategy. The first strategy adds a learning mechanism to accelerate convergence. The local scape operator is applied to escape from local optima. The last strategy is introduced to increase diversity and improve convergence speed. The results show the superior performance of EJSO. The Orthogonal Learning JSO (OLJSO) [43] is the integration of the Orthogonal Learning Strategy into the JSO, which combines two solutions to generate better outcomes. The OJSO enhances the exploitation, avoids becoming stuck in local optima, and improves the exploration. The results demonstrate that the OJSO outperforms the JSO.

Some researchers integrate the JSO with additional algorithms. The hybrid jellyfish search optimizer and particle swarm optimization (HJSPSO) [101] is based on the JSO structure, which applies PSO to enhance exploration capacity. The outcomes indicate that HJSPSO enhances the exploration and exploitation abilities, outperforming other metaheuristic optimization approaches. Another combination is a hybrid of the JSO and

PSO (HJPSO) [102], which aims to enhance the training of the SVM classifier for stock market trend prediction. The HJPSO integrates the global search ability of the PSO and the local search ability of JSO, thereby discovering the optimal parameters for SVM and enhancing classification accuracy. In addition, this algorithm strikes a balance between exploration and exploitation. A hybrid Beluga Whale Optimization based on the jellyfish search optimizer (HBWO-JS) [103] is proposed to solve engineering optimization problems. The movement and hunting strategy of the BWO is incorporated to enhance exploration, and the ocean current of the JSO is utilized to improve exploitation. The results display that the HBWO-JS can handle nonlinear, constrained engineering problems.

Although many significant improvements have been achieved in recent years, the JSO still requires further advancement to handle complex optimization problems, which is the motivation of this study.

3. Problem Definition

In this section, the canonical JSO and its strategies are explained. Additionally, the concepts of a conscious neighborhood and the wandering search strategy are clarified.

3.1. Jellyfish Search Optimizer

The diverse feeding behavior of the ocean and the habitats of jellyfishes inspire the Jellyfish Search Optimizer (JSO) [15]. These creatures can conduct themselves by utilizing their unique features. Under favorable conditions, jellyfishes can form large groups known as blooms. Within this bloom, jellyfishes exhibit two types of movements: passive (type A) and active (type B) [104,105]. The JSO algorithm mimics these behaviors in two phases: exploration and exploitation. During the exploration phase, jellyfishes search for planktonic food by detecting ocean currents. Conversely, during the exploitation phase, they employ both passive and active movements within the swarm to optimize their feeding strategy. Additionally, a time control mechanism is employed to switch between these two phases. Therefore, the JSO algorithm consists of three parts, which are described below.

Ocean Current: The jellyfishes are attracted to many nutrients in the ocean current. The direction of the ocean current (trend) is determined by Equation (1).

$$trend = X^* - 3 \times rand(0,\ 1) \times \mu \tag{1}$$

where X^* and μ indicate the location of the current best jellyfish in the swarm and the mean of all jellyfish's locations. Each jellyfish moves to a new location according to Equation (2).

$$X_i(t+1) = X_i(t) + rand(0,\ 1) \times trend \tag{2}$$

where $X_i(t)$ is the location of jellyfish i at time t.

Jellyfish Swarm: Jellyfishes in the swarm move around their location (passive motion) or another (active motion). In the early stages of a swarm's formation, the majority of jellyfishes primarily demonstrate passive movement, known as type A motion. As the swarm matures, there is a gradual shift towards more active movement, referred to as type B motion, among the jellyfishes. The new location of each jellyfish with type A motion is calculated by Equation (3) to find a better location.

$$X_i(t+1) = X_i(t) + \gamma \times rand(0,\ 1) \times (U_b - L_b) \tag{3}$$

U_b and L_b are the upper and lower bounds of the search space, respectively. The motion coefficient γ is considered 0.1, which is the motion length of the jellyfish's locations. In type B motion, to determine the direction, a random location of the jellyfish j is selected

and compared with the current location of the jellyfish *i*. If the food quality is superior at the location of jellyfish *j*, then jellyfish *i* will advance towards jellyfish *j*; conversely, if the food quality is lacking, jellyfish *i* will retreat from jellyfish *j*'s location. Equations (4)–(7) show the updated location of a jellyfish.

$$\text{Step is simulated as rand } (0, 1) \times \text{Direction} \tag{4}$$

$$Direction = \begin{cases} X_j(t) - X_i(t) & if\ f(X_i) \geq f(X_j) \\ X_i(t) - X_j(t) & if\ f(X_i) < f(X_j) \end{cases} \tag{5}$$

$$Step = X_i(t+1) - X_i(t) \tag{6}$$

$$X_i(t+1) = X_i(t) + Step \tag{7}$$

Time Control Mechanism: There are large amounts of nutrients in the ocean currents, which attract the jellyfishes. A swarm is created when more jellyfishes collect in the ocean current. The ocean current is changed by temperature or wind, then the jellyfishes in the swarm move into another ocean current and form another jellyfish swarm. Jellyfishes inside a swarm display type A and type B motion by switching between them. Initially, type A is favored; type B is selected over time. A time control mechanism is designed for modeling this situation. This mechanism applies a time control function $c(t)$ and a threshold constant C_0. The time control function shown in Equation (8) generates a value that varies randomly between 0 and 1 over time. C_0 is set to 0.5; if $c(t)$ exceeds C_0, jellyfishes follow the ocean current, and when its value is less than C_0, jellyfishes move into the swarm.

$$c(t) = \left| \left(1 - \frac{t}{Max_{iter}}\right) \times (2 \times rand(0,\ 1) - 1) \right| \tag{8}$$

where t and Max_{iter} are the current iteration and the maximum number of iterations, respectively. Function $1 - c(t)$ is applied to simulate the movement of jellyfishes in a swarm (type A or B). If rand (0, 1) exceeds function $1 - c(t)$, a jellyfish displays type A motion, and if rand (0, 1) is lower than $1 - c(t)$, it displays type B motion. The flowchart of the JSO algorithm is shown in Figure 1.

3.2. Conscious Neighborhood Concept

The neighborhood concept in the CCSA algorithm was introduced by Zamani et al. [45] to facilitate understanding of the search space and deliberate selection of movement strategies for solving global optimization problems. The CCSA comprises two strategies: Neighborhood-based Local Search (NLS) and Non-neighborhood-based Global Search (NGS), which utilize the neighborhood concept to enhance both local search and global search. During the initialization phase, a finite set of N crows (or individuals) is distributed uniformly at random across the search space. The crow c_i in iteration t is shown by Equation (9), where X_i (t) and f_i (t) indicate the position and the fitness of crow c_i, respectively. $m_i(t)$ and $fbest_i$ show the position and best fitness of c_i until the iteration t.

$$c_i(t) = \{X_i(t), f_i(t), m_i(t), fbest_i(t)\} \tag{9}$$

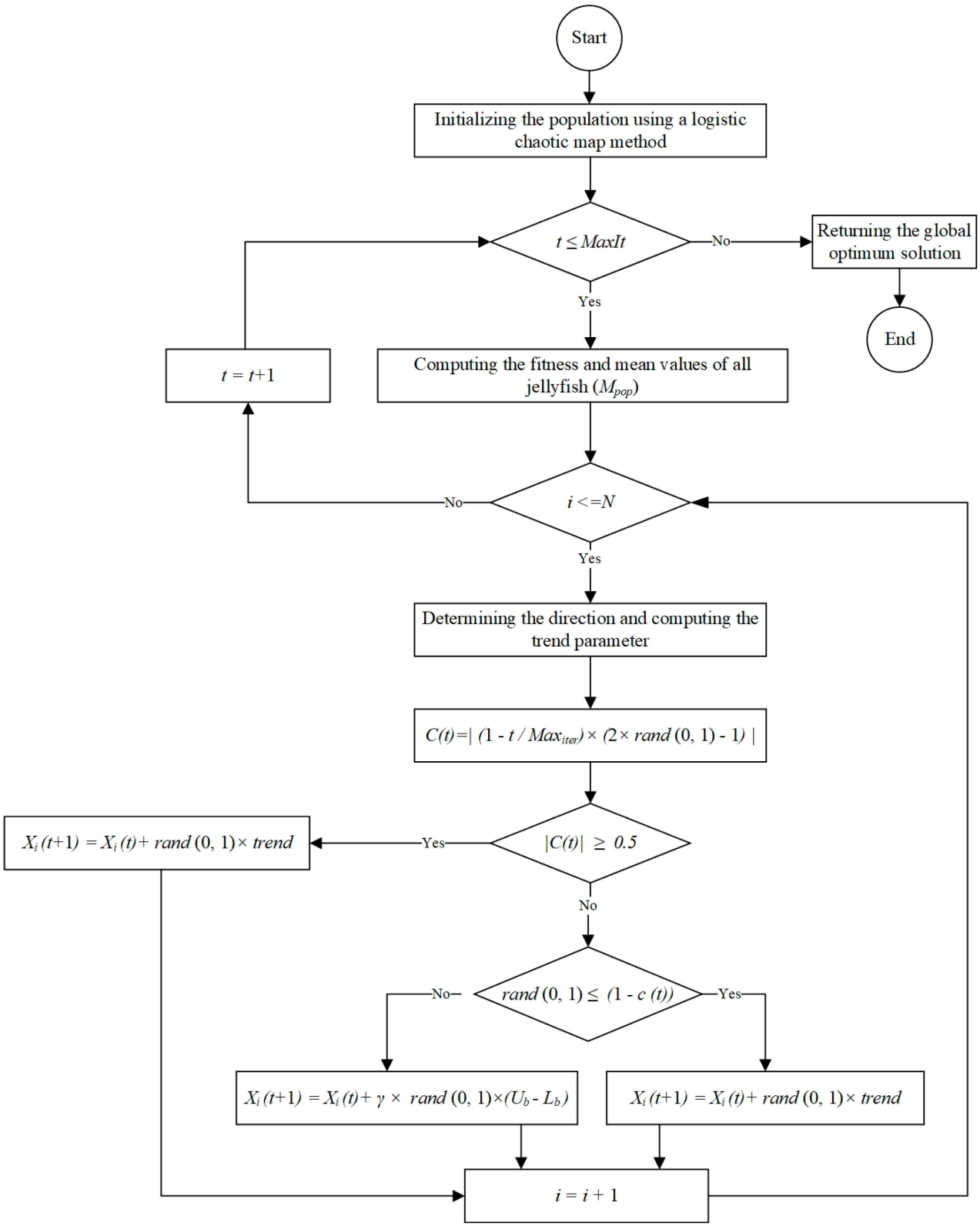


Figure 1. The flowchart of the JSO algorithm.

A conscious neighborhood and non-neighborhood of c_i are obtained by Equations (10) and (11), which are used to determine the movement strategy between NLS or NGS con-

sciously, and enhance balance in the global search and local search capabilities of the algorithm. In addition, two variables, w_{ij} and μ, are calculated using Equations (12) and (13).

$$N(c_i) = \{c_j \mid d(X_i, m_i) \times w_{ij} < \mu \ \ for\ j = 1, \ldots, N\ and\ i \neq j\} \tag{10}$$

$$Non - N(c_i) = \{c_j \mid d(X_i, m_i) \times w_{ij} > \mu \ \ for\ j = 1, \ldots, N\ and\ i \neq j\} \tag{11}$$

$$w_{ij} = \frac{\varepsilon + \left(f_i - fbest_j\right)}{\sum_{k=1}^{N}(f_i - fbest_k)} \tag{12}$$

$$\mu = \frac{1}{N}\sum_{j=1}^{N}\left(d\left(X_i, m_j\right) \times w_{ij}\right) \tag{13}$$

where $d\ (X_i, m_j)$ shows the Euclidean distance between crows c_i and the hiding place of crow c_j. A random crow and the best crow from the neighbor and non-neighbor vicinity of crow c_i are selected, named c_{local} and c_{global}, respectively. If the fitness value of c_{local} is less than the fitness value of c_{global}, the NLS strategy is adopted for the subsequent movement; otherwise, the NGS strategy is selected.

3.3. Wandering Around Search (WAS) Strategy

The WAS strategy analyzes the crows' surrounding environment and changes their position through several jumps. The reason is to recalibrate the positions of crows that have not achieved better fitness values through the NLS or NGS strategies. WAS provides an additional chance for inferior individuals to improve their fitness value. Thus, inferior individuals explore the search space by accomplishing a random number of jumps (NJ), where k dimensions are randomly picked and their values are altered. The WAS strategy is defined in Equation (14).

$$X_{ij}(t+1) = m_{gbest\ j}(t) + r_i \times fl_i(t) \times \left(X_{rj}(t) - X_{ij}(t)\right) \tag{14}$$

where $m_{gbest\ j}$ and $X_{rj}(t)$ denote the value of dimension j for the best hiding place and a randomly chosen crow, respectively. r_i is a uniformly distributed random number in the interval [0, 1], and $fl_i(t)$ is the flight length of the crow c_i at iteration t, which is a linearly decreasing variable and is calculated by Equation (15).

$$fl(j) = 2.02 - \frac{1.08}{NJ} \times j \tag{15}$$

where the number of jumps (NJ) is randomly selected between 1 and 50, and j is from 1 to NJ.

4. Proposed Algorithm

This section describes the proposed Conscious Neighborhood-based JSO (CNJSO) algorithm. To tackle the JSO algorithm's weaknesses, CNJSO introduces a new movement strategy named Best archive and Non-neighborhood-based Global Search, or BNGS, to enhance the exploration. It also adapts and utilizes the concept of conscious neighborhood to select between exploration and exploitation. Moreover, CNJSO employs the Wandering Around Search (WAS) strategy introduced by the CCSA algorithm [45] to improve inferior individuals. The following subsections will provide detailed explanations of how the CNJSO algorithm utilizes the introduced BNGS strategy and the WAS strategy.

4.1. Exploration Improvement Using the Introduced BNGS Strategy

Since the JSO suffers from low exploration and inconsistency between exploration and exploitation, this study introduces a new search strategy called the Best archive and

Non-neighborhood-based Global Search (BNGS) strategy. In addition, the conscious neighborhood concept is employed to determine the movement strategy between the ocean's current and the jellyfish swarm, making a good trade-off between global and local search. To consciously select the movement strategy, the neighbors and non-neighbors of each individual are determined by Equations (10) and (11). Then, an individual is randomly selected from the neighborhood set (local), and an individual with the best fitness value of the non-neighborhood set (global) is picked for individual i, denoted by X_{local} and X_{global}, respectively. If the fitness value of X_{local} (f_{local}) is better than the fitness value of X_{global} (f_{global}), individual i moves within the jellyfish swarm; otherwise, it moves along the ocean's current using the new BNGS search strategy to enhance the exploration of CNJSO. Moreover, the best archive is utilized to maintain the best individual generated in each iteration. The size of the archive is equal to the population size, and when it is full, some previous individuals are randomly removed from it. The introduced BNGS strategy generates new positions according to Equation (16).

$$X_i(t+1) = X_{archive}(t) + c(t) \times \left(X_i(t) - X_{global}(t) \right) \tag{16}$$

where $X_{archive}$ indicates a randomly selected jellyfish from the archive, and X_{global} is a random non-neighbor of individual i. The coefficient $c(t)$ is a time-control parameter calculated by Equation (8).

4.2. Improving Inferior Jellyfishes Using Wandering Around Search (WAS) Strategy

This study employs the Wandering Around Search (WAS) strategy to improve inferior jellyfishes. Accordingly, individual behaviors are examined, and if their current positions are unsatisfactory, they are consistently relocated to more favorable positions. Thus, the objective of WAS is to realign the positions of individuals who have not achieved a good fitness value. As a result, if the new fitness value of individual i is not better than its previous fitness value, individual i moves to another position using a random number of jumps (NJ), where k dimensions are randomly selected for each jump and their values are modified using Equation (17).

$$X_{ij}(t+1) = m_{gbest\ j}(t) + r_i \times f_{l_i}(t) \times \left(X_{rj}(t) - X_{ij}(t) \right) \tag{17}$$

where X_{ij} $(t + 1)$ represents the value of dimension j in the new position of individual i. $m_{gbest\ j}(t)$ and X_{rj} (t) denote the value of dimension j for the best and a randomly selected individual, respectively. fl_i (t) is a linearly decreasing variable, and r_i is a random number uniformly distributed in the interval [0, 1].

Figure 2 illustrates the flowchart of the proposed CNJSO algorithm, highlighting the new components indicated by the grey boxes.

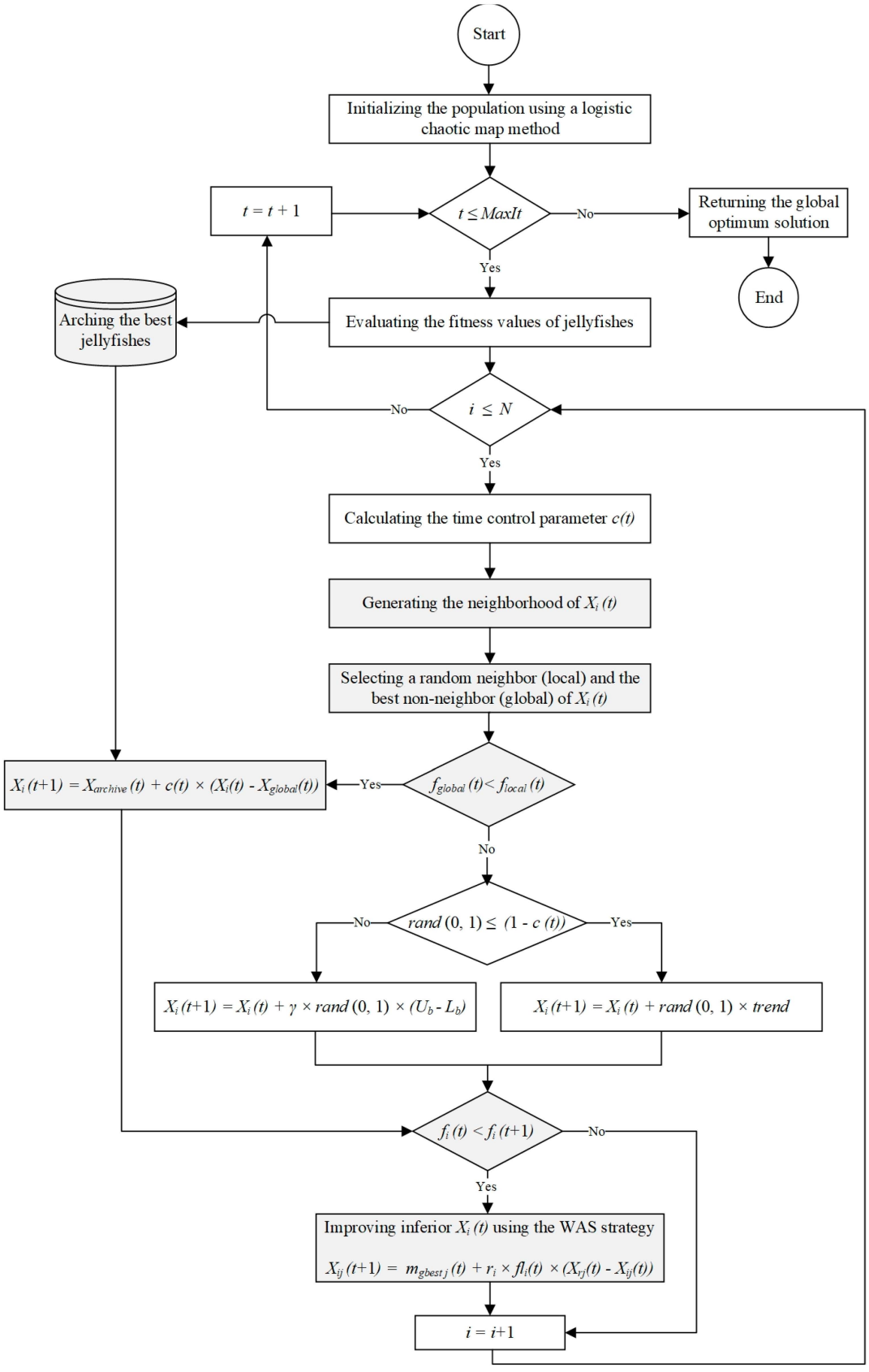


Figure 2. The flowchart of the proposed CNJSO algorithm.

5. Experimental Evaluation and Results

In this study, the performance of CNJSO is assessed on the CEC 2018 benchmark function [50], with dimensions of 30, 50, and 100. Then, results were compared with several of the state-of-the-art swarm intelligence algorithms—PSO, KH, GWO, WOA, EEGWO, HGSO, JSO, TSA, MTBO, and FOA—and the convergence behavior of these algorithms was demonstrated. In addition, the overall performance of CNJSO and comparative algorithms was statistically examined using the Wilcoxon rank-sum and Friedman tests.

5.1. Benchmark Functions

The CEC 2018 benchmark functions, where the complexity levels progressively increase with increasing dimensionality, were used in this study. This benchmark set incorporates 29 optimization problems of various types: unimodal (F1 and F3), multimodal (F4–F10), hybrid (F11–F20), and composite (F21–F30). Because the unimodal functions have a single global optimum, they are appropriate for assessing exploitation ability. As opposed to unimodal functions, multimodal functions have numerous local optima, making them appropriate for evaluating exploration abilities. The capability to strike a balance between exploration and exploitation can be evaluated concurrently using the hybrid and composite functions.

5.2. Experimental Setup

Due to the stochastic nature of swarm intelligence algorithms, their evaluation should be conducted in an impartial setting [5], and all tests should be carefully carried out under fair conditions [106]. Therefore, CNJSO and comparative algorithms were implemented using MATLAB 2018a, and experiments were conducted on an Intel Core i7-6500U CPU (2.50 GHz) with 8 GB main memory.

To ensure fair comparisons and consistent programming approaches across all tests [50], all experiments are run 20 times, while the maximum number of iterations and the population size are set to $10^4 \times$ dimension and 100, respectively. The mean error, standard deviation, and minimum (min) of the global best solution found after 20 runs are compared to assess how well an algorithm performs. Table 1 displays the parameters of the comparative algorithms.

Table 1. Parameter settings.

Algorithms	Settings
PSO [12]	$c_1 = c_2 = 2$
KH [4]	$V_f = 0.02$, $D_{max} = 0.005$, $N_{max} = 0.01$, $Sr = 0$
GWO [14]	a = [2 to 0]
WOA [46]	a =2, $b = 1$
EEGWO [47]	$b_1 = 0.1$, $b_2 = 0.9$, $mo = 1.5$, $a_{initial} = 2$, $a_{final} = 0$
HGSO [48]	$l_1 = 5 \times 10^{-3}$, $l_2 = 100$, $l_3 = 1 \times 10^{-2}$, $alpha = 1$, $beta = 1$, $M_1 = 0.1$, $M_2 = 0.2$
JSO [15]	$C_0 = 0.5$
TSA [16]	$P_{min} = 1$, $P_{max} = 4$
MTBO [49]	$Li \sim U$ [0.25, 0.50], $Ai \sim U$ [0.75, 1.00], $Mi \sim U$ [0.75, 1.00]
FOA [17]	$alpha = 2$, $beta = 1.5$, $gamma = 0.5$, $ground = 0.3$, $tree = 0.4$, $ambush = 0.3$
CNJSO	$C_0 = 0.5$

5.3. Performance Evaluation

Different functions of the CEC 2018 benchmark are employed to evaluate the performance of CNJSO and compare it with several comparative algorithms in terms of exploration, exploitation, and ability to escape from local optima. This subsection reports the numerical results in Tables 2–5, in which the bold letters show the best results. In the last rows of these tables, the number of wins (W), ties (T), and losses (L) is provided.

Table 2. Comparison of the obtained results from unimodal test functions.

F	D	Index	PSO 1997	KH 2012	GWO 2014	WOA 2016	EEGWO 2018	HGSO 2019	JSO 2020	TSA 2020	MTBO 2023	FOA 2024	CNJSO
F1	30	Min	2.54×10^{8}	8.27×10^{2}	1.68×10^{7}	7.79×10^{5}	5.20×10^{10}	3.64×10^{8}	6.19×10^{1}	7.49×10^{9}	5.68×10^{1}	4.97×10^{-1}	1.00×10^{2}
		Mean	1.54×10^{10}	1.59×10^{4}	8.49×10^{8}	3.26×10^{6}	5.97×10^{10}	1.52×10^{10}	1.69×10^{3}	1.57×10^{10}	3.66×10^{3}	6.36×10^{3}	4.97×10^{-15}
		SD	2.14×10^{8}	1.31×10^{3}	2.84×10^{7}	2.38×10^{6}	4.57×10^{9}	3.77×10^{8}	1.65×10^{3}	6.66×10^{9}	4.44×10^{3}	5.91×10^{3}	8.63×10^{-15}
	50	Min	1.94×10^{8}	1.55×10^{3}	3.41×10^{7}	2.53×10^{6}	1.05×10^{11}	3.83×10^{8}	4.99×10^{-1}	2.45×10^{10}	5.27×10^{1}	2.46×10^{2}	1.00×10^{2}
		Mean	3.78×10^{10}	2.31×10^{5}	4.06×10^{9}	9.72×10^{6}	1.16×10^{11}	3.95×10^{10}	1.23×10^{3}	4.06×10^{10}	3.11×10^{3}	8.91×10^{3}	2.42×10^{-14}
		SD	1.54×10^{8}	2.04×10^{3}	4.57×10^{7}	1.16×10^{7}	4.56×10^{9}	3.96×10^{8}	1.69×10^{3}	9.82×10^{9}	3.41×10^{3}	8.13×10^{3}	1.53×10^{-14}
	100	Min	1.13×10^{11}	2.18×10^{6}	2.23×10^{10}	1.77×10^{7}	2.58×10^{11}	1.28×10^{11}	4.88×10^{2}	7.85×10^{10}	9.15×10^{1}	1.24×10^{2}	1.00×10^{2}
		Mean	1.29×10^{11}	1.11×10^{8}	3.27×10^{10}	3.03×10^{7}	2.70×10^{11}	1.60×10^{11}	5.67×10^{3}	1.09×10^{11}	1.63×10^{4}	7.77×10^{4}	2.44×10^{-12}
		SD	8.14×10^{9}	2.59×10^{8}	6.88×10^{9}	8.33×10^{6}	6.94×10^{9}	1.65×10^{10}	3.76×10^{3}	1.54×10^{10}	2.71×10^{4}	1.42×10^{5}	8.57×10^{-12}
F3	30	Min	7.40×10^{7}	3.01×10^{3}	6.87×10^{7}	4.94×10^{4}	7.58×10^{4}	4.22×10^{8}	2.26×10^{3}	2.55×10^{4}	6.31×10^{1}	2.66×10^{2}	3.00×10^{2}
		Mean	4.91×10^{4}	4.53×10^{4}	2.83×10^{4}	1.67×10^{5}	8.88×10^{4}	3.84×10^{4}	4.19×10^{3}	4.42×10^{4}	1.65×10^{3}	5.46×10^{3}	1.99×10^{-14}
		SD	3.41×10^{7}	3.49×10^{3}	8.03×10^{7}	7.80×10^{4}	4.85×10^{3}	4.34×10^{8}	9.34×10^{2}	1.26×10^{4}	1.14×10^{3}	3.00×10^{3}	3.45×10^{-14}
	50	Min	1.41×10^{7}	3.74×10^{3}	8.60×10^{7}	4.40×10^{4}	2.15×10^{5}	4.41×10^{8}	2.08×10^{4}	3.74×10^{4}	7.28×10^{3}	1.55×10^{4}	3.00×10^{2}
		Mean	1.07×10^{5}	1.15×10^{5}	6.57×10^{4}	7.50×10^{4}	1.41×10^{6}	1.39×10^{5}	2.94×10^{4}	8.54×10^{4}	1.89×10^{4}	4.24×10^{4}	5.68×10^{-14}
		SD	$^{-}2.8 \times 10^{7}$	4.22×10^{3}	9.76×10^{7}	2.97×10^{4}	3.19×10^{6}	4.53×10^{8}	5.12×10^{3}	2.06×10^{4}	8.13×10^{3}	1.42×10^{4}	0
	100	Min	3.09×10^{5}	2.53×10^{5}	1.60×10^{5}	3.84×10^{5}	3.19×10^{5}	2.50×10^{5}	1.33×10^{5}	1.51×10^{5}	9.62×10^{4}	1.92×10^{5}	3.00×10^{2}
		Mean	3.75×10^{5}	3.58×10^{5}	1.98×10^{5}	6.03×10^{5}	7.39×10^{6}	2.92×10^{5}	1.61×10^{5}	1.94×10^{5}	1.57×10^{5}	2.39×10^{5}	1.65×10^{-13}
		SD	3.23×10^{4}	5.71×10^{4}	2.28×10^{4}	1.74×10^{5}	2.25×10^{7}	2.07×10^{4}	1.04×10^{4}	2.74×10^{4}	3.68×10^{4}	2.45×10^{4}	5.83×10^{-14}
Rank	30	W/T/L	0/0/2	0/0/2	0/0/2	0/0/2	0/0/2	0/0/2	0/0/2	0/0/2	0/0/2	0/0/2	**2/0/0**
	50	W/T/L	0/0/2	0/0/2	0/0/2	0/0/2	0/0/2	0/0/2	0/0/2	0/0/2	0/0/2	0/0/2	**2/0/0**
	100	W/T/L	0/0/2	0/0/2	0/0/2	0/0/2	0/0/2	0/0/2	0/0/2	0/0/2	0/0/2	0/0/2	**2/0/0**

Table 3. Comparison of the obtained results from multimodal test functions.

F	D	Index	PSO 1997	KH 2012	GWO 2014	WOA 2016	EEGWO 2018	HGSO 2019	JSO 2020	TSA 2020	MTBO 2023	FOA 2024	CNJSO
F4	30	Min	5.32×10^{2}	6.83×10^{1}	9.37×10^{1}	7.85×10^{1}	1.27×10^{4}	1.06×10^{3}	6.78×10^{1}	2.95×10^{2}	4.06×10^{0}	4.26×10^{-3}	4.00×10^{2}
		Mean	9.08×10^{2}	9.87×10^{1}	1.45×10^{2}	1.59×10^{2}	1.86×10^{4}	1.63×10^{3}	9.66×10^{1}	2.32×10^{3}	6.43×10^{1}	4.78×10^{1}	7.53×10^{0}
		SD	1.57×10^{2}	2.03×10^{1}	3.13×10^{1}	4.22×10^{1}	2.81×10^{3}	4.48×10^{2}	2.05×10^{1}	1.89×10^{3}	2.94×10^{1}	3.92×10^{1}	1.85×10^{1}
	50	Min	2.28×10^{3}	7.32×10^{1}	2.08×10^{2}	2.10×10^{2}	3.12×10^{4}	4.51×10^{3}	7.48×10^{1}	2.44×10^{3}	6.30×10^{-2}	2.85×10^{1}	4.00×10^{2}
		Mean	3.38×10^{3}	1.54×10^{2}	4.12×10^{2}	2.81×10^{2}	3.95×10^{4}	7.71×10^{3}	1.41×10^{2}	6.87×10^{3}	9.44×10^{1}	7.22×10^{1}	2.93×10^{1}
		SD	4.21×10^{2}	5.06×10^{1}	1.67×10^{2}	5.53×10^{1}	2.71×10^{3}	1.78×10^{3}	3.94×10^{1}	2.77×10^{3}	4.87×10^{1}	5.27×10^{1}	4.51×10^{1}
	100	Min	1.20×10^{4}	2.20×10^{2}	1.82×10^{3}	3.81×10^{2}	9.01×10^{4}	1.97×10^{4}	2.65×10^{2}	8.60×10^{3}	1.95×10^{2}	1.59×10^{2}	4.00×10^{2}
		Mean	1.39×10^{4}	3.56×10^{2}	2.60×10^{3}	5.35×10^{2}	1.12×10^{5}	2.91×10^{4}	3.19×10^{2}	1.59×10^{4}	2.85×10^{2}	2.28×10^{2}	1.40×10^{0}
		SD	1.05×10^{3}	5.31×10^{1}	5.09×10^{2}	7.35×10^{1}	1.03×10^{4}	5.63×10^{3}	3.84×10^{1}	4.83×10^{3}	5.62×10^{1}	3.65×10^{1}	1.95×10^{0}
F5	30	Min	2.07×10^{2}	9.06×10^{1}	4.71×10^{1}	1.79×10^{2}	4.39×10^{2}	2.56×10^{2}	7.56×10^{1}	1.83×10^{2}	6.47×10^{1}	6.77×10^{1}	5.30×10^{2}
		Mean	2.54×10^{2}	1.37×10^{2}	9.17×10^{1}	2.64×10^{2}	4.68×10^{2}	3.06×10^{2}	1.07×10^{2}	2.95×10^{2}	1.06×10^{2}	1.18×10^{2}	5.80×10^{1}
		SD	2.00×10^{1}	3.14×10^{1}	3.30×10^{1}	5.46×10^{1}	1.73×10^{1}	1.71×10^{1}	1.78×10^{1}	4.84×10^{1}	2.22×10^{1}	3.35×10^{1}	1.34×10^{1}
	50	Min	4.97×10^{2}	2.09×10^{2}	1.21×10^{2}	2.73×10^{2}	6.70×10^{2}	4.80×10^{2}	2.11×10^{2}	4.62×10^{2}	1.73×10^{2}	1.51×10^{2}	5.76×10^{2}
		Mean	5.31×10^{2}	2.56×10^{2}	1.82×10^{2}	4.06×10^{2}	7.45×10^{2}	5.45×10^{2}	2.82×10^{2}	5.93×10^{2}	2.36×10^{2}	2.45×10^{2}	1.29×10^{2}
		SD	1.76×10^{1}	3.11×10^{1}	3.73×10^{1}	7.60×10^{1}	2.63×10^{1}	2.80×10^{1}	4.41×10^{1}	6.85×10^{1}	4.18×10^{1}	4.75×10^{1}	3.57×10^{1}
	100	Min	1.17×10^{3}	6.21×10^{2}	3.73×10^{2}	7.81×10^{2}	1.64×10^{3}	1.22×10^{3}	6.63×10^{2}	1.24×10^{3}	5.84×10^{2}	4.64×10^{2}	7.90×10^{2}
		Mean	1.23×10^{3}	7.34×10^{2}	5.68×10^{2}	9.42×10^{2}	1.69×10^{3}	1.31×10^{3}	7.52×10^{2}	1.49×10^{3}	6.64×10^{2}	6.05×10^{2}	3.57×10^{2}
		SD	2.40×10^{1}	8.43×10^{1}	1.49×10^{2}	8.89×10^{1}	1.77×10^{1}	4.21×10^{1}	6.11×10^{1}	1.35×10^{2}	5.12×10^{1}	8.89×10^{1}	5.64×10^{1}
F6	30	Min	3.53×10^{1}	1.95×10^{1}	1.14×10^{0}	5.02×10^{1}	9.61×10^{1}	4.73×10^{1}	4.13×10^{-1}	2.58×10^{1}	4.94×10^{0}	8.82×10^{0}	6.00×10^{2}
		Mean	4.09×10^{1}	3.55×10^{1}	4.10×10^{0}	6.65×10^{1}	1.04×10^{2}	6.48×10^{1}	2.30×10^{0}	6.39×10^{1}	1.45×10^{1}	1.99×10^{1}	1.14×10^{-13}
		SD	2.80×10^{0}	9.06×10^{0}	1.86×10^{0}	8.97×10^{0}	5.08×10^{0}	6.35×10^{0}	1.84×10^{0}	1.58×10^{1}	6.16×10^{0}	7.66×10^{0}	0
	50	Min	4.33×10^{1}	3.74×10^{1}	5.50×10^{0}	6.58×10^{1}	1.06×10^{2}	7.14×10^{1}	6.64×10^{0}	6.62×10^{1}	1.80×10^{1}	2.70×10^{1}	6.00×10^{2}
		Mean	5.31×10^{1}	5.13×10^{1}	1.05×10^{1}	7.68×10^{1}	1.15×10^{2}	8.24×10^{1}	1.35×10^{1}	8.99×10^{1}	2.90×10^{1}	3.66×10^{1}	9.66×10^{-14}
		SD	3.67×10^{0}	6.46×10^{0}	3.91×10^{0}	9.80×10^{0}	3.06×10^{0}	4.74×10^{0}	6.19×10^{0}	1.49×10^{1}	6.82×10^{0}	7.33×10^{0}	1.08×10^{-13}
	100	Min	6.41×10^{1}	5.14×10^{1}	1.93×10^{1}	7.06×10^{1}	1.14×10^{2}	8.68×10^{1}	2.66×10^{1}	8.40×10^{1}	3.83×10^{1}	3.71×10^{1}	6.00×10^{2}
		Mean	7.19×10^{1}	5.66×10^{1}	2.72×10^{1}	8.04×10^{1}	1.19×10^{2}	9.46×10^{1}	3.84×10^{1}	1.06×10^{2}	4.82×10^{1}	4.89×10^{1}	1.59×10^{-13}
		SD	4.36×10^{0}	3.79×10^{0}	4.54×10^{0}	8.76×10^{0}	2.11×10^{0}	3.86×10^{0}	5.44×10^{0}	1.27×10^{1}	5.18×10^{0}	7.45×10^{0}	1.04×10^{-13}
F7	30	Min	6.21×10^{2}	8.34×10^{1}	7.15×10^{1}	3.37×10^{2}	6.80×10^{2}	3.24×10^{2}	8.09×10^{1}	3.40×10^{2}	8.87×10^{1}	1.05×10^{2}	7.53×10^{2}
		Mean	8.27×10^{2}	1.33×10^{2}	1.26×10^{2}	4.90×10^{2}	7.60×10^{2}	4.01×10^{2}	1.26×10^{2}	4.91×10^{2}	1.59×10^{2}	1.82×10^{2}	8.22×10^{1}
		SD	9.68×10^{1}	2.64×10^{1}	3.14×10^{1}	1.04×10^{2}	4.01×10^{1}	3.32×10^{1}	1.82×10^{1}	8.58×10^{1}	5.81×10^{1}	5.48×10^{1}	1.63×10^{1}
	50	Min	1.61×10^{3}	2.74×10^{2}	2.07×10^{2}	7.66×10^{2}	1.28×10^{3}	7.17×10^{2}	1.76×10^{2}	8.59×10^{2}	2.37×10^{2}	2.94×10^{2}	8.26×10^{2}
		Mean	2.01×10^{3}	3.62×10^{2}	3.35×10^{2}	9.95×10^{2}	1.38×10^{3}	8.29×10^{2}	3.32×10^{2}	9.97×10^{2}	3.62×10^{2}	4.45×10^{2}	1.80×10^{2}
		SD	2.50×10^{2}	5.66×10^{1}	8.59×10^{1}	7.36×10^{1}	4.11×10^{1}	6.43×10^{1}	8.16×10^{1}	9.29×10^{1}	7.01×10^{1}	1.05×10^{2}	3.86×10^{1}
	100	Min	4.46×10^{3}	1.16×10^{3}	8.50×10^{2}	2.38×10^{3}	3.27×10^{3}	2.03×10^{3}	7.04×10^{2}	2.33×10^{3}	1.01×10^{3}	1.41×10^{3}	1.10×10^{3}
		Mean	5.68×10^{3}	1.43×10^{3}	1.02×10^{3}	2.56×10^{3}	3.38×10^{3}	2.45×10^{3}	1.21×10^{3}	2.62×10^{3}	1.40×10^{3}	1.84×10^{3}	5.54×10^{2}
		SD	6.91×10^{2}	1.69×10^{2}	1.11×10^{2}	1.04×10^{2}	4.25×10^{1}	1.61×10^{2}	2.24×10^{2}	1.82×10^{2}	2.65×10^{2}	2.38×10^{2}	1.33×10^{2}
F8	30	Min	2.36×10^{2}	7.36×10^{1}	5.75×10^{1}	1.28×10^{2}	3.22×10^{2}	2.27×10^{2}	6.77×10^{1}	2.04×10^{2}	6.07×10^{1}	5.07×10^{1}	8.34×10^{2}
		Mean	2.65×10^{2}	1.09×10^{2}	7.64×10^{1}	2.08×10^{2}	3.79×10^{2}	2.53×10^{2}	9.49×10^{1}	2.73×10^{2}	8.46×10^{1}	1.02×10^{2}	5.37×10^{1}
		SD	1.30×10^{1}	1.69×10^{1}	1.46×10^{1}	4.75×10^{1}	1.83×10^{1}	1.36×10^{1}	1.66×10^{1}	5.52×10^{1}	2.34×10^{1}	3.53×10^{1}	1.46×10^{1}
	50	Min	4.98×10^{2}	2.09×10^{2}	1.36×10^{2}	2.93×10^{2}	7.05×10^{2}	5.03×10^{2}	1.80×10^{2}	4.48×10^{2}	1.68×10^{2}	1.26×10^{2}	8.82×10^{2}
		Mean	5.25×10^{2}	2.84×10^{2}	1.96×10^{2}	4.15×10^{2}	7.69×10^{2}	5.71×10^{2}	2.45×10^{2}	5.84×10^{2}	2.23×10^{2}	2.40×10^{2}	1.25×10^{2}
		SD	1.81×10^{1}	4.77×10^{1}	3.16×10^{1}	7.35×10^{1}	2.16×10^{1}	2.75×10^{1}	3.82×10^{1}	8.61×10^{1}	2.85×10^{1}	6.73×10^{1}	2.45×10^{1}
	100	Min	1.11×10^{3}	6.85×10^{2}	4.84×10^{2}	8.76×10^{2}	1.81×10^{3}	1.30×10^{3}	5.74×10^{2}	1.34×10^{3}	6.00×10^{2}	5.24×10^{2}	1.03×10^{3}
		Mean	1.22×10^{3}	7.85×10^{2}	5.49×10^{2}	1.06×10^{3}	1.87×10^{3}	1.43×10^{3}	7.54×10^{2}	1.55×10^{3}	7.19×10^{2}	6.49×10^{2}	3.60×10^{2}
		SD	4.72×10^{1}	5.99×10^{1}	4.79×10^{1}	1.16×10^{2}	2.45×10^{1}	7.01×10^{1}	1.37×10^{2}	1.19×10^{2}	7.51×10^{1}	8.74×10^{1}	7.74×10^{1}
F9	30	Min	4.31×10^{3}	9.31×10^{2}	9.54×10^{1}	2.61×10^{3}	1.08×10^{4}	3.17×10^{3}	8.91×10^{0}	3.77×10^{3}	7.62×10^{1}	3.27×10^{2}	9.01×10^{2}
		Mean	5.09×10^{3}	2.31×10^{3}	5.41×10^{2}	5.93×10^{3}	1.27×10^{4}	4.98×10^{3}	1.26×10^{2}	8.95×10^{3}	3.08×10^{2}	1.27×10^{3}	9.24×10^{0}
		SD	5.20×10^{2}	6.62×10^{2}	4.41×10^{2}	1.99×10^{3}	1.04×10^{3}	9.90×10^{2}	1.55×10^{2}	2.76×10^{3}	2.42×10^{2}	6.25×10^{2}	1.22×10^{1}
	50	Min	1.15×10^{4}	7.64×10^{3}	1.51×10^{3}	1.12×10^{4}	3.75×10^{4}	2.05×10^{4}	2.92×10^{2}	2.02×10^{4}	1.18×10^{3}	2.18×10^{3}	9.10×10^{2}
		Mean	1.36×10^{4}	9.41×10^{3}	4.57×10^{3}	1.95×10^{4}	4.41×10^{4}	2.61×10^{4}	1.21×10^{3}	3.31×10^{4}	3.52×10^{3}	5.53×10^{3}	7.28×10^{1}
		SD	1.29×10^{3}	1.36×10^{3}	3.26×10^{3}	4.97×10^{3}	2.77×10^{3}	2.02×10^{3}	5.71×10^{2}	9.11×10^{3}	3.21×10^{3}	3.02×10^{3}	7.31×10^{1}
	100	Min	3.25×10^{4}	1.95×10^{4}	1.03×10^{4}	2.35×10^{4}	7.64×10^{4}	5.87×10^{4}	8.93×10^{3}	6.93×10^{4}	7.02×10^{3}	1.72×10^{4}	1.09×10^{3}
		Mean	4.27×10^{4}	2.19×10^{4}	2.26×10^{4}	3.76×10^{4}	8.81×10^{4}	6.45×10^{4}	2.67×10^{4}	8.96×10^{4}	2.97×10^{4}	3.12×10^{4}	9.57×10^{2}
		SD	5.17×10^{3}	1.59×10^{3}	8.71×10^{3}	1.31×10^{4}	4.09×10^{3}	3.26×10^{3}	9.08×10^{3}	1.65×10^{4}	1.15×10^{4}	6.88×10^{3}	5.29×10^{2}

Table 3. *Cont.*

F	D	Index	PSO 1997	KH 2012	GWO 2014	WOA 2016	EEGWO 2018	HGSO 2019	JSO 2020	TSA 2020	MTBO 2023	FOA 2024	CNJSO
F10	30	Min	6.54×10^{3}	3.37×10^{3}	1.86×10^{3}	3.83×10^{3}	7.17×10^{3}	5.10×10^{3}	2.55×10^{3}	4.51×10^{3}	1.79×10^{3}	3.04×10^{3}	1.94×10^{3}
		Mean	6.98×10^{3}	4.06×10^{3}	2.85×10^{3}	5.23×10^{3}	8.40×10^{3}	5.72×10^{3}	4.67×10^{3}	5.58×10^{3}	5.95×10^{3}	4.42×10^{3}	1.89×10^{3}
		SD	1.97×10^{2}	4.36×10^{2}	5.55×10^{2}	6.40×10^{2}	4.65×10^{2}	3.44×10^{2}	1.34×10^{3}	4.49×10^{2}	1.83×10^{3}	6.32×10^{2}	5.55×10^{2}
	50	Min	1.24×10^{4}	5.33×10^{3}	4.23×10^{3}	7.51×10^{3}	1.47×10^{4}	1.08×10^{4}	4.57×10^{3}	9.07×10^{3}	5.01×10^{3}	6.14×10^{3}	3.83×10^{3}
		Mean	1.34×10^{4}	6.65×10^{3}	5.63×10^{3}	9.07×10^{3}	1.54×10^{4}	1.17×10^{4}	5.87×10^{3}	1.07×10^{4}	1.01×10^{4}	8.72×10^{3}	3.96×10^{3}
		SD	5.11×10^{2}	8.55×10^{2}	6.94×10^{2}	1.30×10^{3}	3.69×10^{2}	6.84×10^{2}	1.27×10^{3}	8.93×10^{2}	3.75×10^{3}	9.64×10^{2}	6.36×10^{2}
	100	Min	2.95×10^{4}	1.27×10^{4}	1.16×10^{4}	1.52×10^{4}	3.01×10^{4}	2.27×10^{4}	1.17×10^{4}	2.24×10^{4}	1.15×10^{4}	1.58×10^{4}	9.83×10^{3}
		Mean	3.01×10^{4}	1.45×10^{4}	1.31×10^{4}	1.98×10^{4}	3.28×10^{4}	2.50×10^{4}	1.59×10^{4}	2.58×10^{4}	2.01×10^{4}	2.11×10^{4}	1.08×10^{4}
		SD	3.58×10^{2}	1.30×10^{3}	1.09×10^{3}	1.92×10^{3}	9.59×10^{2}	7.73×10^{2}	3.81×10^{3}	1.28×10^{3}	8.02×10^{3}	2.39×10^{3}	9.24×10^{2}
Rank	30	W/T/L	0/0/7	0/0/7	0/0/7	0/0/7	0/0/7	0/0/7	0/0/7	0/0/7	0/0/7	0/0/7	**7/0/0**
	50	W/T/L	0/0/7	0/0/7	0/0/7	0/0/7	0/0/7	0/0/7	0/0/7	0/0/7	0/0/7	0/0/7	**7/0/0**
	100	W/T/L	0/0/7	0/0/7	0/0/7	0/0/7	0/0/7	0/0/7	0/0/7	0/0/7	0/0/7	0/0/7	**7/0/0**

Table 4. Comparison of the obtained results from hybrid test functions.

F	D	Index	PSO 1997	KH 2012	GWO 2014	WOA 2016	EEGWO 2018	HGSO 2019	JSO 2020	TSA 2020	MTBO 2023	FOA 2024	CNJSO
F11	30	Min	1.25×10^{3}	1.56×10^{2}	1.48×10^{2}	1.96×10^{2}	4.30×10^{3}	5.80×10^{2}	3.29×10^{1}	3.17×10^{2}	5.00×10^{1}	2.59×10^{1}	1.13×10^{3}
		Mean	1.83×10^{3}	4.02×10^{2}	3.18×10^{2}	3.24×10^{2}	1.07×10^{4}	1.44×10^{3}	6.23×10^{1}	3.84×10^{3}	1.03×10^{2}	1.29×10^{2}	4.18×10^{1}
		SD	3.52×10^{2}	1.84×10^{2}	2.01×10^{2}	7.52×10^{1}	2.42×10^{3}	5.84×10^{2}	1.97×10^{1}	2.02×10^{3}	3.27×10^{1}	4.55×10^{1}	1.85×10^{1}
	50	Min	3.96×10^{3}	1.29×10^{3}	3.63×10^{2}	3.39×10^{2}	1.98×10^{4}	2.51×10^{3}	8.88×10^{1}	7.98×10^{3}	1.30×10^{2}	1.07×10^{2}	1.15×10^{3}
		Mean	5.23×10^{3}	3.56×10^{3}	1.23×10^{3}	5.00×10^{2}	2.44×10^{4}	4.89×10^{3}	1.32×10^{2}	1.20×10^{4}	1.71×10^{2}	1.95×10^{2}	8.65×10^{1}
		SD	8.86×10^{2}	1.69×10^{3}	9.45×10^{2}	1.02×10^{2}	1.80×10^{3}	1.25×10^{3}	2.42×10^{1}	2.24×10^{3}	4.08×10^{1}	4.39×10^{1}	2.19×10^{1}
	100	Min	3.72×10^{4}	4.80×10^{4}	1.46×10^{4}	4.36×10^{3}	2.39×10^{5}	1.13×10^{5}	5.71×10^{2}	3.67×10^{4}	9.46×10^{2}	7.75×10^{2}	1.20×10^{3}
		Mean	4.53×10^{4}	7.37×10^{4}	3.74×10^{4}	6.56×10^{3}	6.61×10^{6}	1.31×10^{5}	6.86×10^{2}	5.98×10^{4}	1.35×10^{3}	1.05×10^{3}	1.76×10^{2}
		SD	5.27×10^{3}	1.27×10^{4}	9.13×10^{3}	1.89×10^{3}	1.40×10^{7}	1.08×10^{4}	7.55×10^{1}	1.35×10^{4}	3.18×10^{2}	1.94×10^{2}	5.41×10^{1}
F12	30	Min	5.96×10^{8}	3.07×10^{5}	1.65×10^{6}	1.17×10^{7}	1.34×10^{10}	5.61×10^{8}	1.61×10^{4}	6.39×10^{7}	3.62×10^{4}	5.22×10^{4}	1.54×10^{3}
		Mean	1.16×10^{9}	2.83×10^{6}	3.15×10^{7}	4.29×10^{7}	1.66×10^{10}	1.27×10^{9}	4.02×10^{4}	2.81×10^{9}	1.89×10^{5}	2.46×10^{5}	8.86×10^{3}
		SD	2.59×10^{8}	1.77×10^{6}	2.85×10^{7}	2.94×10^{7}	1.53×10^{9}	5.32×10^{8}	1.75×10^{4}	2.62×10^{9}	2.25×10^{5}	1.79×10^{5}	7.68×10^{3}
	50	Min	6.17×10^{9}	1.93×10^{6}	2.91×10^{7}	3.88×10^{7}	7.33×10^{10}	8.50×10^{9}	1.20×10^{5}	3.75×10^{9}	1.61×10^{5}	7.36×10^{5}	2.57×10^{3}
		Mean	7.55×10^{9}	1.06×10^{7}	4.74×10^{8}	1.85×10^{8}	9.20×10^{10}	1.57×10^{10}	3.68×10^{5}	1.86×10^{10}	2.05×10^{6}	4.93×10^{6}	8.05×10^{3}
		SD	8.41×10^{8}	9.25×10^{6}	6.19×10^{8}	1.01×10^{8}	9.52×10^{9}	3.89×10^{9}	1.51×10^{5}	9.86×10^{9}	1.87×10^{6}	3.76×10^{6}	4.65×10^{3}
	100	Min	3.77×10^{10}	1.79×10^{7}	9.83×10^{8}	3.37×10^{8}	1.82×10^{11}	3.84×10^{10}	9.99×10^{5}	1.77×10^{10}	3.43×10^{6}	4.40×10^{6}	1.02×10^{4}
		Mean	4.36×10^{10}	7.20×10^{7}	4.33×10^{9}	7.17×10^{8}	2.09×10^{11}	6.45×10^{10}	2.21×10^{6}	5.30×10^{10}	3.43×10^{7}	2.21×10^{7}	2.56×10^{4}
		SD	3.48×10^{9}	6.44×10^{7}	2.95×10^{9}	2.38×10^{8}	1.17×10^{10}	1.49×10^{10}	8.39×10^{5}	1.99×10^{10}	5.15×10^{7}	1.45×10^{7}	1.07×10^{4}
F13	30	Min	1.91×10^{8}	1.49×10^{4}	2.76×10^{4}	3.64×10^{4}	7.20×10^{9}	2.27×10^{8}	2.24×10^{3}	2.60×10^{6}	1.16×10^{3}	1.67×10^{3}	1.32×10^{3}
		Mean	4.15×10^{8}	3.74×10^{4}	8.62×10^{4}	1.10×10^{5}	1.71×10^{10}	4.36×10^{8}	5.51×10^{3}	1.16×10^{9}	2.07×10^{4}	2.57×10^{4}	3.43×10^{1}
		SD	1.15×10^{8}	1.80×10^{4}	6.92×10^{4}	4.59×10^{4}	3.24×10^{9}	1.37×10^{8}	2.73×10^{3}	2.96×10^{9}	1.45×10^{4}	2.27×10^{4}	1.10×10^{1}
	50	Min	1.33×10^{9}	2.22×10^{4}	5.08×10^{4}	4.18×10^{4}	3.78×10^{10}	9.55×10^{8}	4.88×10^{2}	2.39×10^{8}	1.05×10^{3}	1.74×10^{3}	1.34×10^{3}
		Mean	2.35×10^{9}	4.80×10^{4}	8.38×10^{7}	1.55×10^{5}	5.28×10^{10}	2.36×10^{9}	1.95×10^{3}	7.36×10^{9}	5.45×10^{3}	1.22×10^{4}	1.38×10^{2}
		SD	5.84×10^{8}	2.29×10^{4}	1.04×10^{8}	1.12×10^{5}	7.14×10^{9}	9.74×10^{8}	1.18×10^{3}	5.60×10^{9}	4.44×10^{3}	1.23×10^{4}	6.97×10^{1}
	100	Min	6.30×10^{9}	2.17×10^{4}	2.14×10^{5}	4.95×10^{4}	4.64×10^{10}	5.82×10^{9}	3.22×10^{3}	4.24×10^{9}	3.21×10^{3}	4.31×10^{3}	1.52×10^{3}
		Mean	8.23×10^{9}	3.48×10^{4}	6.24×10^{8}	8.42×10^{4}	5.24×10^{10}	1.07×10^{10}	6.67×10^{3}	1.65×10^{10}	9.13×10^{3}	1.39×10^{4}	5.55×10^{2}
		SD	1.03×10^{9}	8.49×10^{3}	4.33×10^{8}	3.33×10^{4}	2.99×10^{9}	3.08×10^{9}	3.75×10^{3}	6.43×10^{9}	4.51×10^{3}	9.93×10^{3}	3.58×10^{2}
F14	30	Min	5.17×10^{4}	1.47×10^{4}	1.61×10^{3}	3.39×10^{4}	4.01×10^{6}	4.05×10^{4}	2.59×10^{2}	1.80×10^{4}	4.57×10^{2}	1.09×10^{3}	1.41×10^{3}
		Mean	1.48×10^{5}	3.45×10^{5}	1.14×10^{5}	9.63×10^{5}	1.43×10^{7}	4.46×10^{5}	2.05×10^{3}	7.39×10^{5}	7.80×10^{3}	6.16×10^{3}	2.12×10^{1}
		SD	6.08×10^{4}	4.58×10^{5}	2.82×10^{5}	1.52×10^{6}	9.41×10^{6}	2.21×10^{5}	2.04×10^{3}	9.65×10^{5}	7.59×10^{3}	4.78×10^{3}	8.34×10^{0}
	50	Min	5.33×10^{5}	2.14×10^{4}	3.41×10^{4}	1.21×10^{5}	6.76×10^{7}	1.69×10^{6}	6.55×10^{3}	1.94×10^{5}	6.52×10^{3}	3.88×10^{3}	1.44×10^{3}
		Mean	1.11×10^{6}	3.55×10^{5}	4.75×10^{5}	5.55×10^{5}	1.87×10^{8}	3.40×10^{6}	2.21×10^{4}	3.44×10^{6}	5.73×10^{4}	1.09×10^{5}	6.95×10^{1}
		SD	4.89×10^{5}	3.41×10^{5}	7.09×10^{5}	4.09×10^{5}	8.97×10^{7}	1.28×10^{6}	1.21×10^{4}	4.47×10^{6}	3.72×10^{4}	6.60×10^{4}	1.84×10^{1}
	100	Min	1.36×10^{7}	1.58×10^{6}	8.64×10^{5}	3.95×10^{5}	9.24×10^{7}	1.02×10^{7}	7.67×10^{4}	1.33×10^{6}	3.56×10^{5}	2.09×10^{5}	1.55×10^{3}
		Mean	2.17×10^{7}	3.64×10^{6}	3.76×10^{6}	1.68×10^{6}	2.05×10^{8}	1.52×10^{7}	9.97×10^{4}	6.57×10^{6}	1.00×10^{6}	1.54×10^{6}	6.75×10^{2}
		SD	6.57×10^{6}	1.47×10^{6}	2.00×10^{6}	7.46×10^{5}	6.41×10^{7}	2.86×10^{6}	1.38×10^{4}	4.33×10^{6}	4.89×10^{5}	8.67×10^{5}	5.21×10^{2}
F15	30	Min	1.31×10^{7}	7.88×10^{3}	1.58×10^{4}	1.02×10^{4}	1.37×10^{8}	6.91×10^{5}	1.66×10^{2}	3.35×10^{4}	1.29×10^{2}	2.31×10^{2}	1.51×10^{3}
		Mean	7.64×10^{7}	1.64×10^{4}	2.34×10^{5}	1.04×10^{5}	5.86×10^{8}	3.28×10^{6}	1.78×10^{3}	2.32×10^{7}	4.21×10^{3}	9.14×10^{3}	2.53×10^{1}
		SD	3.52×10^{7}	6.40×10^{3}	5.82×10^{5}	1.04×10^{5}	2.52×10^{8}	1.64×10^{6}	1.53×10^{3}	7.01×10^{7}	4.93×10^{3}	8.21×10^{3}	1.37×10^{1}
	50	Min	3.74×10^{8}	1.10×10^{4}	2.33×10^{4}	2.06×10^{4}	7.07×10^{9}	1.18×10^{8}	1.41×10^{3}	8.88×10^{5}	4.21×10^{2}	8.62×10^{2}	1.59×10^{3}
		Mean	8.18×10^{8}	2.12×10^{4}	3.59×10^{6}	8.34×10^{4}	1.05×10^{10}	2.31×10^{8}	8.81×10^{3}	1.44×10^{9}	7.99×10^{3}	1.02×10^{4}	1.30×10^{2}
		SD	2.35×10^{8}	7.14×10^{3}	7.45×10^{6}	6.32×10^{4}	2.10×10^{9}	5.50×10^{7}	5.49×10^{3}	2.04×10^{9}	6.00×10^{3}	9.13×10^{3}	4.37×10^{1}
	100	Min	2.59×10^{9}	9.12×10^{3}	6.19×10^{5}	3.27×10^{4}	2.37×10^{10}	9.36×10^{8}	2.21×10^{2}	1.36×10^{8}	3.40×10^{2}	6.48×10^{2}	1.68×10^{3}
		Mean	3.19×10^{9}	2.16×10^{4}	6.85×10^{7}	1.39×10^{5}	2.85×10^{10}	2.64×10^{9}	8.57×10^{2}	7.12×10^{9}	2.25×10^{3}	6.39×10^{3}	2.30×10^{2}
		SD	3.20×10^{8}	5.75×10^{3}	8.56×10^{7}	1.81×10^{5}	2.30×10^{9}	8.49×10^{8}	7.54×10^{2}	4.93×10^{9}	1.66×10^{3}	8.84×10^{3}	4.85×10^{1}
F16	30	Min	1.54×10^{3}	8.12×10^{2}	2.58×10^{2}	1.01×10^{3}	4.39×10^{3}	1.81×10^{3}	3.52×10^{2}	7.44×10^{2}	3.56×10^{2}	2.90×10^{2}	1.62×10^{3}
		Mean	1.75×10^{3}	1.16×10^{3}	6.91×10^{2}	1.81×10^{3}	5.81×10^{3}	2.10×10^{3}	6.72×10^{2}	1.62×10^{3}	7.23×10^{2}	8.64×10^{2}	5.33×10^{2}
		SD	1.46×10^{2}	2.81×10^{2}	2.17×10^{2}	5.07×10^{2}	8.67×10^{2}	1.35×10^{2}	1.93×10^{2}	3.90×10^{2}	2.99×10^{2}	2.34×10^{2}	2.69×10^{2}
	50	Min	3.33×10^{3}	1.12×10^{3}	5.79×10^{2}	1.71×10^{3}	8.00×10^{3}	1.90×10^{3}	6.51×10^{2}	2.19×10^{3}	9.04×10^{2}	9.30×10^{2}	2.22×10^{3}
		Mean	3.79×10^{3}	1.74×10^{3}	1.27×10^{3}	3.34×10^{3}	9.57×10^{3}	2.97×10^{3}	1.08×10^{3}	3.23×10^{3}	1.34×10^{3}	1.67×10^{3}	1.33×10^{3}
		SD	2.39×10^{2}	3.13×10^{2}	3.92×10^{2}	7.45×10^{2}	1.22×10^{3}	4.24×10^{2}	3.29×10^{2}	6.13×10^{2}	3.37×10^{2}	4.45×10^{2}	3.17×10^{2}
	100	Min	8.10×10^{3}	2.97×10^{3}	2.55×10^{3}	5.60×10^{3}	2.14×10^{4}	8.05×10^{3}	2.94×10^{3}	7.22×10^{3}	2.90×10^{3}	2.89×10^{3}	2.96×10^{3}
		Mean	9.62×10^{3}	4.86×10^{3}	3.80×10^{3}	7.69×10^{3}	2.44×10^{4}	1.03×10^{4}	4.00×10^{3}	8.88×10^{3}	4.12×10^{3}	4.43×10^{3}	3.16×10^{3}
		SD	5.51×10^{2}	8.41×10^{2}	8.40×10^{2}	1.31×10^{3}	1.98×10^{3}	8.93×10^{2}	5.62×10^{2}	1.05×10^{3}	7.27×10^{2}	9.13×10^{2}	5.69×10^{2}
F17	30	Min	5.81×10^{2}	9.94×10^{1}	7.07×10^{1}	3.83×10^{2}	2.35×10^{3}	5.23×10^{2}	5.81×10^{1}	1.86×10^{2}	1.54×10^{2}	9.69×10^{1}	1.73×10^{3}
		Mean	8.05×10^{2}	4.62×10^{2}	2.33×10^{2}	7.49×10^{2}	5.44×10^{3}	8.08×10^{2}	1.52×10^{2}	5.85×10^{2}	3.56×10^{2}	3.87×10^{2}	1.54×10^{2}
		SD	1.36×10^{2}	2.13×10^{2}	1.23×10^{2}	2.59×10^{2}	4.23×10^{3}	1.29×10^{2}	7.18×10^{1}	1.66×10^{2}	1.26×10^{2}	2.01×10^{2}	1.34×10^{2}
	50	Min	3.08×10^{3}	9.95×10^{2}	4.41×10^{2}	1.63×10^{3}	8.81×10^{3}	1.54×10^{3}	6.54×10^{2}	1.22×10^{3}	7.51×10^{2}	8.78×10^{2}	1.92×10^{3}
		Mean	3.77×10^{3}	1.64×10^{3}	9.98×10^{2}	2.40×10^{3}	1.42×10^{4}	2.11×10^{3}	1.07×10^{3}	2.09×10^{3}	1.39×10^{3}	1.58×10^{3}	8.66×10^{2}
		SD	3.00×10^{2}	2.82×10^{2}	2.48×10^{2}	3.47×10^{2}	3.77×10^{3}	2.29×10^{2}	2.25×10^{2}	6.41×10^{2}	3.52×10^{2}	3.34×10^{2}	2.74×10^{2}
	100	Min	8.00×10^{3}	2.88×10^{3}	1.69×10^{3}	4.10×10^{3}	2.00×10^{6}	8.24×10^{3}	2.33×10^{3}	4.57×10^{3}	2.31×10^{3}	2.09×10^{3}	3.32×10^{3}
		Mean	9.23×10^{3}	4.10×10^{3}	2.72×10^{3}	5.42×10^{3}	1.59×10^{7}	1.58×10^{4}	3.15×10^{3}	9.28×10^{4}	3.84×10^{3}	3.97×10^{3}	2.49×10^{3}
		SD	5.83×10^{2}	6.44×10^{2}	5.00×10^{2}	9.84×10^{2}	8.84×10^{6}	7.01×10^{3}	5.04×10^{2}	9.49×10^{4}	6.56×10^{2}	8.34×10^{2}	3.92×10^{2}
F18	30	Min	6.52×10^{5}	2.94×10^{4}	3.06×10^{4}	1.10×10^{5}	3.59×10^{7}	8.23×10^{5}	4.78×10^{4}	1.22×10^{5}	6.14×10^{4}	5.19×10^{4}	1.81×10^{3}
		Mean	3.31×10^{6}	3.94×10^{5}	6.53×10^{5}	1.89×10^{6}	1.54×10^{8}	2.23×10^{6}	1.08×10^{5}	6.61×10^{6}	1.96×10^{5}	2.44×10^{5}	2.34×10^{2}
		SD	1.76×10^{6}	4.45×10^{5}	6.85×10^{5}	1.98×10^{6}	8.19×10^{7}	1.40×10^{6}	4.55×10^{4}	1.83×10^{7}	1.24×10^{5}	2.28×10^{5}	3.36×10^{2}
	50	Min	6.08×10^{6}	6.76×10^{5}	3.97×10^{5}	6.09×10^{5}	1.32×10^{8}	4.74×10^{6}	1.08×10^{5}	7.02×10^{5}	9.57×10^{4}	5.85×10^{4}	1.87×10^{3}
		Mean	1.28×10^{7}	2.62×10^{6}	2.70×10^{6}	5.26×10^{6}	2.73×10^{8}	9.12×10^{6}	3.87×10^{5}	9.94×10^{6}	6.60×10^{5}	6.50×10^{5}	2.38×10^{3}
		SD	3.38×10^{6}	1.58×10^{6}	3.96×10^{6}	5.09×10^{6}	7.95×10^{7}	2.60×10^{6}	1.98×10^{5}	1.43×10^{7}	6.52×10^{5}	4.87×10^{5}	2.62×10^{3}
	100	Min	2.82×10^{7}	8.37×10^{5}	1.18×10^{6}	9.86×10^{5}	1.37×10^{8}	1.16×10^{7}	1.58×10^{5}	1.56×10^{6}	2.41×10^{5}	5.53×10^{5}	2.57×10^{3}
		Mean	4.40×10^{7}	2.59×10^{6}	3.33×10^{6}	2.29×10^{6}	3.53×10^{8}	1.93×10^{7}	3.45×10^{5}	6.96×10^{6}	9.13×10^{5}	2.12×10^{6}	9.58×10^{3}
		SD	1.06×10^{7}	1.06×10^{6}	1.58×10^{6}	8.64×10^{5}	1.16×10^{8}	5.85×10^{6}	1.06×10^{5}	6.46×10^{6}	4.43×10^{5}	1.32×10^{6}	7.90×10^{3}

Table 4. *Cont.*

F	D	Index	PSO 1997	KH 2012	GWO 2014	WOA 2016	EEGWO 2018	HGSO 2019	JSO 2020	TSA 2020	MTBO 2023	FOA 2024	CNJSO
F19	30	Min	1.17×10^{7}	5.38×10^{3}	9.69×10^{3}	3.39×10^{4}	4.06×10^{8}	3.00×10^{6}	3.34×10^{2}	1.28×10^{5}	1.61×10^{2}	7.90×10^{1}	1.91×10^{3}
		Mean	9.09×10^{7}	1.20×10^{5}	5.11×10^{5}	2.61×10^{6}	1.41×10^{9}	9.34×10^{6}	5.03×10^{3}	9.37×10^{7}	4.44×10^{3}	1.32×10^{4}	1.78×10^{1}
		SD	4.51×10^{7}	1.28×10^{5}	4.80×10^{5}	2.81×10^{6}	6.13×10^{8}	3.32×10^{6}	3.64×10^{3}	1.82×10^{8}	4.85×10^{3}	1.16×10^{4}	9.68×10^{0}
	50	Min	2.04×10^{8}	1.99×10^{4}	3.79×10^{4}	2.67×10^{4}	3.34×10^{9}	5.75×10^{7}	9.71×10^{3}	2.16×10^{6}	2.33×10^{3}	9.41×10^{2}	1.92×10^{3}
		Mean	3.97×10^{8}	1.66×10^{5}	3.14×10^{6}	2.28×10^{6}	6.12×10^{9}	1.67×10^{8}	2.30×10^{4}	1.10×10^{9}	1.64×10^{4}	1.30×10^{4}	5.67×10^{1}
		SD	1.08×10^{8}	1.18×10^{5}	7.33×10^{6}	1.91×10^{6}	1.33×10^{9}	6.29×10^{7}	7.20×10^{3}	1.52×10^{9}	9.74×10^{3}	1.24×10^{4}	2.66×10^{1}
	100	Min	1.88×10^{9}	6.82×10^{4}	1.89×10^{6}	1.93×10^{6}	2.01×10^{10}	1.05×10^{9}	1.42×10^{2}	2.81×10^{8}	3.85×10^{2}	7.69×10^{2}	2.02×10^{3}
		Mean	3.23×10^{9}	3.63×10^{5}	6.70×10^{7}	1.55×10^{7}	2.74×10^{10}	2.47×10^{9}	1.75×10^{3}	5.66×10^{9}	2.91×10^{3}	7.52×10^{3}	1.85×10^{2}
		SD	5.34×10^{8}	2.59×10^{5}	6.88×10^{7}	5.59×10^{6}	2.83×10^{9}	8.76×10^{8}	1.72×10^{3}	4.75×10^{9}	2.67×10^{3}	9.31×10^{3}	3.96×10^{1}
F20	30	Min	4.68×10^{2}	2.88×10^{2}	1.58×10^{2}	2.31×10^{2}	1.06×10^{3}	4.80×10^{2}	2.14×10^{2}	1.76×10^{2}	1.36×10^{2}	1.53×10^{2}	2.01×10^{3}
		Mean	6.19×10^{2}	5.76×10^{2}	3.93×10^{2}	6.48×10^{2}	1.33×10^{3}	5.91×10^{2}	2.76×10^{2}	6.35×10^{2}	3.07×10^{2}	2.95×10^{2}	1.50×10^{2}
		SD	9.42×10^{1}	2.17×10^{2}	1.74×10^{2}	1.99×10^{2}	1.29×10^{2}	6.82×10^{1}	5.12×10^{1}	1.71×10^{2}	1.43×10^{2}	6.46×10^{1}	9.27×10^{1}
	50	Min	1.54×10^{3}	4.85×10^{2}	4.04×10^{2}	1.34×10^{3}	1.82×10^{3}	1.02×10^{3}	4.44×10^{2}	1.16×10^{3}	3.63×10^{2}	3.33×10^{2}	2.12×10^{3}
		Mean	1.79×10^{3}	1.33×10^{3}	8.03×10^{2}	1.66×10^{3}	2.63×10^{3}	1.40×10^{3}	7.82×10^{2}	1.62×10^{3}	7.44×10^{2}	6.30×10^{2}	4.94×10^{2}
		SD	1.80×10^{2}	3.25×10^{2}	2.47×10^{2}	2.31×10^{2}	2.63×10^{2}	2.14×10^{2}	2.22×10^{2}	2.62×10^{2}	2.57×10^{2}	2.05×10^{2}	1.96×10^{2}
	100	Min	4.40×10^{3}	2.46×10^{3}	1.15×10^{3}	2.97×10^{3}	5.90×10^{3}	4.16×10^{3}	1.61×10^{3}	3.29×10^{3}	1.53×10^{3}	1.66×10^{3}	3.21×10^{3}
		Mean	5.06×10^{3}	3.35×10^{3}	2.30×10^{3}	4.24×10^{3}	6.56×10^{3}	4.58×10^{3}	2.24×10^{3}	4.19×10^{3}	2.56×10^{3}	2.42×10^{3}	2.14×10^{3}
		SD	3.01×10^{2}	5.32×10^{2}	4.78×10^{2}	6.02×10^{2}	2.54×10^{2}	2.41×10^{2}	4.10×10^{2}	5.07×10^{2}	8.33×10^{2}	3.78×10^{2}	4.32×10^{2}
Rank	30	W/T/L	0/0/10	0/0/10	0/0/10	0/0/10	0/0/10	0/0/10	1/0/9	0/0/10	0/0/10	0/0/10	**9/0/1**
	50	W/T/L	0/0/10	0/0/10	0/0/10	0/0/10	0/0/10	0/0/10	1/0/9	0/0/10	0/0/10	0/0/10	**9/0/1**
	100	W/T/L	0/0/10	0/0/10	0/0/10	0/0/10	0/0/10	0/0/10	0/0/10	0/0/10	0/0/10	0/0/10	**10/0/0**

Table 5. Comparison of the obtained results from composite test functions.

F	D	Index	PSO 1997	KH 2012	GWO 2014	WOA 2016	EEGWO 2018	HGSO 2019	JSO 2020	TSA 2020	MTBO 2023	FOA 2024	CNJSO
F21	30	Min	4.27×10^{2}	2.69×10^{2}	2.35×10^{2}	3.38×10^{2}	6.10×10^{2}	3.98×10^{2}	2.56×10^{2}	4.03×10^{2}	2.46×10^{2}	2.51×10^{2}	2.33×10^{3}
		Mean	4.45×10^{2}	3.12×10^{2}	2.76×10^{2}	4.49×10^{2}	7.10×10^{2}	4.67×10^{2}	2.81×10^{2}	4.96×10^{2}	2.80×10^{2}	2.99×10^{2}	2.55×10^{2}
		SD	1.13×10^{1}	2.18×10^{1}	3.22×10^{1}	6.46×10^{1}	4.70×10^{1}	2.50×10^{1}	1.17×10^{1}	4.20×10^{1}	1.81×10^{1}	3.19×10^{1}	1.31×10^{1}
	50	Min	6.81×10^{2}	3.66×10^{2}	3.24×10^{2}	6.04×10^{2}	1.06×10^{3}	7.44×10^{2}	3.17×10^{2}	7.00×10^{2}	3.47×10^{2}	3.22×10^{2}	2.36×10^{3}
		Mean	7.07×10^{2}	4.39×10^{2}	3.73×10^{2}	7.58×10^{2}	1.24×10^{3}	8.20×10^{2}	3.66×10^{2}	8.24×10^{2}	4.08×10^{2}	4.48×10^{2}	3.22×10^{2}
		SD	1.43×10^{1}	3.34×10^{1}	2.67×10^{1}	9.71×10^{1}	8.39×10^{1}	3.33×10^{1}	2.61×10^{1}	7.45×10^{1}	4.52×10^{1}	5.45×10^{1}	3.21×10^{1}
	100	Min	1.44×10^{3}	1.01×10^{3}	6.44×10^{2}	1.56×10^{3}	2.72×10^{3}	1.80×10^{3}	6.13×10^{2}	1.79×10^{3}	6.72×10^{2}	7.41×10^{2}	2.51×10^{3}
		Mean	1.51×10^{3}	1.25×10^{3}	7.65×10^{2}	1.81×10^{3}	3.15×10^{3}	1.96×10^{3}	7.29×10^{2}	1.96×10^{3}	8.37×10^{2}	9.34×10^{2}	5.72×10^{2}
		SD	4.36×10^{1}	1.27×10^{2}	8.10×10^{1}	1.90×10^{2}	2.29×10^{2}	9.62×10^{1}	5.96×10^{1}	1.16×10^{2}	1.06×10^{2}	1.06×10^{2}	6.95×10^{1}
F22	30	Min	1.63×10^{3}	1.00×10^{2}	1.58×10^{2}	1.12×10^{2}	7.01×10^{3}	9.08×10^{2}	1.00×10^{2}	1.50×10^{3}	1.00×10^{2}	1.00×10^{2}	2.30×10^{3}
		Mean	5.50×10^{3}	1.00×10^{2}	2.13×10^{3}	3.72×10^{3}	7.99×10^{3}	1.72×10^{3}	1.01×10^{2}	5.73×10^{3}	1.97×10^{3}	2.78×10^{2}	1.00×10^{2}
		SD	2.52×10^{3}	5.08×10^{-1}	1.53×10^{3}	2.25×10^{3}	4.05×10^{2}	3.65×10^{2}	1.64×10^{0}	1.45×10^{3}	2.80×10^{3}	7.86×10^{2}	9.70×10^{-1}
	50	Min	1.25×10^{4}	6.04×10^{3}	5.05×10^{3}	8.07×10^{3}	1.48×10^{4}	5.41×10^{3}	1.00×10^{2}	4.36×10^{3}	4.99×10^{3}	4.86×10^{3}	2.30×10^{3}
		Mean	1.35×10^{4}	8.21×10^{3}	6.14×10^{3}	9.70×10^{3}	1.59×10^{4}	9.30×10^{3}	1.56×10^{3}	1.11×10^{4}	1.06×10^{4}	8.77×10^{3}	4.38×10^{3}
		SD	4.17×10^{2}	9.28×10^{2}	6.93×10^{2}	1.22×10^{3}	5.56×10^{2}	2.48×10^{3}	3.01×10^{3}	1.82×10^{3}	3.39×10^{3}	1.41×10^{3}	1.39×10^{3}
	100	Min	2.98×10^{4}	1.47×10^{4}	1.17×10^{4}	1.60×10^{4}	3.31×10^{4}	2.63×10^{4}	1.00×10^{2}	2.54×10^{4}	1.10×10^{4}	1.59×10^{4}	1.26×10^{4}
		Mean	3.08×10^{4}	1.78×10^{4}	1.64×10^{4}	2.15×10^{4}	3.42×10^{4}	2.84×10^{4}	1.45×10^{4}	2.76×10^{4}	2.51×10^{4}	2.21×10^{4}	1.17×10^{4}
		SD	6.22×10^{2}	1.30×10^{3}	5.20×10^{3}	3.14×10^{3}	5.01×10^{2}	8.55×10^{2}	5.04×10^{3}	1.27×10^{3}	7.70×10^{3}	2.73×10^{3}	8.75×10^{2}
F23	30	Min	5.69×10^{2}	4.87×10^{2}	3.84×10^{2}	5.56×10^{2}	1.26×10^{3}	6.96×10^{2}	4.15×10^{2}	6.97×10^{2}	4.14×10^{2}	4.22×10^{2}	2.68×10^{3}
		Mean	5.89×10^{2}	5.90×10^{2}	4.39×10^{2}	7.06×10^{2}	1.55×10^{3}	7.85×10^{2}	4.55×10^{2}	8.63×10^{2}	4.65×10^{2}	4.94×10^{2}	4.11×10^{2}
		SD	1.19×10^{1}	5.56×10^{1}	3.93×10^{1}	7.45×10^{1}	1.97×10^{2}	4.75×10^{1}	2.64×10^{1}	1.04×10^{2}	4.18×10^{1}	4.70×10^{1}	1.99×10^{1}
	50	Min	9.06×10^{2}	8.62×10^{2}	5.79×10^{2}	1.04×10^{3}	2.23×10^{3}	1.07×10^{3}	5.63×10^{2}	1.25×10^{3}	6.28×10^{2}	6.43×10^{2}	2.80×10^{3}
		Mean	9.43×10^{2}	1.06×10^{3}	6.24×10^{2}	1.28×10^{3}	2.72×10^{3}	1.35×10^{3}	6.88×10^{2}	1.50×10^{3}	7.02×10^{2}	7.70×10^{2}	5.72×10^{2}
		SD	1.33×10^{1}	1.02×10^{2}	3.65×10^{1}	1.53×10^{2}	2.47×10^{2}	1.27×10^{2}	4.73×10^{1}	1.44×10^{2}	5.08×10^{1}	8.26×10^{1}	4.56×10^{1}
	100	Min	1.63×10^{3}	2.17×10^{3}	9.72×10^{2}	1.75×10^{3}	4.72×10^{3}	2.61×10^{3}	1.11×10^{3}	2.52×10^{3}	1.17×10^{3}	1.03×10^{3}	2.98×10^{3}
		Mean	1.66×10^{3}	2.41×10^{3}	1.12×10^{3}	2.44×10^{3}	5.88×10^{3}	3.93×10^{3}	1.20×10^{3}	2.82×10^{3}	1.37×10^{3}	1.37×10^{3}	7.79×10^{2}
		SD	3.28×10^{1}	1.43×10^{2}	6.90×10^{1}	3.14×10^{2}	5.97×10^{2}	1.04×10^{3}	5.68×10^{1}	2.34×10^{2}	1.27×10^{2}	1.78×10^{2}	4.99×10^{1}
F24	30	Min	6.19×10^{2}	5.79×10^{2}	4.49×10^{2}	6.06×10^{2}	1.56×10^{3}	7.66×10^{2}	4.75×10^{2}	7.81×10^{2}	4.68×10^{2}	4.83×10^{2}	2.87×10^{3}
		Mean	6.36×10^{2}	6.99×10^{2}	4.99×10^{2}	7.61×10^{2}	1.82×10^{3}	8.66×10^{2}	5.29×10^{2}	9.15×10^{2}	5.01×10^{2}	5.45×10^{2}	4.92×10^{2}
		SD	9.49×10^{0}	7.24×10^{1}	4.58×10^{1}	8.56×10^{1}	1.69×10^{2}	6.21×10^{1}	2.59×10^{1}	9.13×10^{1}	2.73×10^{1}	3.34×10^{1}	1.43×10^{1}
	50	Min	9.09×10^{2}	1.04×10^{3}	6.26×10^{2}	1.03×10^{3}	2.63×10^{3}	1.26×10^{3}	6.98×10^{2}	1.25×10^{3}	6.44×10^{2}	6.55×10^{2}	2.99×10^{3}
		Mean	9.43×10^{2}	1.23×10^{3}	6.93×10^{2}	1.27×10^{3}	3.16×10^{3}	1.53×10^{3}	7.84×10^{2}	1.57×10^{3}	7.10×10^{2}	7.90×10^{2}	6.51×10^{2}
		SD	1.57×10^{1}	1.45×10^{2}	6.57×10^{1}	1.38×10^{2}	3.00×10^{2}	1.18×10^{2}	6.38×10^{1}	1.46×10^{2}	5.58×10^{1}	7.24×10^{1}	5.57×10^{1}
	100	Min	2.11×10^{3}	2.80×10^{3}	1.36×10^{3}	3.23×10^{3}	8.78×10^{3}	3.92×10^{3}	1.78×10^{3}	3.54×10^{3}	1.72×10^{3}	1.61×10^{3}	3.57×10^{3}
		Mean	2.16×10^{3}	3.31×10^{3}	1.52×10^{3}	3.62×10^{3}	1.11×10^{4}	4.52×10^{3}	2.01×10^{3}	4.10×10^{3}	1.97×10^{3}	1.89×10^{3}	1.33×10^{3}
		SD	2.66×10^{1}	3.86×10^{2}	8.98×10^{1}	2.29×10^{2}	7.95×10^{2}	2.63×10^{2}	1.49×10^{2}	3.93×10^{2}	1.83×10^{2}	1.79×10^{2}	8.09×10^{1}
F25	30	Min	1.07×10^{3}	3.89×10^{2}	3.92×10^{2}	3.94×10^{2}	2.30×10^{3}	7.08×10^{2}	3.84×10^{2}	4.65×10^{2}	3.84×10^{2}	3.84×10^{2}	2.88×10^{3}
		Mean	1.31×10^{3}	4.20×10^{2}	4.49×10^{2}	4.44×10^{2}	3.27×10^{3}	8.20×10^{2}	3.94×10^{2}	9.61×10^{2}	4.15×10^{2}	3.94×10^{2}	3.89×10^{2}
		SD	1.36×10^{2}	2.08×10^{1}	3.10×10^{1}	3.00×10^{1}	4.76×10^{2}	6.48×10^{1}	1.19×10^{1}	3.94×10^{2}	2.46×10^{1}	1.35×10^{1}	8.48×10^{0}
	50	Min	2.73×10^{3}	5.36×10^{2}	7.03×10^{2}	5.26×10^{2}	1.21×10^{4}	2.80×10^{3}	5.72×10^{2}	1.92×10^{3}	4.63×10^{2}	4.61×10^{2}	2.96×10^{3}
		Mean	3.39×10^{3}	5.91×10^{2}	8.99×10^{2}	6.27×10^{2}	1.35×10^{4}	3.94×10^{3}	6.06×10^{2}	3.91×10^{3}	5.52×10^{2}	5.50×10^{2}	5.57×10^{2}
		SD	3.49×10^{2}	2.42×10^{1}	1.80×10^{2}	4.94×10^{1}	6.32×10^{2}	5.48×10^{2}	1.31×10^{1}	1.37×10^{3}	3.88×10^{1}	4.05×10^{1}	3.55×10^{1}
	100	Min	1.42×10^{4}	7.54×10^{2}	2.11×10^{3}	1.00×10^{3}	2.39×10^{4}	8.57×10^{3}	7.59×10^{2}	5.29×10^{3}	7.64×10^{2}	6.38×10^{2}	3.14×10^{3}
		Mean	1.78×10^{4}	8.50×10^{2}	2.96×10^{3}	1.14×10^{3}	2.71×10^{4}	1.10×10^{4}	8.56×10^{2}	8.34×10^{3}	8.56×10^{2}	7.75×10^{2}	7.64×10^{2}
		SD	1.68×10^{3}	5.89×10^{1}	4.90×10^{2}	7.12×10^{1}	1.56×10^{3}	1.30×10^{3}	4.26×10^{1}	1.98×10^{3}	5.16×10^{1}	7.08×10^{1}	6.24×10^{1}
F26	30	Min	3.72×10^{3}	2.00×10^{2}	1.44×10^{3}	1.63×10^{3}	8.42×10^{3}	3.73×10^{3}	2.00×10^{2}	1.50×10^{3}	2.00×10^{2}	2.00×10^{2}	3.80×10^{3}
		Mean	3.87×10^{3}	3.28×10^{3}	1.83×10^{3}	4.74×10^{3}	9.41×10^{3}	4.44×10^{3}	2.25×10^{3}	5.14×10^{3}	2.28×10^{3}	2.32×10^{3}	1.71×10^{3}
		SD	9.33×10^{1}	1.39×10^{3}	2.12×10^{2}	1.04×10^{3}	6.32×10^{2}	3.72×10^{2}	1.32×10^{3}	1.34×10^{3}	1.05×10^{3}	9.69×10^{2}	2.77×10^{2}
	50	Min	6.34×10^{3}	5.58×10^{3}	2.28×10^{3}	7.94×10^{3}	1.43×10^{4}	7.24×10^{3}	3.01×10^{2}	8.80×10^{3}	3.00×10^{2}	3.39×10^{3}	4.85×10^{3}
		Mean	6.62×10^{3}	7.40×10^{3}	3.25×10^{3}	1.07×10^{4}	1.54×10^{4}	8.64×10^{3}	5.41×10^{3}	1.08×10^{4}	5.64×10^{3}	4.60×10^{3}	2.80×10^{3}
		SD	1.57×10^{2}	8.69×10^{2}	4.77×10^{2}	1.61×10^{3}	5.11×10^{2}	1.11×10^{3}	3.28×10^{3}	1.05×10^{3}	2.54×10^{3}	8.73×10^{2}	3.10×10^{2}
	100	Min	1.59×10^{4}	1.89×10^{4}	7.80×10^{3}	2.47×10^{4}	5.12×10^{4}	2.43×10^{4}	1.68×10^{4}	2.75×10^{4}	1.31×10^{4}	1.11×10^{4}	9.81×10^{3}
		Mean	1.64×10^{4}	2.33×10^{4}	9.71×10^{3}	2.90×10^{4}	5.50×10^{4}	3.18×10^{4}	2.05×10^{4}	2.99×10^{4}	2.05×10^{4}	1.40×10^{4}	8.18×10^{3}
		SD	3.22×10^{2}	1.71×10^{3}	9.83×10^{2}	2.86×10^{3}	1.70×10^{3}	2.62×10^{3}	1.81×10^{3}	1.59×10^{3}	3.85×10^{3}	2.23×10^{3}	6.78×10^{2}
F27	30	Min	5.76×10^{2}	5.75×10^{2}	5.10×10^{2}	5.40×10^{2}	1.90×10^{3}	5.00×10^{2}	5.30×10^{2}	6.18×10^{2}	5.11×10^{2}	5.14×10^{2}	3.20×10^{3}
		Mean	6.13×10^{2}	7.05×10^{2}	5.40×10^{2}	6.43×10^{2}	2.56×10^{3}	5.00×10^{2}	5.56×10^{2}	8.25×10^{2}	5.50×10^{2}	5.54×10^{2}	5.23×10^{2}
		SD	2.11×10^{1}	8.40×10^{1}	2.17×10^{1}	7.29×10^{1}	4.04×10^{2}	8.23×10^{-5}	1.95×10^{1}	1.33×10^{2}	3.00×10^{1}	4.27×10^{1}	1.80×10^{1}
	50	Min	9.11×10^{2}	1.30×10^{3}	6.32×10^{2}	9.80×10^{2}	3.71×10^{3}	5.00×10^{2}	7.51×10^{2}	1.35×10^{3}	6.49×10^{2}	6.30×10^{2}	3.26×10^{3}
		Mean	9.96×10^{2}	1.70×10^{3}	7.89×10^{2}	1.37×10^{3}	5.64×10^{3}	5.00×10^{2}	9.58×10^{2}	1.80×10^{3}	8.85×10^{2}	9.33×10^{2}	6.29×10^{2}
		SD	6.43×10^{1}	2.96×10^{2}	7.01×10^{1}	2.07×10^{2}	7.96×10^{2}	1.60×10^{-4}	9.23×10^{1}	2.98×10^{2}	1.33×10^{2}	1.74×10^{2}	5.35×10^{1}
	100	Min	1.58×10^{3}	2.02×10^{3}	9.17×10^{2}	1.32×10^{3}	7.44×10^{3}	5.00×10^{2}	1.22×10^{3}	2.23×10^{3}	9.39×10^{2}	8.40×10^{2}	3.46×10^{3}
		Mean	1.73×10^{3}	3.01×10^{3}	1.10×10^{3}	2.23×10^{3}	1.30×10^{4}	5.00×10^{2}	1.47×10^{3}	3.05×10^{3}	1.35×10^{3}	1.14×10^{3}	8.60×10^{2}
		SD	1.03×10^{2}	6.58×10^{2}	1.22×10^{2}	6.48×10^{2}	1.61×10^{3}	1.12×10^{-4}	1.08×10^{2}	5.56×10^{2}	2.92×10^{2}	1.72×10^{2}	5.88×10^{1}

Table 5. *Cont.*

F	D	Index	PSO 1997	KH 2012	GWO 2014	WOA 2016	EEGWO 2018	HGSO 2019	JSO 2020	TSA 2020	MTBO 2023	FOA 2024	CNJSO
F28	30	Min	8.75×10^{2}	3.95×10^{2}	4.73×10^{2}	4.38×10^{2}	4.01×10^{3}	5.00×10^{2}	3.90×10^{2}	6.84×10^{2}	3.00×10^{2}	3.00×10^{2}	3.10×10^{3}
		Mean	1.00×10^{3}	4.47×10^{2}	5.55×10^{2}	4.91×10^{2}	5.04×10^{3}	9.19×10^{2}	4.09×10^{2}	1.43×10^{3}	3.81×10^{2}	3.64×10^{2}	3.21×10^{2}
		SD	6.68×10^{1}	2.66×10^{1}	6.08×10^{1}	2.20×10^{1}	4.86×10^{2}	4.56×10^{2}	1.23×10^{1}	6.55×10^{2}	5.29×10^{1}	6.02×10^{1}	4.35×10^{1}
	50	Min	1.43×10^{3}	4.81×10^{2}	6.72×10^{2}	5.70×10^{2}	9.97×10^{3}	5.00×10^{2}	4.93×10^{2}	2.32×10^{3}	4.60×10^{2}	4.59×10^{2}	3.27×10^{3}
		Mean	1.92×10^{3}	5.40×10^{2}	1.15×10^{3}	6.34×10^{2}	1.16×10^{4}	3.46×10^{3}	5.37×10^{2}	4.00×10^{3}	5.03×10^{2}	4.90×10^{2}	4.97×10^{2}
		SD	3.93×10^{2}	3.87×10^{1}	3.47×10^{2}	5.28×10^{1}	8.68×10^{2}	1.60×10^{3}	2.94×10^{1}	1.07×10^{3}	2.81×10^{1}	1.90×10^{1}	1.09×10^{1}
	100	Min	9.17×10^{3}	6.28×10^{2}	2.28×10^{3}	7.78×10^{2}	3.16×10^{4}	1.16×10^{4}	6.10×10^{2}	7.26×10^{3}	5.26×10^{2}	5.32×10^{2}	3.10×10^{3}
		Mean	1.23×10^{4}	6.99×10^{2}	3.66×10^{3}	9.03×10^{2}	3.44×10^{4}	1.62×10^{4}	6.71×10^{2}	1.15×10^{4}	6.56×10^{2}	5.75×10^{2}	4.08×10^{2}
		SD	2.23×10^{3}	4.51×10^{1}	9.82×10^{2}	5.72×10^{1}	1.36×10^{3}	2.01×10^{3}	3.37×10^{1}	1.95×10^{3}	5.22×10^{1}	3.16×10^{1}	1.25×10^{2}
F29	30	Min	1.25×10^{3}	6.77×10^{2}	4.89×10^{2}	1.06×10^{3}	3.91×10^{3}	1.02×10^{3}	4.82×10^{2}	1.08×10^{3}	5.49×10^{2}	5.90×10^{2}	3.26×10^{3}
		Mean	1.54×10^{3}	1.28×10^{3}	7.96×10^{2}	1.92×10^{3}	6.13×10^{3}	1.37×10^{3}	6.57×10^{2}	1.58×10^{3}	9.72×10^{2}	1.08×10^{3}	5.17×10^{2}
		SD	1.55×10^{2}	2.81×10^{2}	1.70×10^{2}	3.51×10^{2}	1.52×10^{3}	2.62×10^{2}	1.07×10^{2}	3.57×10^{2}	2.85×10^{2}	2.92×10^{2}	1.08×10^{2}
	50	Min	2.85×10^{3}	1.62×10^{3}	7.63×10^{2}	2.06×10^{3}	3.81×10^{4}	2.22×10^{3}	8.78×10^{2}	2.22×10^{3}	1.29×10^{3}	1.56×10^{3}	3.32×10^{3}
		Mean	3.48×10^{3}	2.40×10^{3}	1.33×10^{3}	3.77×10^{3}	2.11×10^{5}	3.84×10^{3}	1.35×10^{3}	4.12×10^{3}	1.99×10^{3}	2.10×10^{3}	7.80×10^{2}
		SD	2.83×10^{2}	5.31×10^{2}	2.75×10^{2}	8.36×10^{2}	1.33×10^{5}	1.10×10^{3}	2.57×10^{2}	1.07×10^{3}	3.50×10^{2}	3.56×10^{2}	2.44×10^{2}
	100	Min	1.11×10^{4}	4.42×10^{3}	3.60×10^{3}	7.60×10^{3}	4.88×10^{5}	8.21×10^{3}	2.95×10^{3}	8.67×10^{3}	3.57×10^{3}	3.56×10^{3}	4.92×10^{3}
		Mean	1.32×10^{4}	5.69×10^{3}	4.47×10^{3}	1.04×10^{4}	8.86×10^{5}	1.24×10^{4}	4.11×10^{3}	1.83×10^{4}	4.76×10^{3}	4.75×10^{3}	2.64×10^{3}
		SD	1.21×10^{3}	7.47×10^{2}	4.63×10^{2}	2.07×10^{3}	2.77×10^{5}	3.16×10^{3}	5.02×10^{2}	1.16×10^{4}	6.61×10^{2}	8.09×10^{2}	4.15×10^{2}
F30	30	Min	1.55×10^{7}	1.72×10^{5}	2.05×10^{5}	1.21×10^{6}	6.86×10^{8}	4.06×10^{7}	2.93×10^{3}	4.03×10^{6}	2.49×10^{3}	3.56×10^{3}	4.99×10^{3}
		Mean	5.28×10^{7}	1.91×10^{6}	4.98×10^{6}	9.90×10^{6}	2.33×10^{9}	7.45×10^{7}	3.79×10^{3}	1.19×10^{7}	7.10×10^{3}	9.50×10^{3}	2.16×10^{3}
		SD	1.93×10^{7}	1.49×10^{6}	4.92×10^{6}	6.46×10^{6}	8.45×10^{8}	1.98×10^{7}	7.24×10^{2}	7.09×10^{6}	6.30×10^{3}	4.82×10^{3}	1.53×10^{2}
	50	Min	4.20×10^{8}	1.87×10^{7}	4.18×10^{7}	4.59×10^{7}	5.14×10^{9}	3.74×10^{8}	7.38×10^{5}	3.81×10^{7}	6.84×10^{5}	8.82×10^{5}	5.83×10^{5}
		Mean	7.14×10^{8}	4.48×10^{7}	7.55×10^{7}	8.84×10^{7}	9.51×10^{9}	5.84×10^{8}	8.84×10^{5}	1.00×10^{9}	9.58×10^{5}	1.32×10^{6}	6.85×10^{5}
		SD	1.95×10^{8}	2.13×10^{7}	2.13×10^{7}	2.93×10^{7}	1.83×10^{9}	1.37×10^{8}	1.15×10^{5}	1.21×10^{9}	1.62×10^{5}	4.50×10^{5}	1.10×10^{5}
	100	Min	2.54×10^{9}	4.53×10^{6}	4.58×10^{7}	6.36×10^{7}	4.06×10^{10}	4.65×10^{9}	2.95×10^{3}	6.11×10^{9}	4.62×10^{3}	8.79×10^{3}	5.33×10^{3}
		Mean	3.52×10^{9}	1.16×10^{7}	3.40×10^{8}	2.12×10^{8}	4.62×10^{10}	8.62×10^{9}	4.11×10^{3}	1.20×10^{10}	2.26×10^{4}	2.93×10^{4}	3.38×10^{3}
		SD	3.74×10^{8}	4.36×10^{6}	3.52×10^{8}	9.95×10^{7}	2.68×10^{9}	2.21×10^{9}	5.02×10^{2}	4.48×10^{9}	1.46×10^{4}	3.31×10^{4}	2.28×10^{3}
Rank	30	W/T/L	0/0/10	0/0/10	0/0/10	0/0/10	0/0/10	1/0/9	0/0/10	0/0/10	0/0/10	0/0/10	9/0/1
	50	W/T/L	0/0/10	0/0/10	0/0/10	0/0/10	0/0/10	1/0/9	1/0/9	0/0/10	1/0/9	2/0/8	5/0/5
	100	W/T/L	0/0/10	0/0/10	0/0/10	0/0/10	0/0/10	1/0/9	0/0/10	0/0/10	0/0/10	0/0/10	9/0/1

5.3.1. Evaluation of Exploitation and Exploration

The CNJSO is experimentally appraised by benchmark functions F1 and F3 on different dimensions, 30, 50, and 100. Table 2 shows the experimental results of CNJSO and comparative algorithms, which prove the strong exploitation ability of CNJSO. The benchmark functions F4–F10 have multiple local optima that increase exponentially in dimension, making them appropriate for assessing the exploration ability of CNJSO and comparative algorithms. Table 3 represents the experimental results of CNJSO and comparative algorithms to solve multimodal functions on dimensions 30, 50, and 100. Tables 4 and 5 show the results of CNJSO and competing algorithms on test functions F11–F30, which verify the improvement in exploration and exploitation ability using the conscious neighborhood concept.

The primary reason is that this concept helps determine an effective movement strategy consciously. In this study, each individual's neighborhood and non-neighborhood are evaluated to determine the next movement strategy rather than relying on a time-based mechanism to switch between local and global search. This approach allows the population to adaptively balance exploration and exploitation based on the current search context. Additionally, the proposed BNGS enhances CNJSO's exploration capability through two complementary mechanisms. First, a random individual is selected from an archive containing the best-performing individuals; this allows information from high-quality solutions to influence the population and guides individuals toward promising regions in the search space. Second, a random non-neighborhood individual is selected to incorporate information from diverse areas outside the immediate neighborhood, promoting broader exploration. The combination of these two mechanisms enables CNJSO to explore the search space effectively, avoid premature convergence, and maintain a robust balance between local refinement and global search.

5.3.2. Evaluation of Escape Ability from Local Optima

To evaluate the balance between exploration and exploitation, which sets the stage for escaping from the local optima trap, the hybrid and composite functions are appropriate. The results in Table 4 indicate that the proposed CNJSO outperforms the comparative algorithms on the hybrid functions F11–F20. The results in Table 5 indicate that the CNJSO algorithm handles the composite optimization problems posed by the benchmark functions

F21–F30 more effectively than the comparative algorithms, particularly at a dimensionality of 100. The primary cause for this is that the use of WAS forced those individuals who could not achieve good fitness to adjust their positions. The WAS strategy is used to examine how individuals behave, jumping to another spot if their present position is not satisfactory. Thus, this strategy can strike a balance between exploration and exploitation, thereby avoiding the risk of becoming trapped in local optima.

5.4. Convergence Analysis

The convergent curves of CNJSO and comparative algorithms are illustrated in Figure 3. Regarding these curves, it becomes evident that CNJSO reveals comparable convergence for the majority of the functions. These results demonstrate that CNJSO decreases premature convergence and improves the balance between local and global search by preserving the continuity around the local and global optima in these functions. Compared to the competing algorithms, CNJSO consistently reaches lower objective function values in fewer iterations, indicating faster and more reliable convergence. This improved performance can be attributed to CNJSO's ability to explore the search space effectively while exploiting promising regions, thereby avoiding local traps and achieving a better approximation of the global optimum across various test functions.

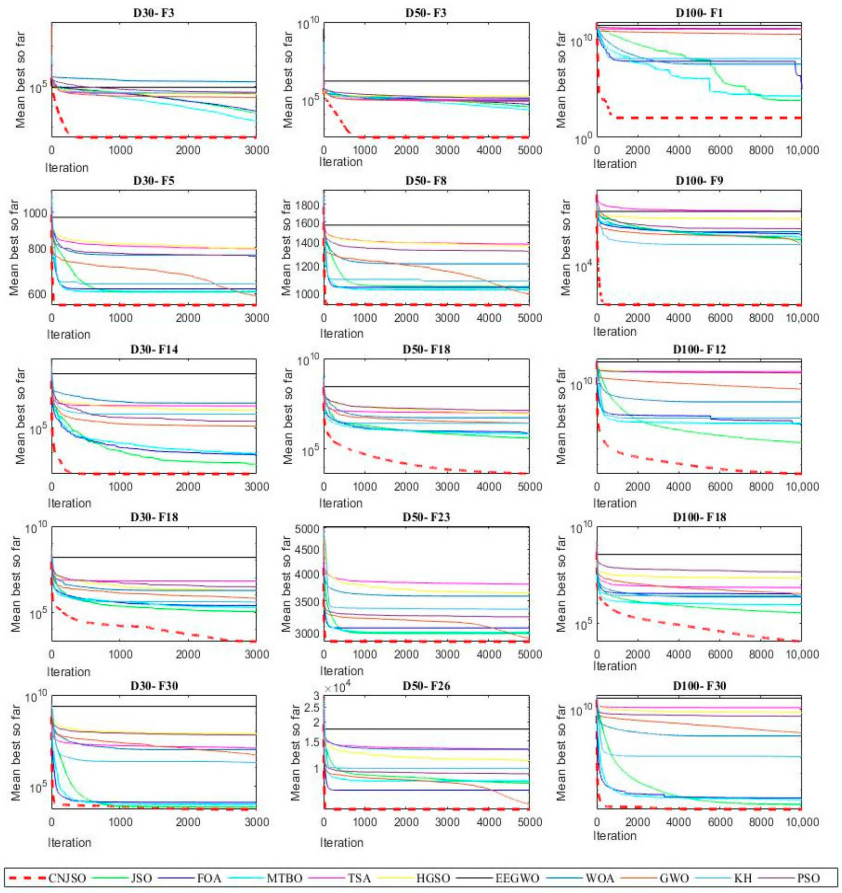


Figure 3. Comparison of convergence behavior of CNJSO and competing algorithms.

5.5. Statistical Analysis

To assess the significance of performance differences between CNJSO and competing algorithms, the non-parametric Wilcoxon rank-sum and Friedman tests were employed.

5.5.1. Non-Parametric Friedman Test

The nonparametric Friedman (F_f) test [107] evaluates whether there are significant differences in performance among two or more algorithms. For each dataset or test case, the algorithms are ranked independently, with the best-performing algorithm assigned rank one and the worst-performing algorithm assigned rank k, while ties are assigned average ranks. The final rank of each algorithm is determined by computing the average of its ranks across all datasets. The Friedman statistic F_f is calculated using Equation (18), where k is the number of algorithms, R_j is the average rank of algorithm j, and n is the number of test cases. This statistic is then compared to a chi-square distribution to test the null hypothesis that all algorithms perform equivalently. The results in Table 6 show that CNJSO outperforms the other algorithms, achieving the top overall rank.

$$F_f = \frac{12n}{k(k+1)}\left[\sum_j R_j^2 - \frac{k(k+1)^2}{4}\right] \tag{18}$$

Table 6. Friedman test results for dimensions 30, 50, and 100.

Alg.	D	F1	F3	F4	F5	F6	F7	F8	F9	F10	F11	F12	F13	F14	F15	F16	F17
PSO	30	7.45	6.60	7.00	6.50	5.75	8.65	7.60	6.95	7.75	7.75	7.30	7.65	5.70	8.05	6.55	7.15
	50	7.55	6.30	7.00	7.30	5.70	9.00	7.10	5.90	7.80	7.30	7.00	7.65	6.70	8.00	7.70	7.95
	100	7.55	6.95	7.40	7.10	6.25	9.00	6.90	6.60	7.95	5.85	7.60	7.55	7.85	7.95	7.45	7.50
KH	30	3.90	6.00	3.65	4.35	5.20	3.45	4.40	5.10	3.60	5.40	4.05	4.00	5.85	4.10	5.00	4.55
	50	4.00	6.55	3.35	3.85	5.30	3.95	4.55	5.00	3.80	6.25	4.00	4.00	4.65	3.85	4.50	4.65
	100	4.20	6.50	3.65	4.10	4.90	4.35	4.25	3.00	3.65	7.00	3.85	4.00	5.40	4.00	4.55	4.55
GWO	30	6.00	4.25	5.15	2.45	2.75	3.10	2.50	3.50	2.10	4.55	5.35	5.00	4.30	5.35	2.90	2.80
	50	6.00	4.40	5.80	2.15	2.35	3.25	2.55	3.80	2.90	5.05	5.65	5.70	4.75	5.60	2.65	2.30
	100	6.00	3.70	6.00	2.30	2.05	2.20	2.00	3.40	2.65	5.15	6.00	6.00	5.30	6.00	2.65	2.15
WOA	30	5.00	8.65	5.55	6.85	7.45	6.85	6.30	7.30	4.95	5.05	5.60	5.65	6.75	5.65	6.65	6.80
	50	5.00	4.90	5.15	6.10	7.25	6.95	6.10	6.95	5.40	4.05	5.30	5.30	5.65	5.35	6.95	6.70
	100	4.80	8.65	4.95	5.85	6.90	6.75	6.05	5.50	5.40	4.00	5.00	5.00	4.00	5.00	6.20	5.80
EEGWO	30	9.00	8.25	9.00	9.00	9.00	8.30	9.00	9.00	9.00	9.00	9.00	9.00	9.00	8.95	9.00	9.00
	50	9.00	9.00	9.00	9.00	9.00	8.00	9.00	9.00	9.00	9.00	9.00	9.00	9.00	9.00	9.00	9.00
	100	9.00	7.75	9.00	9.00	9.00	8.00	9.00	9.00	8.95	9.00	9.00	9.00	9.00	9.00	9.00	9.00
HGSO	30	7.55	5.25	8.00	7.65	7.55	6.20	7.10	6.65	5.85	7.25	7.70	7.35	7.25	6.90	7.50	6.50
	50	7.45	7.85	8.00	7.60	7.75	6.05	7.80	7.90	6.50	7.35	8.00	7.35	8.00	7.00	6.25	6.15
	100	7.45	5.15	7.60	7.90	7.85	6.25	7.95	7.95	6.60	8.00	7.40	7.45	7.15	7.05	7.35	7.50
JSO	30	2.40	2.95	3.30	3.55	2.30	3.25	3.65	2.25	4.35	2.00	2.05	2.20	2.15	2.35	2.65	2.20
	50	2.25	2.95	3.10	4.25	2.70	2.95	3.65	2.05	3.00	2.20	2.10	2.10	2.20	2.80	1.95	2.55
	100	2.55	2.60	3.00	4.35	3.05	3.45	4.15	4.00	3.95	2.00	2.00	2.30	2.00	2.10	3.00	2.65
TSA	30	8.95	7.25	9.25	8.95	8.75	8.40	8.80	9.90	7.05	9.75	9.45	8.60	7.60	8.15	7.55	6.75
	50	9.05	6.85	9.15	9.70	9.60	8.45	9.10	9.85	7.45	10.0	9.45	9.70	8.25	8.80	8.15	7.00
	100	8.35	4.30	9.15	10.00	9.90	8.25	10.0	10.6	8.15	7.95	9.45	9.70	7.45	9.50	8.30	9.85
MTBO	30	2.70	2.05	2.30	3.40	4.00	3.80	3.15	3.20	6.30	2.70	2.90	3.15	3.00	2.65	2.85	4.00
	50	2.75	2.05	2.30	3.55	3.95	3.80	3.25	3.40	5.55	2.75	2.95	2.90	3.05	2.40	3.05	3.80
	100	2.45	2.70	2.40	3.35	4.00	4.00	3.65	4.55	4.80	3.00	3.15	2.70	3.30	2.85	3.20	4.25
FOA	30	3.65	3.50	2.65	4.35	4.95	5.10	4.15	4.90	4.70	3.70	3.70	3.80	3.30	3.75	4.45	5.30
	50	3.70	4.05	2.35	4.10	4.75	5.00	4.15	4.45	5.80	3.45	4.00	3.55	4.15	3.15	4.70	5.15
	100	3.05	5.95	2.35	3.50	4.55	6.05	3.40	5.40	6.05	3.20	3.40	3.65	4.30	3.45	4.20	4.85
CNJSO	30	1.00	1.00	1.05	1.25	1.00	1.40	1.30	1.05	1.10	1.30	1.05	1.00	1.00	1.00	1.90	2.00
	50	1.00	1.00	1.30	1.20	1.00	1.05	1.00	1.00	1.05	1.05	1.00	1.00	1.00	1.00	2.95	1.90
	100	1.00	1.00	1.00	1.05	1.00	1.00	1.05	1.00	1.05	1.00	1.00	1.00	1.00	1.05	1.60	1.60

Alg.		F18	F19	F20	F21	F22	F23	F24	F25	F26	F27	F28	F29	F30	Avg. rank	Overall rank
PSO	30	7.35	8.00	6.80	6.90	6.25	5.65	5.25	8.00	5.50	6.25	7.45	6.50	7.45	6.96	8
	50	7.50	8.00	7.45	6.30	7.90	5.10	4.95	7.25	4.40	5.45	7.15	6.95	7.70	6.97	8
	100	8.00	8.00	7.60	6.20	7.75	4.95	4.65	8.00	3.25	5.10	7.50	7.45	7.10	7.00	7
KH	30	4.00	4.25	5.80	4.75	2.70	5.50	6.25	3.85	5.20	7.70	3.80	5.45	4.35	4.70	5
	50	4.80	4.10	5.40	4.65	4.90	6.10	6.45	3.10	5.50	7.80	3.55	5.10	4.25	4.76	5
	100	5.15	4.00	4.70	5.00	4.00	7.00	7.05	2.80	5.65	7.10	3.45	4.80	4.00	4.71	5
GWO	30	4.25	4.90	3.90	2.30	6.05	2.45	2.10	5.00	2.30	3.55	6.20	3.05	5.10	3.90	4
	50	4.50	5.20	3.15	2.90	3.15	2.00	1.85	6.00	2.10	3.35	6.25	2.50	5.30	3.90	4
	100	5.15	5.85	2.60	2.90	3.20	2.20	1.95	6.00	1.90	2.30	6.00	3.15	5.50	3.87	4
WOA	30	6.20	5.85	6.30	6.75	6.85	6.90	6.70	4.95	7.15	6.50	5.15	7.55	5.55	6.33	6
	50	5.85	5.60	6.85	7.05	5.65	7.15	6.75	4.05	7.80	7.10	5.05	6.85	5.45	6.01	6
	100	4.55	5.15	6.15	7.85	5.10	7.25	7.65	5.00	7.70	5.85	5.00	6.25	5.50	5.82	6
EEGWO	30	9.00	9.00	9.00	9.00	9.00	9.00	9.00	9.00	9.00	9.00	9.00	9.00	9.00	8.95	9
	50	9.00	9.00	9.00	9.00	9.00	9.00	9.00	9.00	9.00	9.00	9.00	9.00	9.00	8.97	9
	100	9.00	9.00	9.00	9.00	9.00	9.00	9.00	9.00	9.00	9.00	9.00	9.00	9.00	8.92	9
HGSO	30	6.95	6.95	6.10	7.35	5.70	7.80	7.80	7.00	6.80	1.10	7.05	5.75	7.55	6.76	7
	50	7.00	7.00	5.75	7.65	5.30	7.65	7.80	7.75	6.60	1.00	6.85	6.90	7.30	6.95	7
	100	7.00	7.00	7.00	6.95	6.20	6.75	6.30	7.00	6.90	7.55	7.50	7.30	7.90	7.17	8

Table 6. *Cont.*

JSO	30	2.60	2.65	2.60	3.20	2.60	3.10	3.45	1.80	3.40	4.40	2.70	2.30	2.20	2.78	2
	50	2.45	2.75	3.05	2.45	1.50	3.25	3.65	3.95	3.90	5.00	3.45	2.60	2.25	2.86	2
	100	2.05	2.25	2.50	2.45	3.00	2.90	3.85	2.80	4.75	3.90	2.85	2.60	2.10	2.94	2
TSA	30	7.10	7.80	7.80	9.35	9.30	9.55	9.40	8.70	8.95	9.75	9.30	7.80	7.45	8.53	10
	50	7.40	8.85	8.10	9.30	7.90	9.65	9.45	9.10	9.25	9.45	9.50	9.05	8.60	8.83	10
	100	7.20	9.55	7.55	9.80	7.60	9.75	9.80	8.30	9.40	8.75	8.60	8.90	10.0	8.83	10
MTBO	30	3.65	2.40	3.15	3.30	4.60	3.25	2.35	3.65	3.55	4.05	2.30	4.20	2.80	3.29	3
	50	2.90	2.35	2.80	3.70	5.65	3.55	2.90	2.10	4.00	4.20	2.05	3.95	2.50	3.25	3
	100	3.10	2.70	3.05	3.60	5.65	3.95	3.50	3.05	4.75	3.15	2.65	3.45	2.75	3.44	3
FOA	30	4.10	3.45	3.60	4.40	3.40	4.25	4.20	2.65	4.10	4.50	2.75	5.25	3.80	4.01	4
	50	3.50	2.65	2.70	5.05	5.45	4.45	4.05	2.25	3.60	5.10	1.95	5.00	3.75	4.00	4
	100	4.95	3.65	3.55	4.55	5.50	4.30	3.80	2.25	3.35	2.80	2.05	3.75	3.35	3.97	3
CNJSO	30	1.00	1.00	1.35	1.45	1.25	1.35	2.10	1.75	2.10	2.45	1.35	1.20	1.00	1.34	**1**
	50	1.00	1.00	1.55	1.30	1.95	1.20	1.65	1.80	1.70	2.10	1.65	1.15	1.25	1.34	**1**
	100	1.00	1.05	2.40	1.05	1.10	1.00	1.05	1.35	1.10	1.05	1.05	1.00	1.15	1.13	**1**

5.5.2. Wilcoxon Rank-Sum

The Wilcoxon rank-sum test [108] is used to evaluate the statistical significance of CNJSO and the competitor algorithm's results. The samples in the rank-sum experiment are assigned ranks, and the sum of the ranks is then determined. In this test, the null hypothesis (H_0) states that there is no significant difference in the performance of the compared algorithms at a significance level of 0.05 when employing the benchmark functions. The *p*-values for dimensions 30, 50, and 100 are shown in Tables 7–9, where an underlined value indicates a *p*-value greater than 0.05. Thus, the results indicate that the null hypothesis is rejected for the majority of functions, and CNJSO demonstrates statistically significant improvements compared to the other algorithms.

Table 7. Wilcoxon signed-rank test results for dimension 30.

F	PSO	KH	GWO	WOA	EEGWO	HGSO	JSO	TSA	MTBO	FOA
1	3.67×10^{-8}	3.67×10^{-8}	3.67×10^{-8}	3.67×10^{-8}	3.67×10^{-8}	3.67×10^{-8}	3.67×10^{-8}	3.67×10^{-8}	3.67×10^{-8}	3.67×10^{-8}
3	3.67×10^{-8}	3.67×10^{-8}	3.67×10^{-8}	3.67×10^{-8}	3.67×10^{-8}	3.67×10^{-8}	3.67×10^{-8}	3.67×10^{-8}	3.67×10^{-8}	3.67×10^{-8}
4	6.28×10^{-8}	6.28×10^{-8}	6.28×10^{-8}	6.28×10^{-8}	6.28×10^{-8}	6.28×10^{-8}	6.28×10^{-8}	6.28×10^{-8}	3.67×10^{-7}	7.17×10^{-6}
5	6.80×10^{-8}	6.80×10^{-8}	6.61×10^{-5}	6.80×10^{-8}	6.80×10^{-8}	6.80×10^{-8}	9.17×10^{-8}	6.80×10^{-8}	4.54×10^{-7}	1.92×10^{-7}
6	8.01×10^{-9}	8.01×10^{-9}	8.01×10^{-9}	8.01×10^{-9}	8.01×10^{-9}	8.01×10^{-9}	8.01×10^{-9}	8.01×10^{-9}	8.01×10^{-9}	8.01×10^{-9}
7	6.80×10^{-8}	7.95×10^{-7}	2.04×10^{-5}	6.80×10^{-8}	6.80×10^{-8}	6.80×10^{-8}	1.20×10^{-6}	6.80×10^{-8}	1.58×10^{-6}	9.17×10^{-8}
8	6.80×10^{-8}	1.23×10^{-7}	4.17×10^{-5}	6.80×10^{-8}	6.80×10^{-8}	6.80×10^{-8}	3.42×10^{-7}	6.80×10^{-8}	9.75×10^{-6}	3.99×10^{-6}
9	6.79×10^{-8}	6.79×10^{-8}	6.79×10^{-8}	6.79×10^{-8}	6.79×10^{-8}	6.79×10^{-8}	7.94×10^{-7}	6.79×10^{-8}	6.79×10^{-8}	6.79×10^{-8}
10	6.80×10^{-8}	6.80×10^{-8}	2.60×10^{-5}	6.80×10^{-8}	6.80×10^{-8}	6.80×10^{-8}	1.92×10^{-7}	6.80×10^{-8}	1.38×10^{-6}	6.80×10^{-8}
11	6.80×10^{-8}	6.80×10^{-8}	6.80×10^{-8}	6.80×10^{-8}	6.80×10^{-8}	6.80×10^{-8}	4.16×10^{-4}	6.80×10^{-8}	1.20×10^{-6}	3.50×10^{-6}
12	6.80×10^{-8}	6.80×10^{-8}	6.80×10^{-8}	6.80×10^{-8}	6.80×10^{-8}	6.80×10^{-8}	2.56×10^{-7}	6.80×10^{-8}	6.80×10^{-8}	6.80×10^{-8}
13	6.80×10^{-8}	6.80×10^{-8}	6.80×10^{-8}	6.80×10^{-8}	6.80×10^{-8}	6.80×10^{-8}	6.80×10^{-8}	6.80×10^{-8}	6.80×10^{-8}	6.80×10^{-8}
14	6.80×10^{-8}	6.80×10^{-8}	6.80×10^{-8}	6.80×10^{-8}	6.80×10^{-8}	6.80×10^{-8}	6.80×10^{-8}	6.80×10^{-8}	6.80×10^{-8}	6.80×10^{-8}
15	6.80×10^{-8}	6.80×10^{-8}	6.80×10^{-8}	6.80×10^{-8}	6.80×10^{-8}	6.80×10^{-8}	6.80×10^{-8}	6.80×10^{-8}	6.80×10^{-8}	6.80×10^{-8}
16	6.80×10^{-8}	5.23×10^{-7}	4.99×10^{-2}	7.90×10^{-8}	6.80×10^{-8}	6.80×10^{-8}	$\underline{1.02 \times 10^{-1}}$	1.43×10^{-7}	$\underline{7.64 \times 10^{-2}}$	6.22×10^{-4}
17	7.90×10^{-8}	2.92×10^{-5}	1.55×10^{-2}	2.22×10^{-7}	6.80×10^{-8}	1.66×10^{-7}	$\underline{3.79 \times 10^{-1}}$	5.23×10^{-7}	$\underline{2.60 \times 10^{-5}}$	7.41×10^{-5}
18	6.80×10^{-8}	6.80×10^{-8}	6.80×10^{-8}	6.80×10^{-8}	6.80×10^{-8}	6.80×10^{-8}	6.80×10^{-8}	6.80×10^{-8}	6.80×10^{-8}	6.80×10^{-8}
19	6.80×10^{-8}	6.80×10^{-8}	6.80×10^{-8}	6.80×10^{-8}	6.80×10^{-8}	6.80×10^{-8}	6.80×10^{-8}	6.80×10^{-8}	6.80×10^{-8}	6.80×10^{-8}
20	6.80×10^{-8}	1.06×10^{-7}	3.07×10^{-6}	1.43×10^{-7}	6.80×10^{-8}	6.80×10^{-8}	1.04×10^{-4}	1.66×10^{-7}	3.75×10^{-4}	1.41×10^{-5}
21	6.80×10^{-8}	9.17×10^{-8}	2.14×10^{-3}	6.80×10^{-8}	6.80×10^{-8}	6.80×10^{-8}	2.36×10^{-6}	6.80×10^{-8}	5.25×10^{-5}	1.25×10^{-5}
22	1.51×10^{-8}	5.28×10^{-6}	1.51×10^{-8}	1.51×10^{-8}	1.51×10^{-8}	1.51×10^{-8}	1.75×10^{-6}	1.51×10^{-8}	1.42×10^{-7}	8.56×10^{-7}
23	6.80×10^{-8}	6.80×10^{-8}	1.93×10^{-2}	6.80×10^{-8}	6.80×10^{-8}	6.80×10^{-8}	3.07×10^{-6}	6.80×10^{-8}	8.60×10^{-6}	9.13×10^{-7}
24	6.80×10^{-8}	6.80×10^{-8}	$\underline{6.95 \times 10^{-1}}$	6.80×10^{-8}	6.80×10^{-8}	6.80×10^{-8}	4.68×10^{-5}	6.80×10^{-8}	$\underline{3.65 \times 10^{-1}}$	3.50×10^{-6}
25	6.80×10^{-8}	3.42×10^{-7}	$\underline{1.23 \times 10^{-7}}$	1.43×10^{-7}	6.80×10^{-8}	6.80×10^{-8}	$\underline{2.39 \times 10^{-1}}$	6.80×10^{-8}	1.16×10^{-4}	2.75×10^{-2}
26	1.92×10^{-7}	1.61×10^{-4}	$\underline{9.09 \times 10^{-2}}$	3.42×10^{-7}	6.80×10^{-8}	6.80×10^{-8}	$\underline{9.79 \times 10^{-3}}$	7.95×10^{-7}	6.22×10^{-4}	3.75×10^{-4}
27	6.80×10^{-8}	6.80×10^{-8}	$\underline{1.23 \times 10^{-2}}$	2.22×10^{-7}	6.80×10^{-8}	1.60×10^{-5}	9.75×10^{-6}	6.80×10^{-8}	4.60×10^{-4}	5.63×10^{-4}
28	2.96×10^{-8}	1.20×10^{-7}	2.96×10^{-8}	2.96×10^{-8}	2.96×10^{-8}	2.96×10^{-8}	7.19×10^{-6}	2.96×10^{-8}	2.55×10^{-5}	1.37×10^{-5}
29	6.80×10^{-8}	9.17×10^{-8}	4.54×10^{-6}	6.80×10^{-8}	6.80×10^{-8}	6.80×10^{-8}	4.60×10^{-4}	6.80×10^{-8}	4.54×10^{-7}	2.56×10^{-7}
30	6.80×10^{-8}	6.80×10^{-8}	6.80×10^{-8}	6.80×10^{-8}	6.80×10^{-8}	6.80×10^{-8}	6.80×10^{-8}	6.80×10^{-8}	9.17×10^{-8}	6.80×10^{-8}

Table 8. Wilcoxon signed-rank test results for dimension 50.

F	PSO	KH	GWO	WOA	EEGWO	HGSO	JSO	TSA	MTBO	FOA
1	4.81×10^{-8}	4.81×10^{-8}	4.81×10^{-8}	4.81×10^{-8}	4.81×10^{-8}	4.81×10^{-8}	4.81×10^{-8}	4.81×10^{-8}	4.81×10^{-8}	4.81×10^{-8}
3	8.01×10^{-9}	8.01×10^{-9}	8.01×10^{-9}	8.01×10^{-9}	8.01×10^{-9}	8.01×10^{-9}	8.01×10^{-9}	8.01×10^{-9}	8.01×10^{-9}	8.01×10^{-9}
4	6.64×10^{-8}	1.18×10^{-6}	6.64×10^{-8}	6.64×10^{-8}	6.64×10^{-8}	6.64×10^{-8}	6.78×10^{-7}	6.64×10^{-8}	8.19×10^{-5}	1.22×10^{-3}
5	6.80×10^{-8}	9.17×10^{-8}	1.79×10^{-4}	6.80×10^{-8}	6.80×10^{-8}	6.80×10^{-8}	9.17×10^{-8}	6.80×10^{-8}	6.01×10^{-7}	3.94×10^{-7}

Table 8. *Cont.*

F	PSO	KH	GWO	WOA	EEGWO	HGSO	JSO	TSA	MTBO	FOA
6	1.94×10^{-8}	1.94×10^{-8}	1.94×10^{-8}	1.94×10^{-8}	1.94×10^{-8}	1.94×10^{-8}	1.94×10^{-8}	1.94×10^{-8}	1.94×10^{-8}	1.94×10^{-8}
7	6.80×10^{-8}	7.90×10^{-8}	2.22×10^{-7}	6.80×10^{-8}	6.80×10^{-8}	6.80×10^{-8}	5.23×10^{-7}	6.80×10^{-8}	1.43×10^{-7}	6.80×10^{-8}
8	6.80×10^{-8}	6.80×10^{-8}	6.92×10^{-7}	6.80×10^{-8}	6.80×10^{-8}	6.80×10^{-8}	6.80×10^{-8}	6.80×10^{-8}	6.80×10^{-8}	4.54×10^{-7}
9	6.80×10^{-8}	6.80×10^{-8}	6.80×10^{-8}	6.80×10^{-8}	6.80×10^{-8}	6.80×10^{-8}	7.90×10^{-8}	6.80×10^{-8}	6.80×10^{-8}	6.80×10^{-8}
10	6.80×10^{-8}	6.80×10^{-8}	6.01×10^{-7}	6.80×10^{-8}	6.80×10^{-8}	6.80×10^{-8}	2.56×10^{-7}	6.80×10^{-8}	6.80×10^{-8}	6.80×10^{-8}
11	6.80×10^{-8}	6.80×10^{-8}	6.80×10^{-8}	6.80×10^{-8}	6.80×10^{-8}	6.80×10^{-8}	4.54×10^{-6}	6.80×10^{-8}	1.43×10^{-7}	1.06×10^{-7}
12	6.80×10^{-8}	6.80×10^{-8}	6.80×10^{-8}	6.80×10^{-8}	6.80×10^{-8}	6.80×10^{-8}	6.80×10^{-8}	6.80×10^{-8}	6.80×10^{-8}	6.80×10^{-8}
13	6.80×10^{-8}	6.80×10^{-8}	6.80×10^{-8}	6.80×10^{-8}	6.80×10^{-8}	6.80×10^{-8}	6.80×10^{-8}	6.80×10^{-8}	6.80×10^{-8}	6.80×10^{-8}
14	6.80×10^{-8}	6.80×10^{-8}	6.80×10^{-8}	6.80×10^{-8}	6.80×10^{-8}	6.80×10^{-8}	6.80×10^{-8}	6.80×10^{-8}	6.80×10^{-8}	6.80×10^{-8}
15	6.80×10^{-8}	6.80×10^{-8}	6.80×10^{-8}	6.80×10^{-8}	6.80×10^{-8}	6.80×10^{-8}	6.80×10^{-8}	6.80×10^{-8}	6.80×10^{-8}	6.80×10^{-8}
16	6.80×10^{-8}	7.58×10^{-4}	$\underline{4.73 \times 10^{-1}}$	1.06×10^{-7}	6.80×10^{-8}	6.80×10^{-8}	1.55×10^{-2}	6.80×10^{-8}	$\underline{9.46 \times 10^{-1}}$	5.56×10^{-3}
17	6.80×10^{-8}	2.22×10^{-7}	$\underline{9.09 \times 10^{-2}}$	6.80×10^{-8}	6.80×10^{-8}	6.80×10^{-8}	1.93×10^{-2}	1.06×10^{-7}	$\underline{5.25 \times 10^{-5}}$	1.05×10^{-6}
18	6.80×10^{-8}	6.80×10^{-8}	$\underline{6.80 \times 10^{-8}}$	6.80×10^{-8}	6.80×10^{-8}	6.80×10^{-8}	6.80×10^{-8}	6.80×10^{-8}	6.80×10^{-8}	6.80×10^{-8}
19	6.80×10^{-8}	6.80×10^{-8}	6.80×10^{-8}	6.80×10^{-8}	6.80×10^{-8}	6.80×10^{-8}	6.80×10^{-8}	6.80×10^{-8}	6.80×10^{-8}	6.80×10^{-8}
20	6.80×10^{-8}	6.01×10^{-7}	2.75×10^{-4}	6.80×10^{-8}	6.80×10^{-8}	6.80×10^{-8}	3.38×10^{-4}	6.80×10^{-8}	9.21×10^{-4}	$\underline{7.20 \times 10^{-2}}$
21	6.80×10^{-8}	7.90×10^{-8}	1.41×10^{-5}	6.80×10^{-8}	6.80×10^{-8}	6.80×10^{-8}	1.79×10^{-4}	6.80×10^{-8}	4.54×10^{-7}	$\underline{3.42 \times 10^{-7}}$
22	6.80×10^{-8}	1.06×10^{-7}	8.60×10^{-6}	6.80×10^{-8}	6.80×10^{-8}	2.56×10^{-7}	1.23×10^{-3}	3.42×10^{-7}	3.94×10^{-7}	3.94×10^{-7}
23	6.80×10^{-8}	6.80×10^{-8}	2.75×10^{-4}	6.80×10^{-8}	6.80×10^{-8}	6.80×10^{-8}	1.80×10^{-6}	6.80×10^{-8}	3.94×10^{-7}	1.43×10^{-7}
24	6.80×10^{-8}	6.80×10^{-8}	2.94×10^{-2}	6.80×10^{-8}	6.80×10^{-8}	6.80×10^{-8}	2.36×10^{-6}	6.80×10^{-8}	1.78×10^{-3}	3.07×10^{-6}
25	6.80×10^{-8}	2.34×10^{-3}	6.80×10^{-8}	2.30×10^{-5}	6.80×10^{-8}	6.80×10^{-8}	3.07×10^{-6}	6.80×10^{-8}	$\underline{5.98 \times 10^{-1}}$	$\underline{4.90 \times 10^{-1}}$
26	6.80×10^{-8}	6.80×10^{-8}	8.36×10^{-4}	6.80×10^{-8}	6.80×10^{-8}	6.80×10^{-8}	3.15×10^{-2}	6.80×10^{-8}	1.60×10^{-5}	9.17×10^{-8}
27	6.80×10^{-8}	6.80×10^{-8}	7.95×10^{-7}	6.80×10^{-8}	6.80×10^{-8}	6.80×10^{-8}	6.80×10^{-8}	6.80×10^{-8}	1.92×10^{-7}	3.94×10^{-7}
28	6.73×10^{-8}	2.03×10^{-5}	6.73×10^{-8}	6.73×10^{-8}	6.73×10^{-8}	3.47×10^{-6}	2.05×10^{-6}	6.73×10^{-8}	$\underline{4.25 \times 10^{-1}}$	$\underline{8.82 \times 10^{-1}}$
29	6.80×10^{-8}	6.80×10^{-8}	2.69×10^{-6}	6.80×10^{-8}	6.80×10^{-8}	6.80×10^{-8}	1.58×10^{-6}	6.80×10^{-8}	$\underline{6.80 \times 10^{-8}}$	$\underline{6.80 \times 10^{-8}}$
30	6.80×10^{-8}	6.80×10^{-8}	6.80×10^{-8}	6.80×10^{-8}	6.80×10^{-8}	6.80×10^{-8}	2.04×10^{-5}	6.80×10^{-8}	7.58×10^{-6}	1.66×10^{-7}

Table 9. Wilcoxon signed-rank test results for dimension 100.

F	PSO	KH	GWO	WOA	EEGWO	HGSO	JSO	TSA	MTBO	FOA
1	6.28×10^{-8}	6.28×10^{-8}	6.28×10^{-8}	6.28×10^{-8}	6.28×10^{-8}	6.28×10^{-8}	6.28×10^{-8}	6.28×10^{-8}	6.28×10^{-8}	6.28×10^{-8}
3	2.43×10^{-8}	2.43×10^{-8}	2.43×10^{-8}	2.43×10^{-8}	2.43×10^{-8}	2.43×10^{-8}	2.43×10^{-8}	2.43×10^{-8}	2.43×10^{-8}	2.43×10^{-8}
4	6.69×10^{-8}	6.69×10^{-8}	6.69×10^{-8}	6.69×10^{-8}	6.69×10^{-8}	6.69×10^{-8}	6.69×10^{-8}	6.69×10^{-8}	6.69×10^{-8}	6.69×10^{-8}
5	6.80×10^{-8}	6.80×10^{-8}	6.01×10^{-7}	6.80×10^{-8}	6.80×10^{-8}	6.80×10^{-8}	6.80×10^{-8}	6.80×10^{-8}	6.80×10^{-8}	9.17×10^{-8}
6	4.36×10^{-8}	4.36×10^{-8}	4.36×10^{-8}	4.36×10^{-8}	4.36×10^{-8}	4.36×10^{-8}	4.36×10^{-8}	4.36×10^{-8}	4.36×10^{-8}	4.36×10^{-8}
7	6.80×10^{-8}	6.80×10^{-8}	1.23×10^{-7}	6.80×10^{-8}	6.80×10^{-8}	6.80×10^{-8}	1.43×10^{-7}	6.80×10^{-8}	6.80×10^{-8}	6.80×10^{-8}
8	6.80×10^{-8}	6.80×10^{-8}	7.95×10^{-7}	6.80×10^{-8}	6.80×10^{-8}	6.80×10^{-8}	6.80×10^{-8}	6.80×10^{-8}	6.80×10^{-8}	9.17×10^{-8}
9	6.80×10^{-8}	6.80×10^{-8}	6.80×10^{-8}	6.80×10^{-8}	6.80×10^{-8}	6.80×10^{-8}	6.80×10^{-8}	6.80×10^{-8}	6.80×10^{-8}	6.80×10^{-8}
10	6.80×10^{-8}	6.80×10^{-8}	1.92×10^{-7}	6.80×10^{-8}	6.80×10^{-8}	6.80×10^{-8}	1.43×10^{-7}	6.80×10^{-8}	5.23×10^{-7}	6.80×10^{-8}
11	6.80×10^{-8}	6.80×10^{-8}	6.80×10^{-8}	6.80×10^{-8}	6.80×10^{-8}	6.80×10^{-8}	6.80×10^{-8}	6.80×10^{-8}	6.80×10^{-8}	6.80×10^{-8}
12	6.80×10^{-8}	6.80×10^{-8}	6.80×10^{-8}	6.80×10^{-8}	6.80×10^{-8}	6.80×10^{-8}	6.80×10^{-8}	6.80×10^{-8}	6.80×10^{-8}	6.80×10^{-8}
13	6.80×10^{-8}	6.80×10^{-8}	6.80×10^{-8}	6.80×10^{-8}	6.80×10^{-8}	6.80×10^{-8}	6.80×10^{-8}	6.80×10^{-8}	6.80×10^{-8}	6.80×10^{-8}
14	6.80×10^{-8}	6.80×10^{-8}	6.80×10^{-8}	6.80×10^{-8}	6.80×10^{-8}	6.80×10^{-8}	6.80×10^{-8}	6.80×10^{-8}	6.80×10^{-8}	6.80×10^{-8}
15	6.80×10^{-8}	6.80×10^{-8}	6.80×10^{-8}	6.80×10^{-8}	6.80×10^{-8}	6.80×10^{-8}	1.58×10^{-6}	6.80×10^{-8}	6.80×10^{-8}	6.80×10^{-8}
16	6.80×10^{-8}	5.23×10^{-7}	6.56×10^{-3}	6.80×10^{-8}	6.80×10^{-8}	6.80×10^{-8}	1.44×10^{-4}	6.80×10^{-8}	8.29×10^{-5}	9.28×10^{-5}
17	6.80×10^{-8}	1.23×10^{-7}	$\underline{1.33 \times 10^{-1}}$	6.80×10^{-8}	6.80×10^{-8}	6.80×10^{-8}	1.61×10^{-4}	6.80×10^{-8}	1.38×10^{-6}	1.20×10^{-6}
18	6.80×10^{-8}	6.80×10^{-8}	$\underline{6.80 \times 10^{-8}}$	6.80×10^{-8}	6.80×10^{-8}	6.80×10^{-8}	6.80×10^{-8}	6.80×10^{-8}	6.80×10^{-8}	6.80×10^{-8}
19	6.80×10^{-8}	6.80×10^{-8}	6.80×10^{-8}	6.80×10^{-8}	6.80×10^{-8}	6.80×10^{-8}	1.38×10^{-6}	6.80×10^{-8}	6.80×10^{-8}	6.80×10^{-8}
20	6.80×10^{-8}	2.96×10^{-7}	$\underline{3.23 \times 10^{-1}}$	6.80×10^{-8}	6.80×10^{-8}	6.80×10^{-8}	$\underline{6.17 \times 10^{-1}}$	6.80×10^{-8}	$\underline{1.90 \times 10^{-1}}$	2.94×10^{-2}
21	6.80×10^{-8}	6.80×10^{-8}	$\underline{2.56 \times 10^{-7}}$	6.80×10^{-8}	6.80×10^{-8}	6.80×10^{-8}	$\underline{3.94 \times 10^{-7}}$	6.80×10^{-8}	$\underline{1.43 \times 10^{-7}}$	6.80×10^{-8}
22	6.80×10^{-8}	6.80×10^{-8}	6.01×10^{-7}	6.80×10^{-8}	6.80×10^{-8}	6.80×10^{-8}	1.60×10^{-5}	6.80×10^{-8}	9.13×10^{-7}	6.80×10^{-8}
23	6.80×10^{-8}	6.80×10^{-8}	6.80×10^{-8}	6.80×10^{-8}	6.80×10^{-8}	6.80×10^{-8}	6.80×10^{-8}	6.80×10^{-8}	6.80×10^{-8}	6.80×10^{-8}
24	6.80×10^{-8}	6.80×10^{-8}	1.38×10^{-6}	6.80×10^{-8}	6.80×10^{-8}	6.80×10^{-8}	6.80×10^{-8}	6.80×10^{-8}	6.80×10^{-8}	6.80×10^{-8}
25	6.80×10^{-8}	2.75×10^{-4}	6.80×10^{-8}	6.80×10^{-8}	6.80×10^{-8}	6.80×10^{-8}	5.90×10^{-5}	6.80×10^{-8}	5.25×10^{-5}	$\underline{5.08 \times 10^{-1}}$
26	6.80×10^{-8}	6.80×10^{-8}	1.41×10^{-5}	6.80×10^{-8}	6.80×10^{-8}	6.80×10^{-8}	6.80×10^{-8}	6.80×10^{-8}	6.80×10^{-8}	$\underline{6.80 \times 10^{-8}}$
27	6.80×10^{-8}	6.80×10^{-8}	1.92×10^{-7}	6.80×10^{-8}	6.80×10^{-8}	6.80×10^{-8}	6.80×10^{-8}	6.80×10^{-8}	1.06×10^{-7}	2.69×10^{-6}
28	4.94×10^{-8}	4.94×10^{-8}	4.94×10^{-8}	4.94×10^{-8}	4.94×10^{-8}	4.94×10^{-8}	4.94×10^{-8}	4.94×10^{-8}	1.65×10^{-7}	1.15×10^{-5}
29	6.80×10^{-8}	6.80×10^{-8}	6.80×10^{-8}	6.80×10^{-8}	6.80×10^{-8}	6.80×10^{-8}	1.06×10^{-7}	6.80×10^{-8}	6.80×10^{-8}	6.80×10^{-8}
30	6.80×10^{-8}	6.80×10^{-8}	6.80×10^{-8}	6.80×10^{-8}	6.80×10^{-8}	6.80×10^{-8}	9.13×10^{-7}	6.80×10^{-8}	2.22×10^{-7}	1.66×10^{-7}

5.6. Sensitivity Analysis

Three sets of experiments were conducted to analyze the sensitivity of the CNJSO, using population sizes of 30, 50, and 100 and varying γ values for a problem dimension of 10. Table 10 displays the experimental results of CNJSO gained for all the benchmark functions, including unimodal, multimodal, hybrid, and composite with different parameters γ, and the results of the Friedman test. In the first set of experiments, the population size was fixed at 30, and the algorithm's performance was assessed using four different values of γ: 0.05, 0.1, 0.2, and 3.0. The results demonstrate the impact of varying the γ parameter on performance rankings, as measured using the Friedman test for a population size of 30. With γ = 0.05, the algorithm achieved the lowest rank, 4th place, indicating comparatively weaker performance.

Increasing γ to 0.1 improved the results, yielding a rank of 3. At γ = 0.2, performance was further enhanced with a rank of 2, showing a consistent upward trend. Finally, at γ = 1.0, the algorithm achieved the best rank, 1st place, indicating that this setting optimizes performance under the given conditions.

Table 10. Sensitivity analysis results for dimension 10.

	N = 30				N = 50				N = 100			
Fun	γ = 0.05	γ = 0.1	γ = 0.2	γ = 0.3	γ = 0.05	γ = 0.1	γ = 0.2	γ = 0.3	γ = 0.05	γ = 0.1	γ = 0.2	γ = 0.3
1	1.13×10^{-12}	2.47×10^{-13}	5.68×10^{-15}	7.53×10^{-14}	5.17×10^{9}	7.11×10^{-16}	4.97×10^{-15}	5.23×10^{-13}	0	0	0	0
3	0	0	0	0	3.82×10^{4}	0	0	0	0	0	0	0
4	7.67×10^{-14}	1.25×10^{-13}	1.25×10^{-13}	8.81×10^{-14}	5.11×10^{2}	3.41×10^{-14}	4.55×10^{-14}	2.56×10^{-14}	3.98×10^{-14}	1.99×10^{-14}	4.26×10^{-14}	1.99×10^{-14}
5	9.05×10^{0}	6.67×10^{0}	6.37×10^{0}	6.07×10^{0}	7.10×10^{1}	5.97×10^{0}	5.92×10^{0}	6.17×10^{0}	5.62×10^{0}	7.21×10^{0}	5.87×10^{0}	4.88×10^{0}
6	0	0	0	0	2.84×10^{1}	0	0	0	0	0	0	0
7	1.54×10^{1}	1.58×10^{1}	1.76×10^{1}	1.55×10^{1}	1.52×10^{2}	1.58×10^{1}	1.47×10^{1}	1.56×10^{1}	1.48×10^{1}	1.46×10^{1}	1.54×10^{1}	1.47×10^{1}
8	9.05×10^{0}	6.67×10^{0}	6.57×10^{0}	7.11×10^{0}	8.24×10^{1}	7.36×10^{0}	6.07×10^{0}	8.71×10^{0}	6.42×10^{0}	7.16×10^{0}	5.42×10^{0}	4.68×10^{0}
9	8.95×10^{-3}	4.48×10^{-3}	0	0	1.46×10^{3}	0	0	0	0	0	0	0
10	2.22×10^{2}	2.26×10^{2}	1.55×10^{2}	1.66×10^{2}	1.79×10^{3}	1.33×10^{2}	1.45×10^{2}	1.38×10^{2}	1.09×10^{2}	1.12×10^{2}	1.49×10^{2}	9.60×10^{1}
11	3.90×10^{0}	4.08×10^{0}	4.89×10^{0}	4.63×10^{0}	5.53×10^{2}	4.11×10^{0}	3.49×10^{0}	3.03×10^{0}	3.25×10^{0}	2.62×10^{0}	3.71×10^{0}	3.08×10^{0}
12	1.28×10^{2}	1.46×10^{2}	1.45×10^{2}	1.67×10^{2}	7.66×10^{7}	1.94×10^{2}	1.03×10^{2}	8.05×10^{1}	1.18×10^{2}	1.19×10^{2}	1.30×10^{2}	1.16×10^{2}
13	7.24×10^{0}	6.48×10^{0}	6.61×10^{0}	8.86×10^{0}	9.42×10^{4}	6.59×10^{0}	5.95×10^{0}	6.69×10^{0}	4.84×10^{0}	6.73×10^{0}	5.53×10^{0}	5.27×10^{0}
14	3.88×10^{0}	4.08×10^{0}	3.04×10^{0}	3.13×10^{0}	1.28×10^{3}	3.08×10^{0}	3.63×10^{0}	2.89×10^{0}	3.23×10^{0}	2.84×10^{0}	2.29×10^{0}	2.69×10^{0}
15	1.26×10^{0}	1.95×10^{0}	1.62×10^{0}	9.98×10^{-1}	6.80×10^{5}	2.11×10^{0}	1.48×10^{0}	1.05×10^{0}	1.32×10^{0}	1.32×10^{0}	1.46×10^{0}	9.11×10^{-1}
16	6.32×10^{1}	3.37×10^{1}	2.57×10^{1}	2.46×10^{1}	4.36×10^{2}	2.52×10^{1}	4.41×10^{1}	2.41×10^{1}	9.81×10^{-1}	3.20×10^{1}	6.78×10^{0}	1.41×10^{0}
17	1.41×10^{1}	7.38×10^{0}	7.03×10^{0}	4.80×10^{0}	2.63×10^{2}	1.27×10^{1}	5.85×10^{0}	1.42×10^{0}	5.20×10^{0}	2.92×10^{0}	1.62×10^{0}	1.61×10^{0}
18	5.18×10^{-1}	3.15×10^{-1}	7.23×10^{-1}	3.59×10^{-1}	5.35×10^{5}	6.20×10^{-1}	6.21×10^{-1}	7.71×10^{-1}	4.07×10^{-1}	6.18×10^{-1}	5.17×10^{-1}	5.04×10^{-1}
19	7.20×10^{-1}	3.74×10^{-1}	6.18×10^{-1}	4.29×10^{-1}	6.59×10^{5}	3.30×10^{-1}	4.17×10^{-1}	2.30×10^{-1}	4.21×10^{-1}	2.14×10^{-1}	3.57×10^{-1}	4.17×10^{-1}
20	4.92×10^{-1}	2.71×10^{0}	4.11×10^{-1}	1.02×10^{0}	1.59×10^{2}	4.95×10^{-1}	3.64×10^{-1}	1.31×10^{-1}	4.26×10^{-1}	4.68×10^{-2}	2.30×10^{-1}	1.96×10^{-1}
21	1.58×10^{2}	1.79×10^{2}	1.85×10^{2}	1.56×10^{2}	2.49×10^{2}	1.73×10^{2}	1.45×10^{2}	1.62×10^{2}	1.51×10^{2}	1.50×10^{2}	1.55×10^{2}	1.28×10^{2}
22	9.44×10^{1}	9.68×10^{1}	9.87×10^{1}	1.02×10^{2}	9.59×10^{2}	9.34×10^{1}	9.09×10^{1}	9.24×10^{1}	8.48×10^{1}	9.73×10^{1}	9.75×10^{1}	8.87×10^{1}
23	3.13×10^{2}	3.11×10^{2}	3.13×10^{2}	3.11×10^{2}	3.86×10^{2}	3.13×10^{2}	3.14×10^{2}	3.10×10^{2}	3.12×10^{2}	3.10×10^{2}	3.10×10^{2}	3.10×10^{2}
24	3.09×10^{2}	3.25×10^{2}	3.27×10^{2}	3.22×10^{2}	4.02×10^{2}	3.32×10^{2}	2.95×10^{2}	2.85×10^{2}	2.62×10^{2}	2.61×10^{2}	2.81×10^{2}	2.92×10^{2}
25	4.23×10^{2}	4.29×10^{2}	4.30×10^{2}	4.29×10^{2}	7.80×10^{2}	4.16×10^{2}	4.27×10^{2}	4.29×10^{2}	4.20×10^{2}	4.15×10^{2}	4.31×10^{2}	4.22×10^{2}
26	2.67×10^{2}	4.10×10^{2}	2.88×10^{2}	3.00×10^{2}	9.78×10^{2}	2.65×10^{2}	3.13×10^{2}	3.12×10^{2}	3.02×10^{2}	3.00×10^{2}	2.99×10^{2}	2.90×10^{2}
27	3.96×10^{2}	3.96×10^{2}	3.96×10^{2}	3.95×10^{2}	4.75×10^{2}	3.95×10^{2}	3.95×10^{2}	3.95×10^{2}	3.94×10^{2}	3.95×10^{2}	3.93×10^{2}	3.93×10^{2}
28	4.19×10^{2}	3.38×10^{2}	3.31×10^{2}	3.57×10^{2}	8.75×10^{2}	2.90×10^{2}	3.46×10^{2}	3.28×10^{2}	3.16×10^{2}	2.85×10^{2}	3.24×10^{2}	3.10×10^{2}
29	2.59×10^{2}	2.61×10^{2}	2.54×10^{2}	2.67×10^{2}	5.95×10^{2}	2.54×10^{2}	2.49×10^{2}	2.52×10^{2}	2.44×10^{2}	2.48×10^{2}	2.48×10^{2}	2.40×10^{2}
30	8.22×10^{4}	5.43×10^{2}	4.14×10^{4}	4.14×10^{4}	7.53×10^{6}	6.02×10^{2}	6.07×10^{2}	5.19×10^{2}	4.14×10^{4}	5.83×10^{2}	5.54×10^{2}	7.13×10^{2}
Friedman Rank	4.00	3.00	2.00	1.00	4.00	3.00	2.00	1.00	1.00	2.00	3.00	4.00

For the second set of experiments, the population size was set to 50, and the algorithm was evaluated with γ values of 0.05, 0.1, 0.2, and 0.3. The results show a clear trend of improved performance with increasing γ. Specifically, with γ = 0.05, the algorithm ranked 4th, indicating the weakest performance. Increasing γ to 0.1 and 0.2 led to ranks of 3 and 2, respectively. The best performance was achieved at γ = 0.3, where the algorithm obtained the top rank, 1st place. For the third set of experiments, the population size was increased to 100, and the algorithm was tested with γ values of 0.05, 0.1, 0.2, and 0.3. The results differed from those of other comparative population sizes and revealed that the most suitable performance was obtained when γ = 0.05. Therefore, the results verify that the effect of parameter γ decreases as the population size increases. These results indicated that variations in population size and the γ coefficient influence the performance of the CNJSO algorithm.

6. Applicability of CNJSO for Solving Optimal Power Flow Problems

The Optimal Power Flow (OPF) problem is a fundamental challenge in electrical engineering, focused on optimizing the distribution of electrical power across a network. It represents a class of non-linear optimization problems that are constrained by the operational limits of the power system and the governing power flow equations [109]. This optimization ensures the network operates efficiently, adhering to various constraints, including power balance, voltage limits, and system stability. These problems are inherently complex and representative of real-world power system operations. As such, they provide a rigorous test for optimization algorithms. This section investigates the applicability of CNJSO in addressing complex OPF problems, using the IEEE 30-bus and 118-bus systems as benchmark cases.

6.1. Optimal Power Flow Problem for IEEE 30-Bus System

The IEEE 30–bus system comprises six generators, four transformers, and nine shunt VAR compensation buses. The lower and upper bounds of the transformer tap are set to 0.9 and 1.1 p.u. The minimum and maximum values of voltages for all generator buses and the shunt VAR compensations are 0.95, 1.1, 0.0, and 0.05 p.u, respectively. The schematic of the IEEE 30-bus is shown in Figure 4.

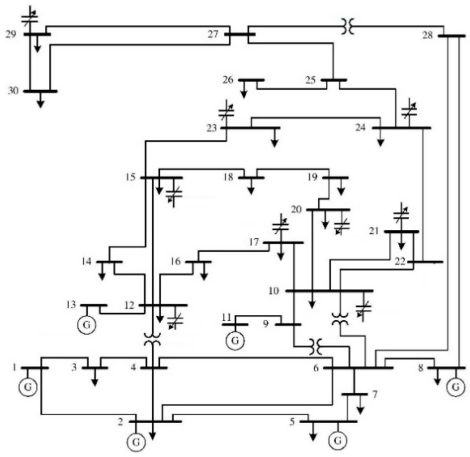


Figure 4. IEEE 30-bus test system single-line diagram.

Case 1: Minimization of the fuel cost

The minimization of fuel cost for all generators is defined as the objective function f_1 and is computed using Equation (19).

$$f_1 = \sum_{i=1}^{NG}\left(a_i + b_i P_{Gi} + c_i P_{Gi}^2\right) \tag{19}$$

where a_i, b_i, and c_i specify the cost coefficients of the generator i. For P_{Gi} (in MW), the coefficients a_i, b_i, and c_i are expressed in \$/hr, \$/MWh, and S/MW^{2}h, respectively.

Case 2: Voltage profile improvement

The objective function f_2 considers both fuel cost minimization and voltage deviation minimization and is calculated using Equation (20).

$$f_2 = \sum_{i=1}^{NG}\left(a_i + b_i P_{Gi} + c_i P_{Gi}^2\right) + w_v \sum_{i=1}^{NL} |V_i - 1.0| \tag{20}$$

where the weighting factor for voltage deviation is w_v, and its value is set to 200.

6.2. Optimal Power Flow Problem for IEEE 118-Bus System

The IEEE 118-bus test problem has 54 generators, 186 branches, nine transformers, two reactors, and 12 capacitors. The control variables consist of the 54 generator outputs, nine settings for transformers, and 12 shunt capacitor reactive power injections. The voltage limits of all buses are between 0.94 and 1.06 p.u. The transformer tap settings are within the interval of 0.90–1.10 p.u. The available reactive powers of shunt capacitors are considered in the range of 0–30 MVAR. Similar to Cases 1 and 2, the objectives of this problem are to minimize the total fuel cost of all generators and improve the voltage profile. The schematic of the system is shown in Figure 5.

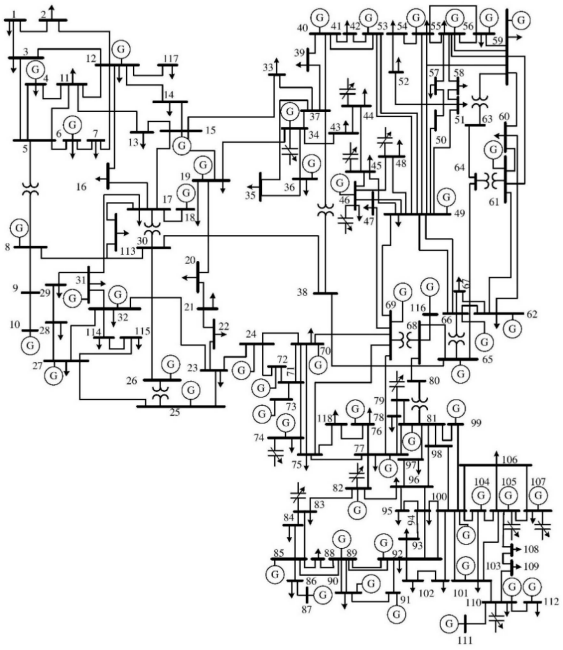


Figure 5. IEEE 118-bus test system single-line diagram.

Tables 11–14 tabulate the findings of the comparative algorithms and CNJSO to solve OPF problems. The population size, maximum number of iterations, and number of runs are set at 50, 200, and 20, respectively. The experimental results demonstrate that the proposed CNJSO algorithm outperforms the competing algorithms in addressing these engineering problems.

Table 11. OPF problem results for Case 1 using the IEEE 30-bus test system.

DVs	PSO	KH	GWO	WOA	EEGWO	HGSO	JSO	TSA	MTBO	FOA	CNJSO
P_{G1} (MW)	186.735	176.423	181.154	174.540	162.171	179.079	176.882	171.501	177.059	177.114	177.117
P_{G2} (MW)	52.375	48.924	48.275	49.837	48.990	36.109	48.476	32.319	48.714	48.677	48.716
P_{G5} (MW)	20.786	21.308	22.908	19.989	19.507	31.926	21.375	23.096	21.382	21.410	21.383
P_{G8} (MW)	12.085	20.848	15.088	22.013	17.259	13.366	21.574	34.892	21.263	21.345	21.269
P_{G11} (MW)	10.000	13.160	12.736	10.985	27.963	12.756	11.967	14.801	12.010	11.879	11.946
P_{G13} (MW)	12.000	12.000	12.664	15.412	16.462	20.164	12.157	15.199	12.003	12.006	12.000
V_{G1} (p.u.)	1.087	1.078	1.088	1.072	1.073	1.051	1.083	1.075	1.084	1.083	1.084
V_{G2} (p.u.)	1.062	1.060	1.070	1.059	1.063	1.014	1.063	1.049	1.065	1.064	1.065
V_{G5} (p.u.)	1.003	1.031	1.043	1.039	1.003	0.958	1.032	1.013	1.033	1.033	1.034
V_{G8} (p.u.)	1.035	1.041	1.043	1.034	1.033	0.985	1.036	1.023	1.038	1.037	1.038
V_{G11} (p.u.)	1.050	1.041	1.061	1.088	1.028	1.062	1.085	1.047	1.081	1.082	1.093
V_{G13} (p.u.)	1.036	1.004	1.035	1.021	1.083	0.988	1.054	1.014	1.047	1.046	1.043
$T_{11(6-9)}$ (p.u.)	1.100	0.985	1.004	0.973	1.091	1.001	1.009	0.929	1.029	1.081	1.035
$T_{12(6-10)}$ (p.u.)	0.975	1.046	0.985	0.973	1.017	1.014	0.969	1.076	0.941	0.900	0.940
$T_{15(4-12)}$ (p.u.)	0.949	1.000	0.948	1.093	0.984	1.010	0.980	1.032	0.969	0.968	0.964
$T_{36(28-27)}$ (p.u.)	0.949	1.031	0.969	0.974	0.981	0.905	0.982	0.981	0.972	0.972	0.974
Q_{C10} (MVAR)	0.000	2.315	2.250	1.416	3.058	2.182	2.551	4.491	4.935	3.425	0.272
Q_{C12} (MVAR)	5.000	1.257	1.960	3.850	3.857	3.718	1.582	4.261	2.427	2.617	1.858
Q_{C15} (MVAR)	5.000	1.036	2.736	3.237	3.319	3.201	2.864	1.845	3.366	4.173	4.351
Q_{C17} (MVAR)	5.000	1.239	3.681	2.658	2.343	0.234	4.824	4.860	2.640	4.982	4.999
Q_{C20} (MVAR)	0.000	2.591	2.131	0.468	0.072	2.199	4.605	3.937	4.045	4.758	4.252
Q_{C21} (MVAR)	2.925	2.587	2.165	0.768	1.039	2.485	1.757	2.992	4.997	4.959	5.000
Q_{C23} (MVAR)	0.000	3.052	0.175	1.934	1.123	3.399	4.354	1.998	3.556	2.208	3.298
Q_{C24} (MVAR)	4.240	2.621	4.955	3.633	0.778	2.530	4.749	2.408	4.984	4.993	5.000
Q_{C29} (MVAR)	0.000	4.663	0.907	1.507	1.918	0.034	2.718	4.726	2.656	2.297	2.543
Cost ($/h)	804.280	801.545	801.538	802.686	812.159	817.978	800.623	809.378	800.539	800.532	**800.521**
Ploss (MW)	10.582	9.263	9.424	9.374	8.951	10.000	9.031	8.409	9.032	9.031	**9.031**
VD (p.u.)	0.376	0.451	0.687	0.394	0.412	0.507	0.827	0.293	0.912	0.878	**0.908**

Table 12. OPF problem results for Case 2 using the IEEE 30-bus test system.

DVs	PSO	KH	GWO	WOA	EEGWO	HGSO	JSO	TSA	MTBO	FOA	CNJSO
P_{G1} (MW)	184.317	174.586	145.215	186.910	147.127	163.265	170.502	178.676	176.146	177.074	175.895
P_{G2} (MW)	63.362	44.213	58.991	44.166	54.029	44.769	48.357	26.450	48.916	49.216	48.918
P_{G5} (MW)	15.000	21.272	26.123	26.431	25.618	15.435	22.080	27.009	21.568	21.722	21.676
P_{G8} (MW)	10.000	20.329	30.949	12.559	16.026	21.369	22.334	31.109	23.491	22.156	22.481
P_{G11} (MW)	10.000	15.406	14.851	11.262	17.916	21.097	17.006	16.129	11.211	10.900	12.347
P_{G13} (MW)	12.000	17.188	15.191	12.814	30.496	26.831	12.670	13.057	12.006	12.370	12.000
V_{G1} (p.u.)	1.053	1.039	1.049	1.049	1.073	1.039	1.032	1.054	1.036	1.038	1.040
V_{G2} (p.u.)	1.026	1.027	1.033	1.040	1.054	1.034	1.019	1.029	1.025	1.022	1.025
V_{G5} (p.u.)	1.002	1.014	1.020	1.028	1.018	0.983	1.018	0.994	1.015	1.018	1.016
V_{G8} (p.u.)	0.999	1.002	1.000	1.002	1.028	1.002	1.004	1.001	1.007	1.002	1.009
V_{G11} (p.u.)	1.035	1.024	1.010	1.007	1.017	1.065	1.015	1.055	1.031	1.036	1.012
V_{G13} (p.u.)	1.032	1.021	1.003	0.999	1.035	0.977	1.008	0.993	0.988	0.998	0.989
$T_{11(6–9)}$ (p.u.)	0.908	0.948	0.997	0.974	0.925	0.995	1.029	0.922	1.050	1.053	1.029
$T_{12(6–10)}$ (p.u.)	1.100	0.976	0.913	0.951	1.031	1.008	0.901	1.027	0.900	0.900	0.900
$T_{15(4–12)}$ (p.u.)	0.977	0.991	0.948	0.936	1.060	0.916	0.965	0.941	0.943	0.955	0.942
$T_{36(28–27)}$ (p.u.)	0.947	0.961	0.958	0.944	0.934	0.967	0.963	0.927	0.972	0.968	0.966
Q_{C10} (MVAR)	0.000	2.728	1.967	0.883	1.428	3.266	4.073	2.393	4.951	4.999	4.966
Q_{C12} (MVAR)	3.646	2.271	1.557	4.735	0.311	0.712	1.547	2.989	2.150	0.296	0.220
Q_{C15} (MVAR)	0.000	3.202	4.142	3.144	1.500	0.431	2.916	4.522	5.000	5.000	4.999
Q_{C17} (MVAR)	5.000	2.551	2.464	1.603	2.966	0.356	0.769	2.054	0.004	0.000	0.000
Q_{C20} (MVAR)	4.701	3.027	2.620	2.215	3.886	2.228	4.870	0.555	5.000	4.996	5.000
Q_{C21} (MVAR)	5.000	2.732	4.097	1.650	0.182	1.933	4.632	4.369	5.000	4.933	4.998
Q_{C23} (MVAR)	0.000	2.056	1.089	3.441	3.528	4.111	4.302	2.726	5.000	5.000	5.000
Q_{C24} (MVAR)	4.665	4.889	4.178	0.246	0.315	0.712	4.972	2.143	5.000	4.999	5.000
Q_{C29} (MVAR)	4.940	2.647	4.387	3.503	1.086	1.861	2.301	4.192	2.785	2.559	2.080
Cost ($/h)	811.671	805.224	812.395	807.981	818.441	816.400	805.137	815.700	804.108	804.164	**804.065**
Ploss (MW)	11.279	9.594	7.920	10.742	7.813	9.366	9.550	9.029	9.938	10.037	**9.917**
VD (p.u.)	0.221	0.156	0.146	0.184	0.335	0.348	0.101	0.272	0.093	0.094	**0.094**

Table 13. OPF problem results for Case 1 using the IEEE 118-bus test system.

DVs	PSO	KH	GWO	WOA	EEGWO	HGSO	JSO	TSA	MTBO	FOA	CNJSO	DVs	PSO	KH	GWO	WOA	EEGWO	HGSO	JSO	TSA	MTBO	FOA	CNJSO
P_{G1}	100.00	68.52	35.51	7.60	51.62	29.22	40.18	72.498	28.83	26.297	24.81	P_{G77}	0.00	68.74	81.11	23.84	53.09	14.73	43.78	54.352	37.79	0.046	0.21
P_{G4}	100.00	10.17	62.67	8.55	56.90	17.53	36.80	26.478	19.00	9.215	0.51	P_{G80}	577.00	4.86	273.42	67.11	385.78	319.82	294.70	157.636	389.36	412.871	425.96
P_{G6}	0.00	81.06	39.58	64.69	47.35	14.28	51.57	17.278	30.60	5.761	2.06	P_{G85}	0.67	41.27	53.24	0.00	65.47	58.22	37.77	6.413	0.00	0.315	0.05
P_{G8}	0.00	7.90	58.37	9.72	44.85	72.12	40.68	80.322	40.54	0.632	0.24	P_{G87}	0.00	48.13	46.45	21.32	15.78	37.34	8.08	8.243	0.47	2.805	3.56
P_{G10}	344.48	444.81	141.56	161.67	283.27	159.92	246.85	207.692	396.97	386.136	400.88	P_{G89}	0.00	565.51	233.21	372.98	341.72	58.75	245.37	667.992	372.39	434.370	466.88
P_{G12}	185.00	89.73	40.45	124.28	151.87	48.41	77.52	19.188	66.90	87.813	85.65	P_{G90}	0.00	46.80	25.35	74.05	45.98	33.06	17.88	53.100	18.40	0.237	0.14
P_{G15}	0.00	47.41	28.94	69.34	27.98	42.71	44.62	18.223	0.00	2.250	15.20	P_{G91}	100.00	78.92	29.69	21.54	44.68	24.10	47.07	73.627	0.37	0.065	0.40
P_{G18}	0.00	76.36	91.46	39.38	7.84	99.28	47.63	68.431	0.04	77.853	14.68	P_{G92}	0.00	96.69	59.29	69.72	88.13	75.76	51.41	30.123	37.76	35.963	0.04
P_{G19}	0.00	83.94	44.95	61.73	45.61	29.94	39.61	97.224	6.82	13.389	12.48	P_{G99}	100.00	64.77	81.55	62.84	99.45	24.15	42.92	32.060	35.53	0.611	0.36
P_{G24}	100.00	32.08	56.92	4.83	39.39	50.89	7.28	60.156	0.02	2.045	0.12	P_{G100}	352.00	140.90	222.78	189.64	103.94	189.69	167.36	326.910	218.90	218.429	230.29
P_{G25}	320.00	205.72	247.63	193.43	37.44	272.85	146.13	219.506	202.74	184.939	194.49	P_{G103}	140.00	6.42	93.59	88.38	9.64	27.74	46.01	102.790	35.21	30.847	37.62
P_{G26}	0.00	87.64	24.02	121.51	295.13	25.17	210.40	15.566	269.98	252.457	278.71	P_{G104}	0.00	72.32	66.16	19.36	70.53	27.51	11.56	26.308	38.93	0.602	1.00
P_{G27}	0.00	36.62	25.06	53.52	67.12	52.79	43.11	93.687	0.16	16.048	7.49	P_{G105}	100.00	78.26	48.48	11.49	70.73	11.46	40.96	11.468	0.03	43.494	14.91
P_{G31}	0.00	99.13	48.92	8.54	84.38	91.23	12.74	6.295	5.21	7.405	6.98	P_{G107}	100.00	58.46	29.71	69.93	77.65	18.73	31.04	57.846	8.88	0.582	31.14
P_{G32}	0.00	53.85	33.75	42.14	35.82	15.61	41.25	51.424	0.02	0.252	22.16	P_{G110}	100.00	79.30	34.74	73.19	95.24	69.90	3.27	52.256	37.61	70.171	3.99
P_{G34}	100.00	32.08	80.68	33.56	22.90	34.09	39.09	1.466	0.44	1.019	3.44	P_{G111}	0.00	43.26	65.47	3.93	24.97	134.73	42.63	32.864	30.88	53.602	35.60
P_{G36}	100.00	72.64	50.67	49.93	49.12	18.83	36.87	30.670	62.92	0.000	5.15	P_{G112}	100.00	8.33	37.38	39.96	36.97	92.34	51.79	49.830	24.07	3.609	46.76
P_{G40}	0.00	83.55	29.47	3.46	82.82	25.20	57.39	32.097	13.65	23.325	56.72	P_{G113}	0.00	74.97	76.86	87.69	86.42	52.53	39.89	73.818	23.35	1.097	0.89
P_{G42}	100.00	1.07	18.09	62.22	38.49	15.78	43.89	85.998	52.61	66.968	61.14	P_{G116}	0.00	51.48	46.90	72.89	18.39	35.12	19.11	12.754	1.02	1.152	0.07
P_{G46}	0.00	78.33	48.03	80.79	114.55	80.49	17.35	48.381	14.44	15.779	18.82	V_{G1}	1.06	0.98	0.99	1.03	0.99	1.05	1.01	1.040	0.99	0.991	0.99
P_{G49}	0.00	256.48	91.60	241.76	184.95	123.28	151.99	227.506	159.60	204.494	192.35	V_{G4}	1.06	1.00	1.00	1.03	0.98	1.01	1.01	1.033	1.00	0.992	1.02
P_{G54}	0.00	42.52	54.37	106.85	56.96	40.04	82.18	45.473	33.94	50.699	50.56	V_{G6}	1.06	1.00	1.00	1.03	0.99	1.01	1.01	1.056	1.00	1.018	1.01
P_{G55}	0.00	8.14	48.71	19.35	99.84	88.17	37.00	31.047	63.50	63.147	47.04	V_{G8}	0.94	1.01	0.96	1.03	0.96	0.98	1.01	0.949	1.03	1.013	1.04
P_{G56}	100.00	7.59	35.79	67.87	67.57	2.32	47.73	91.370	43.25	17.972	45.29	V_{G10}	1.06	1.03	1.02	1.03	0.97	0.95	1.01	0.985	1.01	1.003	1.05
P_{G59}	0.00	20.01	129.98	166.48	0.55	33.66	121.82	150.804	139.15	147.190	148.27	V_{G12}	1.06	1.01	1.00	1.03	1.01	1.04	1.02	1.023	1.00	1.013	1.00
P_{G61}	45.84	25.62	136.61	157.54	6.55	13.43	144.42	52.498	154.83	131.336	146.18	V_{G15}	0.94	0.99	0.97	1.03	0.97	1.04	1.00	1.059	0.99	0.995	1.00
P_{G62}	100.00	67.11	67.82	66.13	32.45	39.60	43.29	29.467	1.01	27.075	0.29	V_{G18}	0.94	0.98	0.96	1.03	0.98	1.01	1.01	1.034	1.00	0.998	1.00
P_{G65}	0.00	72.44	37.63	15.80	6.08	340.02	250.32	154.521	325.69	316.913	348.89	V_{G19}	0.94	0.98	0.97	1.03	1.00	0.96	1.00	1.039	0.99	0.991	0.99
P_{G66}	492.00	132.67	463.61	166.41	12.42	456.58	256.83	40.561	348.24	325.005	343.19	V_{G24}	1.06	1.04	0.98	1.03	0.97	0.96	1.00	0.947	1.00	1.014	1.02
P_{G70}	100.00	39.81	53.88	3.34	34.65	59.30	62.43	39.711	1.64	33.874	1.25	V_{G25}	1.06	0.96	1.02	1.03	1.00	0.97	1.02	0.976	1.00	1.042	1.05
P_{G72}	0.00	45.03	52.27	66.54	9.33	41.17	40.95	82.478	0.04	1.477	0.13	V_{G26}	0.94	1.03	0.96	1.03	1.00	0.96	1.01	0.989	0.96	1.059	1.06
P_{G73}	0.00	2.17	69.59	13.13	86.70	1.43	10.42	82.542	0.04	2.789	1.32	V_{G27}	0.94	1.04	1.00	1.03	1.06	1.03	1.01	0.962	1.00	1.032	1.01
P_{G74}	0.00	30.39	40.20	33.84	99.40	52.23	55.38	27.011	56.02	59.835	6.75	V_{G31}	0.94	1.03	0.98	1.03	0.99	0.98	1.00	1.038	1.02	1.022	1.00
P_{G76}	100.00	82.59	52.41	61.81	17.81	3.77	45.50	95.277	41.76	32.956	32.81	V_{G32}	0.94	0.98	0.98	1.03	1.01	0.97	1.01	1.013	1.00	1.022	1.00
V_{G34}	1.04	1.02	0.97	1.04	0.94	0.98	1.00	1.00	1.00	1.01	1.02	V_{G103}	0.94	0.97	1.02	1.03	1.03	0.98	1.01	1.04	1.00	0.98	1.00
V_{G36}	1.06	1.03	0.96	1.03	0.97	0.97	1.00	0.98	1.00	1.00	1.02	V_{G104}	0.94	1.01	1.02	1.03	0.98	0.94	1.00	0.98	1.00	0.98	1.00
V_{G40}	1.06	0.99	1.06	1.03	0.97	0.99	1.00	1.00	1.00	0.97	1.00	V_{G105}	0.94	1.00	1.00	1.03	0.99	0.95	1.01	1.01	1.00	0.98	0.99
V_{G42}	1.06	0.95	0.94	1.03	0.95	0.95	1.01	0.99	0.99	0.96	1.00	V_{G107}	0.94	1.05	0.97	1.03	1.02	1.04	1.02	0.94	1.00	0.98	0.99
V_{G46}	1.06	1.03	1.02	1.03	1.02	1.03	1.00	0.98	0.99	1.01	1.00	V_{G110}	0.99	1.03	1.02	1.03	1.04	0.98	1.00	1.02	1.00	1.00	1.01
V_{G49}	1.06	1.03	1.02	1.03	0.97	1.02	1.01	1.05	1.02	1.00	1.02	V_{G111}	1.06	0.98	1.03	1.03	1.05	1.05	1.00	1.02	1.00	1.00	1.03
V_{G54}	0.94	0.98	1.05	1.03	0.96	0.97	1.01	1.01	1.01	1.02	0.99	V_{G112}	0.94	0.95	1.02	1.03	0.97	0.98	1.02	1.02	0.99	1.00	1.01
V_{G55}	0.94	0.94	1.03	1.03	0.98	0.98	1.00	1.01	1.01	1.01	0.99	V_{G113}	0.94	0.98	0.99	1.03	0.95	0.97	1.00	1.03	1.01	1.01	1.01
V_{G56}	0.94	0.96	1.04	1.03	0.97	0.97	1.01	1.01	1.01	1.01	0.99	V_{G116}	1.06	0.94	0.99	1.03	0.96	1.01	0.99	0.96	0.97	1.00	1.03
V_{G59}	0.94	1.02	1.01	1.03	0.94	1.05	1.01	0.95	1.02	0.99	1.02	$T_{(5-8)}$	0.90	1.00	0.90	0.93	0.97	0.96	0.98	0.94	0.97	0.92	1.00
V_{G61}	0.94	1.04	1.03	1.03	0.96	1.02	1.00	1.02	0.99	1.02	1.01	$T_{(25-26)}$	0.90	1.07	0.97	1.02	1.02	1.09	0.97	1.00	0.97	1.01	1.01
V_{G62}	0.95	1.03	1.02	1.03	0.96	0.97	0.99	1.05	0.99	1.00	1.01	$T_{(17-30)}$	0.90	1.04	1.01	0.95	0.91	0.94	0.98	1.01	0.98	1.01	1.01
V_{G65}	1.06	0.97	1.01	1.03	0.97	1.01	1.01	0.99	1.02	1.04	1.04	$T_{(37-38)}$	1.10	1.03	1.08	0.94	1.07	1.00	1.01	0.97	1.00	1.01	0.99
V_{G66}	1.06	0.95	1.01	1.03	1.02	0.99	1.00	1.06	1.00	0.97	1.03	$T_{(59-63)}$	1.10	0.92	0.91	0.95	0.96	0.95	0.99	1.05	0.98	1.06	0.99
V_{G69}	1.06	0.97	1.04	1.06	1.01	1.01	1.01	0.95	1.06	1.04	1.05	$T_{(61-64)}$	1.10	0.91	0.97	0.95	0.96	1.06	1.02	1.00	1.04	0.96	1.02
V_{G70}	1.03	1.02	1.03	1.03	0.99	0.98	1.01	0.96	1.02	1.01	1.02	$T_{(65-66)}$	0.97	1.06	1.00	1.02	0.98	0.98	0.99	0.93	1.02	1.08	1.00
V_{G72}	1.06	1.01	0.96	1.03	0.97	0.97	1.03	0.98	0.99	1.06	1.02	$T_{(68-69)}$	0.90	1.07	1.01	0.93	1.07	0.92	1.00	1.06	1.00	0.98	0.95
V_{G73}	0.94	0.98	1.05	1.03	0.95	0.99	1.00	1.06	1.02	0.99	1.03	$T_{(80-81)}$	0.90	1.01	1.09	0.95	1.03	1.05	0.94	1.08	0.97	0.97	0.98

Table 13. *Cont.*

DVs	PSO	KH	GWO	WOA	EEGWO	HGSO	JSO	TSA	MTBO	FOA	CNJSO	DVs	PSO	KH	GWO	WOA	EEGWO	HGSO	JSO	TSA	MTBO	FOA	CNJSO
V_{G74}	1.06	1.02	0.99	1.03	0.95	1.00	0.99	1.00	1.01	0.99	1.00	Q_{C34}	0.00	7.09	20.72	17.19	5.91	13.35	13.99	23.90	24.12	6.94	14.01
V_{G76}	1.06	1.02	0.96	1.03	1.06	1.02	0.99	1.01	0.99	0.98	0.99	Q_{C44}	30.00	4.95	16.63	17.54	11.86	27.13	15.93	10.53	17.58	18.66	1.74
V_{G77}	1.06	1.01	1.00	1.03	1.02	0.95	1.00	0.97	1.01	1.00	1.02	Q_{C45}	30.00	13.46	7.37	20.18	22.97	16.34	15.40	7.90	3.85	0.00	5.89
V_{G80}	1.06	1.03	0.99	1.03	1.00	1.00	1.02	0.99	0.99	1.02	1.03	Q_{C46}	30.00	19.45	19.40	2.01	3.35	14.26	16.54	17.82	8.86	16.24	19.57
V_{G85}	0.94	1.01	1.04	1.02	1.02	0.97	1.00	1.00	0.99	0.99	1.03	Q_{C48}	30.00	11.62	20.39	18.72	21.58	24.14	19.18	10.70	28.84	29.82	3.29
V_{G87}	0.94	0.96	1.04	1.03	1.00	1.05	1.02	1.05	1.01	1.03	1.01	Q_{C74}	30.00	20.25	8.60	19.58	3.48	7.52	16.02	25.23	18.37	11.52	18.25
V_{G89}	0.94	0.97	1.02	1.03	0.94	1.00	1.00	1.05	1.01	1.01	1.06	Q_{C79}	30.00	8.95	22.36	14.62	11.52	29.14	14.98	11.02	27.95	1.08	22.17
V_{G90}	1.06	0.96	0.94	1.03	1.00	0.97	1.00	0.94	0.99	1.03	1.02	Q_{C82}	30.00	20.75	12.81	8.00	19.35	2.12	16.46	17.25	9.30	19.11	12.47
V_{G91}	1.06	0.97	0.96	1.03	0.97	1.04	1.01	1.04	1.02	1.05	1.01	Q_{C83}	30.00	10.98	15.45	0.00	0.15	9.05	17.23	12.88	17.16	4.98	7.13
V_{G92}	0.94	0.99	1.00	1.03	1.03	1.02	0.99	0.98	0.99	1.00	1.01	Q_{C105}	0.00	17.09	12.06	0.00	9.97	28.72	16.22	29.82	22.15	9.80	10.10
V_{G99}	0.94	1.03	1.01	1.03	1.00	1.03	1.01	1.01	1.01	1.01	1.01	Q_{C107}	30.00	18.19	9.60	22.54	21.51	20.04	15.88	7.43	0.00	3.86	17.73
V_{G100}	0.94	0.98	1.03	1.03	1.01	0.97	1.00	1.03	1.00	0.99	1.01	Q_{C110}	30.00	13.37	26.90	7.22	23.70	17.56	14.07	15.60	19.55	13.73	10.52

Final Results	PSO	KH	GWO	WOA	EEGWO	HGSO	JSO	TSA	MTBO	FOA	CNJSO
Cost ($/h)	159,418.75	168,544.16	153,293.89	146,312.53	161,971.59	162,825.44	135,128.76	150,093.16	131,633.71	131,409.51	**130,286.972**
Ploss (MW)	190.611	190.261	88.693	59.391	117.800	130.523	56.92	175.04	91.46	93.19	**86.926**
VD (p.u.)	2.851	1.235	1.082	1.434	1.410	1.598	0.51	1.20	0.70	0.80	**0.855**

Table 14. OPF problem results for Case 2 using the IEEE 118-bus test system.

DVs	PSO	KH	GWO	WOA	EEGWO	HGSO	JSO	TSA	MTBO	FOA	CNJSO	DVs	PSO	KH	GWO	WOA	EEGWO	HGSO	JSO	TSA	MTBO	FOA	CNJSO
P_{G1}	0	96.58	60.05	69.77	51.62	29.22	31.63	67.68	14.62	52.12	23.93	P_{G77}	0	20.62	72.7	2.88	53.09	14.73	42.32	28.34	25.87	0.85	0.11
P_{G4}	0	47.19	39.9	91.33	56.9	17.53	39.88	47.96	0.62	1.98	0.55	P_{G80}	0	214.67	219.84	200.55	385.78	319.82	317.09	407.01	375.38	406.89	423.72
P_{G6}	100	60.93	18.09	53.05	47.35	14.28	38.93	67.83	4.00	3.97	0.99	P_{G85}	0	28.27	75.01	6.42	65.47	58.22	38.84	29.28	0.23	2.08	0.13
P_{G8}	77.21	51.82	35.58	41.26	44.85	72.12	43.85	23.33	0.04	0.05	0.65	P_{G87}	0	39.28	1.2	7.65	15.78	37.34	2.55	20.37	4.86	2.12	3.59
P_{G10}	550	28.91	101.75	219.34	283.27	159.92	198.92	480.53	374.72	346.40	395.19	P_{G89}	707	67.77	395.29	485.46	341.72	58.75	362.61	38.08	429.27	399.54	464.30
P_{G12}	185	34.55	12.67	55.79	151.87	48.41	86.74	55.82	86.00	78.18	85.20	P_{G90}	0	41.77	28.15	17.56	45.98	33.06	51.34	48.88	0.05	0.57	0.13
P_{G15}	0	70.38	43.99	77.79	27.98	42.71	56.78	5.77	3.00	33.75	23.21	P_{G91}	26.4	38.53	39.38	17.33	44.68	24.1	43.27	39.94	0.11	1.05	0.15
P_{G18}	0	78.02	42.46	41.87	7.84	99.28	29.12	63.29	15.80	28.51	13.92	P_{G92}	100	39.52	5.39	49.42	88.13	75.76	35.20	40.24	42.88	0.08	0.14
P_{G19}	0	9.03	22.62	58.03	45.61	29.94	20.49	64.29	49.94	93.97	22.34	P_{G99}	100	67.7	18.84	24.62	99.45	24.15	17.69	84.47	1.09	0.02	0.25
P_{G24}	100	12.21	35.65	9.22	39.39	50.89	36.01	46.27	40.63	0.10	0.30	P_{G100}	0	48.14	129.12	237.14	103.94	189.69	143.26	65.90	213.57	220.17	233.38
P_{G25}	320	103.26	112.78	162.58	37.44	272.85	127.21	318.59	188.77	163.65	194.06	P_{G103}	140	118.55	111.53	66.79	9.64	27.74	55.26	63.35	39.01	38.97	38.50
P_{G26}	0	312.96	162.27	58.4	295.13	25.17	205.16	101.82	218.34	247.94	276.20	P_{G104}	100	61.96	77.47	11.53	70.53	27.51	6.22	75.57	33.00	10.43	2.91
P_{G27}	100	51.19	33.17	59.64	67.12	52.79	44.03	5.54	60.48	37.96	8.00	P_{G105}	0	8.13	60.85	7.31	70.73	11.46	17.12	66.37	26.55	10.82	14.86
P_{G31}	0	43.73	26.95	22.77	84.38	91.23	10.30	47.88	0.09	6.04	7.54	P_{G107}	100	30.57	26.37	82.58	77.65	18.73	54.67	79.22	51.81	37.81	32.37
P_{G32}	0	88.69	68.82	77.1	35.82	15.61	36.18	42.59	33.54	58.52	13.70	P_{G110}	0	74.13	7.78	18.63	95.24	69.9	46.33	13.94	0.04	34.30	11.71
P_{G34}	25.65	13.97	37.82	5.62	22.9	34.09	52.16	21.43	44.29	0.54	3.52	P_{G111}	136	47.58	55.68	73.26	24.97	134.73	70.34	13.05	35.88	33.45	34.89
P_{G36}	100	33.14	52.06	29.62	49.12	18.83	44.50	89.59	0.57	0.23	6.54	P_{G112}	0	30.14	53.92	68.5	36.97	92.34	33.57	6.57	31.16	24.07	37.03
P_{G40}	0	64.03	58.65	70.65	82.82	25.2	51.44	65.06	57.59	84.56	56.79	P_{G113}	0	4.87	24.22	40.36	86.42	52.53	38.04	24.04	39.90	61.36	0.39
P_{G42}	0	38.15	23.77	39.96	38.49	15.78	40.73	37.23	41.55	36.39	62.89	P_{G116}	0	81.01	57.18	64.31	18.39	35.12	42.03	82.57	0.11	0.70	0.09
P_{G46}	0	57.71	40.59	71.71	114.55	80.49	29.86	20.67	19.59	18.73	19.18	V_{G1}	0.94	1	0.97	1.02	0.99	1.05	0.99	0.95	0.97	0.96	0.98
P_{G49}	0	37.59	121.15	12.58	184.95	123.28	143.98	109.53	179.22	169.62	195.35	V_{G4}	0.94	1	0.95	1.02	0.98	1.01	1.03	1.01	1.00	1.01	1.01
P_{G54}	0	142.91	38.01	80.79	56.96	40.04	70.15	4.30	50.45	59.93	49.86	V_{G6}	0.94	1.02	0.96	1.02	0.99	1.01	1.00	0.98	0.99	0.98	1.00
P_{G55}	100	98.23	53.6	46.68	99.84	88.17	50.30	84.25	50.02	36.66	44.19	V_{G8}	1.06	0.98	1.01	1.02	0.96	0.98	1.01	1.03	0.98	0.98	1.03
P_{G56}	0	39.28	20.68	41.99	67.57	2.32	54.27	31.52	23.04	27.86	45.74	V_{G10}	1.06	0.99	1.05	1.02	0.97	0.95	1.00	1.06	1.00	1.00	1.06
P_{G59}	0	20.47	101.57	128.84	0.55	33.66	145.25	83.60	152.53	142.98	147.72	V_{G12}	0.94	1.05	0.96	1.02	1.01	1.04	1.00	1.00	1.00	0.97	1.00

Table 14. *Cont.*

DVs	PSO	KH	GWO	WOA	EEGWO	HGSO	JSO	TSA	MTBO	FOA	CNJSO	DVs	PSO	KH	GWO	WOA	EEGWO	HGSO	JSO	TSA	MTBO	FOA	CNJSO
P_{G61}	260	28.87	128.08	233.59	6.55	13.43	126.36	135.06	124.18	138.73	147.51	V_{G15}	0.94	1.02	0.96	1.02	0.97	1.04	0.99	1.00	1.00	0.95	1.01
P_{G62}	0	60.06	38.05	81.27	32.45	39.6	43.34	58.33	1.36	0.88	0.07	V_{G18}	0.94	0.99	0.97	1.02	0.98	1.01	1.00	1.03	0.99	0.96	1.02
P_{G65}	491	436.44	17.9	22.84	6.08	340.02	196.72	124.93	324.92	339.52	346.01	V_{G19}	0.94	1.01	0.96	1.02	1	0.96	0.99	1.00	1.00	0.96	1.01
P_{G66}	0	398.97	305.55	115.04	12.42	456.58	249.15	168.22	339.61	302.18	342.83	V_{G24}	1.06	1.01	1	1.02	0.97	0.96	0.99	1.03	1.02	1.01	1.02
P_{G70}	0	16.35	83.77	74.38	34.65	59.3	50.66	31.33	3.65	0.00	0.59	V_{G25}	0.94	0.97	1.01	1.02	1	0.97	1.00	0.99	1.00	1.02	1.04
P_{G72}	0	73.3	47.13	29.29	9.33	41.17	51.09	96.55	0.40	11.56	0.84	V_{G26}	0.94	1.05	0.99	1.02	1	0.96	0.99	1.01	0.99	1.00	1.06
P_{G73}	0	16.32	87.17	79.18	86.7	1.43	21.72	84.24	1.22	0.24	0.39	V_{G27}	1.06	1.05	0.98	1.03	1.06	1.03	0.99	1.03	0.98	1.03	1.01
P_{G74}	0	50.66	89.54	16.19	99.4	52.23	39.99	46.89	35.66	68.37	19.15	V_{G31}	1.06	0.96	1.03	1.02	0.99	0.98	0.99	0.97	1.01	0.99	1.00
P_{G76}	100	90.76	26.41	25.71	17.81	3.77	42.05	23.05	0.29	28.12	26.43	V_{G32}	1.06	1.02	1	1.03	1.01	0.97	0.99	1.05	0.99	1.01	1.01
V_{G34}	0.94	0.96	1.04	1.02	0.94	0.98	1.01	1.03	1.01	0.985	1.01	V_{G103}	0.94	0.95	0.98	1.02	1.03	0.98	1.01	0.95	1.01	1.01	1.01
V_{G36}	0.94	0.94	1.04	1.02	0.97	0.97	1.01	1.04	1.01	0.983	1.00	V_{G104}	0.94	0.99	0.95	1.02	0.98	0.94	1.00	0.98	1.00	1.00	1.00
V_{G40}	0.94	1.02	1.04	1.02	0.97	0.99	1.00	0.97	0.98	1.021	1.00	V_{G105}	0.94	0.98	0.94	1.03	0.99	0.95	1.00	0.99	1.00	1.00	1.00
V_{G42}	0.95	0.98	0.99	1.02	0.95	0.95	0.99	0.95	1.01	1.007	1.00	V_{G107}	0.96	1.05	0.94	1.02	1.02	1.04	1.00	1.01	1.01	1.00	1.00
V_{G46}	1.06	1	1.01	1.03	1.02	1.03	1.00	1.06	1.02	1.003	1.00	V_{G110}	0.98	1.02	0.98	1.02	1.04	0.98	1.00	1.00	0.99	1.00	0.99
V_{G49}	0.98	0.97	1.01	1.02	0.97	1.02	1.01	0.99	0.99	0.999	1.02	V_{G111}	0.94	1.04	0.95	1.02	1.05	1.05	1.01	1.00	1.01	1.04	1.00
V_{G54}	0.94	1	0.97	1.02	0.96	0.97	1.00	1.03	1.00	1.005	1.01	V_{G112}	1.06	0.96	1.02	1.02	0.97	0.98	1.01	0.97	0.97	0.98	0.98
V_{G55}	0.94	0.98	0.97	1.01	0.98	0.98	0.99	1.02	1.00	0.998	1.01	V_{G113}	0.94	1.03	1	1.02	0.95	0.97	1.00	1.00	1.02	0.96	1.03
V_{G56}	0.94	0.99	0.97	1.01	0.97	0.97	0.99	1.02	1.00	0.999	1.01	V_{G116}	1.06	1	0.98	1.02	0.96	1.01	0.99	1.04	0.98	1.00	1.02
V_{G59}	1.06	0.96	1.04	1.02	0.94	1.05	0.99	1.03	1.03	0.962	1.02	$T_{(5–8)}$	1.1	0.92	0.96	0.98	0.97	0.96	0.98	1.07	0.98	0.98	1.01
V_{G61}	1.06	0.96	1.06	1.02	0.96	1.02	0.99	1.06	1.03	0.996	1.01	$T_{(25–26)}$	1.1	1.07	0.98	0.99	1.02	1.09	1.02	1.06	1.00	1.01	1.05
V_{G62}	1.06	0.97	1.05	1.02	0.96	0.97	0.99	1.04	1.01	0.992	1.01	$T_{(17–30)}$	1.1	1	1.05	0.99	0.91	0.94	1.00	1.10	0.98	1.03	0.99
V_{G65}	1.06	1	1.02	1.03	0.97	1.01	1.00	1.06	1.01	1.024	1.03	$T_{(37–38)}$	1.1	0.99	0.93	1	1.07	1	0.98	0.95	0.97	1.05	0.98
V_{G66}	1.03	1.01	1.04	1.02	1.02	0.99	1.00	1.00	1.00	1.037	1.03	$T_{(59–63)}$	0.9	0.91	0.94	0.98	0.96	0.95	1.02	0.95	0.98	1.08	0.97
V_{G69}	1.06	0.97	1.02	1.02	1.01	1.01	1.05	0.95	0.99	1.027	1.04	$T_{(61–64)}$	0.97	0.95	0.92	0.99	0.96	1.06	0.99	1.03	0.99	1.09	0.99
V_{G70}	1.06	1.01	1.03	1.02	0.99	0.98	1.00	1.01	0.99	1.007	1.00	$T_{(65–66)}$	1.1	1.06	1.07	1	0.98	0.98	0.99	1.07	1.00	0.95	0.99
V_{G72}	0.94	0.96	1.05	1.02	0.97	0.97	1.00	1.01	1.01	1.018	1.01	$T_{(68–69)}$	0.9	1.02	0.9	0.99	1.07	0.92	0.99	1.09	1.06	0.90	0.93
V_{G73}	1.06	1.05	1.03	1.02	0.95	0.99	0.98	1.01	1.00	1.019	1.00	$T_{(80–81)}$	0.9	0.94	0.95	1	1.03	1.05	1.01	1.09	0.94	0.97	0.97
V_{G74}	1.06	1.03	1.02	1.02	0.95	1	1.00	1.01	0.96	0.995	0.98	Q_{C34}	0	19.38	29.69	7.06	5.91	13.35	16.04	10.93	22.99	11.91	8.81
V_{G76}	1.06	1.03	0.99	1.01	1.06	1.02	0.99	1.02	0.94	0.983	0.97	Q_{C44}	30	18.31	1.99	15.9	11.86	27.13	13.94	29.23	23.31	22.33	0.71
V_{G77}	1.04	1.02	0.98	1.02	1.02	0.95	1.01	0.94	0.99	1.014	1.00	Q_{C45}	30	21.87	17.53	15.21	22.97	16.34	12.92	8.13	1.18	1.45	17.71
V_{G80}	1.06	1.03	1.01	1.02	1	1	1.02	1.02	1.01	1.041	1.02	Q_{C46}	30	3.25	29.46	14.71	3.35	14.26	19.87	3.24	12.94	17.32	14.95
V_{G85}	1.06	0.95	1	1.02	1.02	0.97	1.00	0.96	1.00	0.998	1.02	Q_{C48}	30	15.53	16.08	14.57	21.58	24.14	14.01	15.93	0.22	29.89	0.90
V_{G87}	1.06	1.01	1.02	1.02	1	1.05	1.00	1.03	1.01	0.991	1.00	Q_{C74}	30	10.75	10.65	16.37	3.48	7.52	11.42	19.24	10.14	7.16	27.39
V_{G89}	1.06	0.99	1.03	1.03	0.94	1	1.01	1.04	1.02	1.008	1.05	Q_{C79}	30	21.29	2.69	13.7	11.52	29.14	13.22	22.55	2.45	7.41	14.66
V_{G90}	0.94	0.95	1.04	1.02	1	0.97	0.99	0.98	1.01	0.994	0.99	Q_{C82}	30	16.89	5.25	12.48	19.35	2.12	14.00	8.37	15.65	9.95	12.90
V_{G91}	0.94	1.03	0.96	1.02	0.97	1.04	0.99	0.96	0.99	1.005	0.98	Q_{C83}	0	15.87	30	16.03	0.15	9.05	15.81	10.01	9.44	16.83	8.55
V_{G92}	0.94	1	0.97	1.03	1.03	1.02	0.99	0.99	0.99	0.990	1.00	Q_{C105}	0	22.98	6.67	8.75	9.97	28.72	18.69	9.86	29.83	5.61	2.34
V_{G99}	0.94	1	1.05	1.02	1	1.03	1.00	1.00	1.00	1.014	1.01	Q_{C107}	30	19.46	19.72	3.63	21.51	20.04	14.91	14.51	29.96	0.50	12.30
V_{G100}	0.94	0.97	0.97	1.03	1.01	0.97	1.02	0.99	1.01	1.006	1.01	Q_{C110}	0	6.06	16.33	19.57	23.7	17.56	11.64	26.66	12.03	23.32	12.89

Final Results	PSO	KH	GWO	WOA	EEGWO	HGSO	JSO	TSA	MTBO	FOA	CNJSO
Cost ($/h)	163,613.92	156,723.9	145,878.78	145,671.54	161,971.59	162,825.44	135,837.32	149,195.31	131,440.76	131,641.62	**130,334.31**
Ploss (MW)	242.265	100.941	113.197	80.798	117.8	130.523	62.32	137.31	87.27	83.70	**87.11**
VD (p.u.)	3.059	1.374	1.737	1.053	1.41	1.598	0.63	1.43	0.81	1.07	**0.60**

7. Conclusions

OPF and global optimization problems are a class of complex, nonlinear, and large-scale optimization problems that pose significant computational challenges. Although these challenges make them well-suited for metaheuristic algorithms, which are capable of efficiently exploring complex search spaces and maintaining a balance between exploration and exploitation, many existing algorithms still face limitations such as premature convergence, insufficient exploration, or an imbalance between exploration and exploitation. The JSO is a successful metaheuristic algorithm, which mimics the foraging behavior of the jellyfishes in the ocean. This algorithm suffers from low exploration and an imbalance between exploration and exploitation. To tackle these drawbacks, this study introduced an improved JSO called Conscious Neighborhood-based JSO (CNJSO), which the new movement strategy BNGS proposes to enhance search space exploration. In addition, this algorithm adapted and utilized the concept of conscious neighborhood to decide between exploration and exploitation, and employed the Wandering Around Search (WAS) strategy to improve inferior individuals. The performance of CNJSO was assessed by conducting the CEC 2018 benchmark functions, and the results were statistically analyzed. In addition, the applicability of CNJSO was evaluated by solving the optimal power flow problems for the IEEE 30-bus and 118-bus systems. To sum up, the outcomes of the experiment and analysis can be described as follows.

- Using the conscious neighborhood concept enables the algorithm to consciously determine the movement strategy between the ocean's current and the jellyfish swarm and makes a good trade-off between exploration and exploitation.
- Proposing the Best archive and Non-neighborhood-based Global Search (BNGS) strategy enhances exploration ability.
- The WAS strategy decreases premature convergence and improves the balance between local and global search.
- The proposed CNJSO algorithm performed better than competitor algorithms for different test functions.
- CNJSO can be used to resolve engineering design problems.

Although the proposed CNJSO has indicated superior performance on OPF problems, this study has a particular limitation. The CNJSO requires a longer execution time compared to conventional approaches, which can be a significant limitation in real-time applications. The proposed CNJSO algorithm is applied to solve single-objective and continuous problems. As future work, it can be extended to optimize binary and multi-objective problems. Since multi-objective optimization requires constructing Pareto frontiers, an external archive of non-dominated solutions can be applied. In addition, using the conscious neighborhood concept, the population can learn from different non-dominated solutions instead of a single one. Additionally, CNJSO can be utilized for solving optimization problems in various applications and domains.

Author Contributions: M.H.N.-S.: Conceptualization, methodology, software, validation, formal analysis, investigation, writing—original draft, writing—review & editing, supervision, project administration; M.B.-D.: Conceptualization, methodology, software, validation, formal analysis, investigation, writing- original draft, writing—review & editing; H.Z.: Conceptualization, methodology, software, validation, formal analysis, investigation, writing- original draft, writing—review & editing. All authors have read and agreed to the published version of the manuscript.

Funding: This research received no external funding.

Data Availability Statement: The original contributions presented in this study are included in the article. Further inquiries can be directed to the corresponding author.

Conflicts of Interest: The authors have no competing interests to declare that are relevant to the content of this article.

Nomenclature

The nomenclature table:

Variable Name	Description
t and Max_{iter}	Current iteration and the maximum number of iterations
$X_i(t)$	Position of the i-th jellyfish at time t
$X_{ij}(t+1)$	The j-th dimension of the i-th jellyfish's position
$f(X_i)$	Fitness value of the i-th jellyfish at time t
X^*	Position of the current best jellyfish in the swarm
μ	Mean position of all jellyfish positions
γ	Motion coefficient
U_b and L_b	Upper and lower bounds of the search space
$c(t)$ and C_0	Time control function and a threshold constant
$m_i(t)$ and $fbest_i$	Position and best fitness value of the i-th jellyfish
m_{gbestj} and $X_{rj}(t)$	The j-th dimension of the best hiding place and the r-th random search agent
r_i	A random value in the interval (0, 1)
$fl_i(t)$	Flight length for the i-th search agent in the current iteration t
$X_{archive}$	A randomly selected jellyfish from the archive
X_{global}	A random non-neighbor of individual i
NJ	Number of jumps

References

1. Li, S.; Chen, H.; Wang, M.; Heidari, A.A.; Mirjalili, S. Slime mould algorithm: A new method for stochastic optimization. *Future Gener. Comput. Syst.* **2020**, *111*, 300–323. [CrossRef]
2. Chen, H.; Jiao, S.; Heidari, A.A.; Wang, M.; Chen, X.; Zhao, X. An opposition-based sine cosine approach with local search for parameter estimation of photovoltaic models. *Energy Convers. Manag.* **2019**, *195*, 927–942. [CrossRef]
3. Rashedi, E.; Nezamabadi-pour, H.; Saryazdi, S. GSA: A gravitational search algorithm. *Inf. Sci.* **2009**, *179*, 2232–2248. [CrossRef]
4. Gandomi, A.H.; Alavi, A.H. Krill herd: A new bio-inspired optimization algorithm. *Commun. Nonlinear Sci. Numer. Simul.* **2012**, *17*, 4831–4845. [CrossRef]
5. Talbi, E.-G. *Metaheuristics: From Design to Implementation*; Wiley Publishing: Hoboken, NJ, USA, 2009.
6. Abdel-Basset, M.; Mohamed, R.; Elhoseny, M. applications. In *Metaheuristics Algorithms for Medical Applications*; Abdel-Basset, M., Mohamed, R., Elhoseny, M., Eds.; Academic Press: Cambridge, MA, USA, 2024; pp. 1–26. [CrossRef]
7. Khosravy, M.; Gupta, N.; Patel, N.; Senjyu, T. *Frontier Applications of Nature Inspired Computation*; Springer: Singapore, 2020.
8. Wolpert, D.H.; Macready, W.G. No free lunch theorems for optimization. *IEEE Trans. Evol. Comput.* **1997**, *1*, 67–82. [CrossRef]
9. Mandal, P.K. A review of classical methods and Nature-Inspired Algorithms (NIAs) for optimization problems. *Results Control Optim.* **2023**, *13*, 100315. [CrossRef]
10. Beyer, H.-G.; Schwefel, H.-P. Evolution strategies—A comprehensive introduction. *Nat. Comput.* **2002**, *1*, 3–52. [CrossRef]
11. Grefenstette, J.J. Genetic algorithms and machine learning. In Proceedings of the Sixth Annual Conference on Computational Learning Theory, Association for Computing Machinery, Santa Cruz, CA, USA, 1 August 1993; pp. 3–4. [CrossRef]
12. Eberhart, R.; Kennedy, J. A new optimizer using particle swarm theory. In Proceedings of the Sixth International Symposium on Micro Machine and Human Science, Nagoya, Japan, 4–6 October 1995. [CrossRef]
13. Dorigo, M.; Caro, G.D. Ant colony optimization: A new meta-heuristic. In Proceedings of the 1999 Congress on Evolutionary Computation-CEC99 (Cat. No. 99TH8406), Washington, DC, USA, 6–9 July 1999. [CrossRef]
14. Mirjalili, S.; Lewis, A. Grey wolf optimizer. *Adv. Eng. Softw.* **2014**, *69*, 46–61. [CrossRef]
15. Chou, J.-S.; Truong, D.-N. A novel metaheuristic optimizer inspired by behavior of jellyfish in ocean. *Appl. Math. Comput.* **2021**, *389*, 125535. [CrossRef]
16. Kaur, S.; Awasthi, L.K.; Sangal, A.L.; Dhiman, G. Tunicate Swarm Algorithm: A new bio-inspired based metaheuristic paradigm for global optimization. *Eng. Appl. Artif. Intell.* **2020**, *90*, 103541. [CrossRef]
17. Hamadneh, T.; Batiha, B.; Werner, F.; Montazeri, Z.; Dehghani, M.; Gulnara, B.; Eguchi, K. Fossa Optimization Algorithm: A New Bio-Inspired Metaheuristic Algorithm for Engineering Applications. *Int. J. Intell. Eng. Syst.* **2024**, *17*, 1038–1047. [CrossRef]

18. Rao, R.V.; Savsani, V.J.; Vakharia, D.P. Teaching–learning-based optimization: A novel method for constrained mechanical design optimization problems. *Comput.-Aided Des.* **2011**, *43*, 303–315. [CrossRef]
19. Ida Evangeline, S.; Rathika, P. Wind farm incorporated optimal power flow solutions through multi-objective horse herd optimization with a novel constraint handling technique. *Expert Syst. Appl.* **2022**, *194*, 116544. [CrossRef]
20. Nadimi-Shahraki, M.H.; Taghian, S.; Javaheri, D.; Sadiq, A.S.; Khodadadi, N.; Mirjalili, S. MTV-SCA: Multi-trial vector-based sine cosine algorithm. *Clust. Comput.* **2024**, *27*, 13471–13515. [CrossRef]
21. Kaveh, A.; Kaveh, A.; Nasrollahi, A. Charged system search and particle swarm optimization hybridized for optimal design of engineering structures. *Sci. Iran.* **2014**, *21*, 295–305.
22. Varaee, H.; Safaeian Hamzehkolaei, N.; Safari, M. A Hybrid Generalized Reduced Gradient-Based Particle Swarm Optimizer for Constrained Engineering Optimization Problems. *J. Soft Comput. Civ. Eng.* **2021**, *5*, 86–119. [CrossRef]
23. Wu, H.; Bagherzadeh, S.A.; D'oRazio, A.; Habibollahi, N.; Karimipour, A.; Goodarzi, M.; Bach, Q.-V. Present a new multi objective optimization statistical Pareto frontier method composed of artificial neural network and multi objective genetic algorithm to improve the pipe flow hydrodynamic and thermal properties such as pressure drop and heat transfer coefficient for non-Newtonian binary fluids. *Phys. A Stat. Mech. Appl.* **2019**, *535*, 122409. [CrossRef]
24. Abdel-Basset, M.; El-Shahat, D.; El-Henawy, I.; de Albuquerque, V.H.C.; Mirjalili, S. A new fusion of grey wolf optimizer algorithm with a two-phase mutation for feature selection. *Expert Syst. Appl.* **2020**, *139*, 112824. [CrossRef]
25. Banaie-Dezfouli, M.; Nadimi-Shahraki, M.H.; Beheshti, Z. BE-GWO: Binary extremum-based grey wolf optimizer for discrete optimization problems. *Appl. Soft Comput.* **2023**, *146*, 110583. [CrossRef]
26. Dezfuly, M.; Sajedi, H. Predict Survival of Patients with Lung Cancer Using an Ensemble Feature Selection Algorithm and Classification Methods in Data Mining. *J. Inf.* **2015**, *1*, 1–11. [CrossRef]
27. Beheshti, Z. BMPA-TVSinV: A Binary Marine Predators Algorithm using time-varying sine and V-shaped transfer functions for wrapper-based feature selection. *Knowl. Based Syst.* **2022**, *252*, 109446. [CrossRef]
28. Ouadfel, S.; Elaziz, M.A. Efficient high-dimension feature selection based on enhanced equilibrium optimizer. *Expert Syst. Appl.* **2022**, *187*, 115882. [CrossRef]
29. Dezfouli, M.B.; Nadimi-Shahraki, M.-H.; Zamani, H. A novel tour planning model using big data. In Proceedings of the 2018 International Conference on Artificial Intelligence and Data Processing (IDAP), New York, NY, USA, 28–30 September 2018. [CrossRef]
30. Ghazzai, H.; Yaacoub, E.; Alouini, M.-S. Optimized LTE Cell Planning for Multiple User Density Subareas Using Meta-Heuristic Algorithms. In Proceedings of the 2014 IEEE 80th Vehicular Technology Conference (VTC2014-Fall), Vancouver, BC, Canada, 14–17 September 2014. [CrossRef]
31. Chiang, H.-S.; Huang, T.-C. User-adapted travel planning system for personalized schedule recommendation. *Inf. Fusion* **2015**, *21*, 3–17. [CrossRef]
32. Nadimi-Shahraki, M.H.; Moeini, E.; Taghian, S.; Mirjalili, S. Discrete Improved Grey Wolf Optimizer for Community Detection. *J. Bionic Eng.* **2023**, *20*, 2331–2358. [CrossRef]
33. Pérez-Peló, S.; Sánchez-Oro, J.; Gonzalez-Pardo, A.; Duarte, A. A fast variable neighborhood search approach for multi-objective community detection. *Appl. Soft Comput.* **2021**, *112*, 107838. [CrossRef]
34. Altan, A.; Karasu, S.; Bekiros, S. Digital currency forecasting with chaotic meta-heuristic bio-inspired signal processing techniques. *Chaos Solitons Fractals* **2019**, *126*, 325–336. [CrossRef]
35. Dashti, S.E.; Rahmani, A.M. Dynamic VMs placement for energy efficiency by PSO in cloud computing. *J. Exp. Theor. Artif. Intell.* **2015**, *28*, 97–112. [CrossRef]
36. Nadimi-Shahraki, M.H.; Banaie-Dezfouli, M.; Zamani, H.; Taghian, S.; Mirjalili, S. B-MFO: A Binary Moth-Flame Optimization for Feature Selection from Medical Datasets. *Computers* **2021**, *10*, 136. [CrossRef]
37. Li, Q.; Chen, H.; Huang, H.; Zhao, X.; Cai, Z.; Tong, C.; Liu, W.; Tian, X. An Enhanced Grey Wolf Optimization Based Feature Selection Wrapped Kernel Extreme Learning Machine for Medical Diagnosis. *Comput. Math. Methods Med.* **2017**, *2017*, 9512741. [CrossRef]
38. Abualigah, L.M.; Khader, A.T.; Hanandeh, E.S. A new feature selection method to improve the document clustering using particle swarm optimization algorithm. *J. Comput. Sci.* **2018**, *25*, 456–466. [CrossRef]
39. Zhang, S.; Zhou, Y. Grey Wolf Optimizer Based on Powell Local Optimization Method for Clustering Analysis. *Discret. Dyn. Nat. Soc.* **2015**, *2015*, 481360. [CrossRef]
40. Abasi, A.K.; Khader, A.T.; Al-Betar, M.A.; Naim, S.; Makhadmeh, S.N.; Alyasseri, Z.A.A. Link-based multi-verse optimizer for text documents clustering. *Appl. Soft Comput.* **2020**, *87*, 106002. [CrossRef]
41. Hu, G.; Wang, J.; Li, M.; Hussien, A.G.; Abbas, M. EJS: Multi-Strategy Enhanced Jellyfish Search Algorithm for Engineering Applications. *Mathematics* **2023**, *11*, 851. [CrossRef]
42. Lei, Y.; Fan, L.; Yang, J.; Si, W.; Lawrynczuk, M. Fractional-Order Boosted Jellyfish Search Optimizer with Gaussian Mutation for Income Forecast of Rural Resident. *Comput. Intell. Neurosci.* **2022**, *2022*, 3343505. [CrossRef]

43. Manita, G.; Zermani, A. A Modified Jellyfish Search Optimizer with Orthogonal Learning Strategy. *Procedia Comput. Sci.* **2021**, *192*, 697–708. [CrossRef]
44. Shaheen, A.M.; El-Sehiemy, R.A.; Alharthi, M.M.; Ghoneim, S.S.; Ginidi, A.R. Multi-objective jellyfish search optimizer for efficient power system operation based on multi-dimensional OPF framework. *Energy* **2021**, *237*, 121478. [CrossRef]
45. Zamani, H.; Nadimi-Shahraki, M.H.; Gandomi, A.H. CCSA: Conscious Neighborhood-based Crow Search Algorithm for Solving Global Optimization Problems. *Appl. Soft Comput.* **2019**, *85*, 105583. [CrossRef]
46. Mirjalili, S.; Lewis, A. The whale optimization algorithm. *Adv. Eng. Softw.* **2016**, *95*, 51–67. [CrossRef]
47. Long, W.; Jiao, J.; Liang, X.; Tang, M. An exploration-enhanced grey wolf optimizer to solve high-dimensional numerical optimization. *Eng. Appl. Artif. Intell.* **2018**, *68*, 63–80. [CrossRef]
48. Hashim, F.A.; Houssein, E.H.; Mabrouk, M.S.; Al-Atabany, W.; Mirjalili, S. Henry gas solubility optimization: A novel physics-based algorithm. *Futur. Gener. Comput. Syst.* **2019**, *101*, 646–667. [CrossRef]
49. Faridmehr, I.; Nehdi, M.L.; Davoudkhani, I.F.; Poolad, A. Mountaineering Team-Based Optimization: A Novel Human-Based Metaheuristic Algorithm. *Mathematics* **2023**, *11*, 1273. [CrossRef]
50. Awad, N.H.; Ali, M.Z.; Suganthan, P.N.; Liang, J.J.; Qu, B.Y. *Problem Definitions and Evaluation Criteria for the CEC 2017 Special Session and Competition on Single Objective Bound Constrained Real-Parameter Numerical Optimization*; Technical Report; Nanyang Technological University: Singapore, 2016.
51. Mohamed, A.W.; Hadi, A.A.; Mohamed, A.K. Gaining-sharing knowledge based algorithm for solving optimization problems: A novel nature-inspired algorithm. *Int. J. Mach. Learn. Cybern.* **2019**, *11*, 1501–1529. [CrossRef]
52. Askari, Q.; Younas, I.; Saeed, M. Political Optimizer: A novel socio-inspired meta-heuristic for global optimization. *Knowl. Based Syst.* **2020**, *195*, 105709. [CrossRef]
53. Del Ser, J.; Osaba, E.; Molina, D.; Yang, X.-S.; Salcedo-Sanz, S.; Camacho, D.; Das, S.; Suganthan, P.N.; Coello, C.A.C.; Herrera, F. Bio-inspired computation: Where we stand and what's next. *Swarm Evol. Comput.* **2019**, *48*, 220–250. [CrossRef]
54. Koza, J.R. Genetic programming as a means for programming computers by natural selection. *Stat. Comput.* **1994**, *4*, 87–112. [CrossRef]
55. Storn, R.; Price, K. Differential evolution—A simple and efficient heuristic for global optimization over continuous spaces. *J. Glob. Optim.* **1997**, *11*, 341–359. [CrossRef]
56. Cuevas, E.; Zaldívar, D.; Pérez-Cisneros, M.; Oliva, D. Block-matching algorithm based on differential evolution for motion estimation. *Eng. Appl. Artif. Intell.* **2012**, *26*, 488–498. [CrossRef]
57. Awad, N.H.; Ali, M.Z.; Mallipeddi, R.; Suganthan, P.N. An efficient Differential Evolution algorithm for stochastic OPF based active–reactive power dispatch problem considering renewable generators. *Appl. Soft Comput.* **2019**, *76*, 445–458. [CrossRef]
58. Salman, A.; Engelbrecht, A.P.; Omran, M.G. Empirical analysis of self-adaptive differential evolution. *Eur. J. Oper. Res.* **2007**, *183*, 785–804. [CrossRef]
59. Zhang, J. and A.C. Sanderson, JADE: Adaptive differential evolution with optional external archive. *IEEE Trans. Eviron. Comp.* **2009**, *13*, 945–958. [CrossRef]
60. Tanabe, R.; Fukunaga, A. Success-history based parameter adaptation for Differential Evolution. In Proceedings of the 2013 IEEE Congress on Evolutionary Computation, Cancun, Mexico, 20–23 June 2013. [CrossRef]
61. Tanabe, R.; Fukunaga, A.S. Improving the search performance of SHADE using linear population size reduction. In Proceedings of the 2014 IEEE Congress on Evolutionary Computation (CEC), Beijing, China, 6–11 July 2014. [CrossRef]
62. Brest, J.; Maučec, M.S.; Bošković, B. iL-SHADE: Improved L-SHADE algorithm for single objective real-parameter optimization. In Proceedings of the 2016 IEEE Congress on Evolutionary Computation (CEC), Vancouver, BC, Canada, 24–29 July 2016. [CrossRef]
63. Meng, Z.; Pan, J.-S. Quasi-affine transformation evolution with external archive (QUATRE-EAR): An enhanced structure for differential evolution. *Knowl. Based Sys.* **2018**, *155*, 35–53. [CrossRef]
64. Nadimi-Shahraki, M.H.; Taghian, S.; Mirjalili, S.; Faris, H. MTDE: An effective multi-trial vector-based differential evolution algorithm and its applications for engineering design problems. *App. Soft Comp.* **2020**, *97*, 106761. [CrossRef]
65. Erol, O.K.; Eksin, I. A new optimization method: Big Bang–Big Crunch. *Adv. Eng. Softw.* **2006**, *37*, 106–111. [CrossRef]
66. Kaveh, A.; Talatahari, S. Charged system search for optimal design of frame structures. *Appl. Soft Comput.* **2012**, *12*, 382–393. [CrossRef]
67. Hatamlou, A. Black hole: A new heuristic optimization approach for data clustering. *Inf. Sci.* **2013**, *222*, 175–184. [CrossRef]
68. Zhao, W.; Wang, L.; Zhang, Z. Atom search optimization and its application to solve a hydrogeologic parameter estimation problem. *Knowl. Based Syst.* **2019**, *163*, 283–304. [CrossRef]
69. Kaveh, A.; Khayatazad, M. A new meta-heuristic method: Ray Optimization. *Comput. Struct.* **2012**, *112–113*, 283–294. [CrossRef]
70. Kaveh, A.; Khayatazad, M. Ray optimization for size and shape optimization of truss structures. *Comput. Struct.* **2013**, *117*, 82–94. [CrossRef]
71. Kaur, A.; Kumar, Y. A new metaheuristic algorithm based on water wave optimization for data clustering. *Evol. Intell.* **2021**, *15*, 759–783. [CrossRef]

72. Alatas, B. A novel chemistry based metaheuristic optimization method for mining of classification rules. *Expert Syst. Appl.* **2012**, *39*, 11080–11088. [CrossRef]
73. Ghasemi, M.R.; Varaee, H. A fast multi-objective optimization using an efficient ideal gas molecular movement algorithm. *Eng. Comput.* **2016**, *33*, 477–496. [CrossRef]
74. Wang, H.; Chen, S.; Luo, L. A diffusion algorithm based on P systems for continuous global optimization. *J. Comput. Sci.* **2020**, *44*, 101112. [CrossRef]
75. Yang, B.; Zhang, M.; Zhang, X.; Wang, J.; Shu, H.; Li, S.; He, T.; Yang, L.; Yu, T. Fast atom search optimization based MPPT design of centralized thermoelectric generation system under heterogeneous temperature difference. *J. Clean. Prod.* **2020**, *248*, 119301. [CrossRef]
76. Korashy, A.; Kamel, S.; Houssein, E.H.; Jurado, F.; Hashim, F.A. Development and application of evaporation rate water cycle algorithm for optimal coordination of directional overcurrent relays. *Expert Syst. Appl.* **2021**, *185*, 115538. [CrossRef]
77. Al-Betar, M.A.; Awadallah, M.A.; Abu Zitar, R.; Assaleh, K. Economic load dispatch using memetic sine cosine algorithm. *J. Ambient. Intell. Humaniz. Comput.* **2022**, *14*, 11685–11713. [CrossRef]
78. Eslami, M.; Neshat, M.; Khalid, S.A. A Novel Hybrid Sine Cosine Algorithm and Pattern Search for Optimal Coordination of Power System Damping Controllers. *Sustainability* **2022**, *14*, 541. [CrossRef]
79. Abdel-Mawgoud, H.; Kamel, S.; Khasanov, M.; Khurshaid, T. A strategy for PV and BESS allocation considering uncertainty based on a modified Henry gas solubility optimizer. *Electr. Power Syst. Res.* **2021**, *191*, 106886. [CrossRef]
80. Hashim, F.A.; Houssein, E.H.; Hussain, K.; Mabrouk, M.S.; Al-Atabany, W. A modified Henry gas solubility optimization for solving motif discovery problem. *Neural Comput. Appl.* **2019**, *32*, 10759–10771. [CrossRef]
81. Moosavi, S.; Bardsiri, S.H.; Khatibi, V. Poor and rich optimization algorithm: A new human-based and multi populations algorithm. *Eng. Appl. Artif. Intell.* **2019**, *86*, 165–181. [CrossRef]
82. Mousavirad, S.J.; Ebrahimpour-Komleh, H. Human mental search: A new population-based metaheuristic optimization algorithm. *Appl. Intell.* **2017**, *47*, 850–887. [CrossRef]
83. Dehghani, M.; Mardaneh, M.; Guerrero, J.M.; Malik, O.P.; Ramirez-Mendoza, R.A.; Matas, J.; Vasquez, J.C.; Parra-Arroyo, L. A New "Doctor and Patient" Optimization Algorithm: An Application to Energy Commitment Problem. *Appl. Sci.* **2020**, *10*, 5791. [CrossRef]
84. Chen, X.; Xu, B.; Mei, C.; Ding, Y.; Li, K. Teaching–learning–based artificial bee colony for solar photovoltaic parameter estimation. *Appl. Energy* **2018**, *212*, 1578–1588. [CrossRef]
85. Al-Betar, M.A.; Alyasseri, Z.A.A.; Awadallah, M.A.; Abu Doush, I. Coronavirus herd immunity optimizer (CHIO). *Neural Comput. Appl.* **2020**, *33*, 5011–5042. [CrossRef]
86. Karaboga, D.; Basturk, B. A powerful and efficient algorithm for numerical function optimization: Artificial bee colony (ABC) algorithm. *J. Glob. Optim.* **2007**, *39*, 459–471. [CrossRef]
87. Askarzadeh, A. A novel metaheuristic method for solving constrained engineering optimization problems: Crow search algorithm. *Comput. Struct.* **2016**, *169*, 1–12. [CrossRef]
88. Heidari, A.A.; Mirjalili, S.; Faris, H.; Aljarah, I.; Mafarja, M.; Chen, H. Harris hawks optimization: Algorithm and applications. Futur. Gener. *Comput. Syst.* **2019**, *97*, 849–872. [CrossRef]
89. Arora, S.; Singh, S. Butterfly optimization algorithm: A novel approach for global optimization. *Soft Comput.* **2018**, *23*, 715–734. [CrossRef]
90. Mirjalili, S.; Gandomi, A.H.; Mirjalili, S.Z.; Saremi, S.; Faris, H.; Mirjalili, S.M. Salp Swarm Algorithm: A bio-inspired optimizer for engineering design problems. *Adv. Eng. Softw.* **2017**, *114*, 163–191. [CrossRef]
91. Gandomi, A.H.; Yang, X.-S.; Alavi, A.H. Cuckoo search algorithm: A metaheuristic approach to solve structural optimization problems. *Eng. Comput.* **2012**, *29*, 245. [CrossRef]
92. Mirjalili, S. The Ant Lion Optimizer. *Adv. Eng. Softw.* **2015**, *83*, 80–98. [CrossRef]
93. Faris, H.; Aljarah, I.; Alqatawna, J. Optimizing Feedforward neural networks using Krill Herd algorithm for E-mail spam detection. In Proceedings of the 2015 IEEE Jordan Conference on Applied Electrical Engineering and Computing Technologies (AEECT), The Dead Sea, Jordan, 3–5 November 2015; pp. 1–5. [CrossRef]
94. Thaher, T.; Heidari, A.A.; Mafarja, M.; Dong, J.S.; Mirjalili, S. Binary Harris Hawks optimizer for high-dimensional, low sample size feature selection. In *Evolutionary Machine Learning Techniques*; Springer: Singapore, 2020; pp. 251–272. [CrossRef]
95. Shi, Y.; Pun, C.-M.; Hu, H.; Gao, H. An improved artificial bee colony and its application. *Knowl. Based Syst.* **2016**, *107*, 14–31. [CrossRef]
96. Banaie-Dezfouli, M.; Nadimi-Shahraki, M.H.; Beheshti, Z. R-GWO: Representative-based grey wolf optimizer for solving engineering problems. *App. Sof. Com.* **2021**, *106*, 107328. [CrossRef]
97. Li, X.; Yi, P.; Jiang, Y.; Zhang, F. An Improved Salp Swarm Algorithm Based on Cosine Decline and Chaos Crossover Strategies. In Proceedings of the 2020 IEEE 6th International Conference on Computer and Communications (ICCC), Chengdu, China, 11–14 December 2020. [CrossRef]

98. Saxena, A.; Soni, B.P.; Kumar, R.; Gupta, V. Intelligent Grey Wolf Optimizer—Development and application for strategic bidding in uniform price spot energy market. *Appl. Soft Comput.* **2018**, *69*, 1–13. [CrossRef]
99. Jayabarathi, T.; Raghunathan, T.; Adarsh, B.R.; Suganthan, P.N. Economic dispatch using hybrid grey wolf optimizer. *Energy* **2016**, *111*, 630–641. [CrossRef]
100. Nadimi-Shahraki, M.H.; Taghian, S.; Zamani, H.; Mirjalili, S.; Elaziz, M.A.; Oliva, D. MMKE: Multi-trial vector-based monkey king evolution algorithm and its applications for engineering optimization problems. *PLoS ONE* **2023**, *18*, e0280006. [CrossRef] [PubMed]
101. Nayyef, H.M.; Ibrahim, A.A.; Zainuri, M.A.A.M.; Zulkifley, M.A.; Shareef, H. A Novel Hybrid Algorithm Based on Jellyfish Search and Particle Swarm Optimization. *Mathematics* **2023**, *11*, 3210. [CrossRef]
102. Kuo, R.; Chiu, T.-H. Hybrid of jellyfish and particle swarm optimization algorithm-based support vector machine for stock market trend prediction. *Appl. Soft Comput.* **2024**, *154*, 111394. [CrossRef]
103. Yuan, X.; Hu, G.; Zhong, J.; Wei, G. HBWO-JS: Jellyfish search boosted hybrid beluga whale optimization algorithm for engineering applications. *J. Comput. Des. Eng.* **2023**, *10*, 1615–1656. [CrossRef]
104. Mariottini, G.L.; Pane, L. Mediterranean Jellyfish Venoms: A Review on Scyphomedusae. *Mar. Drugs* **2010**, *8*, 1122–1152. [CrossRef]
105. Zavodnik, D. Spatial aggregations of the swarming jellyfish Pelagia noctiluca (Scyphozoa). *Mar. Biol.* **1987**, *94*, 265–269. [CrossRef]
106. Dhaenens, C.; Jourdan, L. *Metaheuristics for Big Data*; Wiley: Hoboken, NJ, USA, 2016; pp. i–xvi. [CrossRef]
107. Derrac, J.; García, S.; Molina, D.; Herrera, F. A practical tutorial on the use of nonparametric statistical tests as a methodology for comparing evolutionary and swarm intelligence algorithms. *Swarm Evol. Comput.* **2011**, *1*, 3–18. [CrossRef]
108. Wilcoxon, F. Individual comparisons by ranking methods. In *Breakthroughs in Statistics: Methodology and Distribution*; Kotz, S., Johnson, N.L., Eds.; Springer: New York, NY, USA, 1992; pp. 196–202. [CrossRef]
109. Yang, Z.; Zhong, H.; Xia, Q.; Kang, C. Fundamental Review of the OPF Problem: Challenges, Solutions, and State-of-the-Art Algorithms. *J. Energy Eng.* **2017**, *144*, 04017075. [CrossRef]

Disclaimer/Publisher's Note: The statements, opinions and data contained in all publications are solely those of the individual author(s) and contributor(s) and not of MDPI and/or the editor(s). MDPI and/or the editor(s) disclaim responsibility for any injury to people or property resulting from any ideas, methods, instructions or products referred to in the content.